SHEYENNE RIVER
Geomorphology Study

Prepared for
U.S. Army Corps of Engineers
St. Paul District
Contract DACW37-00-D-0001
Task Order No. 0005

Prepared by
WEST Consultants, Inc.
11848 Bernardo Plaza Court
Suite 140B
San Diego, CA 92128

November 2001

WEST CONSULTANTS, INC.

TABLE OF CONTENTS

APPENDICES

LIST OF FIGURES

LIST OF TABLES

1 Introduction

1.1 Purpose and Authorization

The purpose of this study is to provide reasonable predictions of the future behavior of the Sheyenne River (North Dakota) under different hydrologic and project assumptions. Two hydrologic scenarios and three project conditions under each scenario were considered for pumping of excess water from the Devils Lake Basin to the Sheyenne River (the future without project condition plus two pumping conditions). A combination of fluvial geomorphology, hydrology, and hydraulic engineering approaches were used to arrive at the predicted river states. The predicted changes in channel size and/or planform (meander characteristics, sinuosity, etc.) are expected to help the U.S. Army Corps of Engineers, Saint Paul District (the District) determine project feasibility and costs, including possible mitigation measures. This Saint Paul District authorized this study under contract DACW37-00-D-0001, Delivery Order Number 0005.

1.2 Scope

The scope of the study revolved around the efforts to predict future conditions of the river under the different hydrologic scenarios. The future scenarios considered were:

1. **Design (Moderate) Scenario**: This scenario assumes the climate and hydrologic conditions will be similar to 1980-1999 until the year 2015. After that it is assumed that the conditions will be similar to the period 1950-1999.
2. **Wet Scenario**: This scenario assumes the climate and hydrologic conditions will be similar to the period 1993-1999 until Devils Lake naturally overflows to the Sheyenne River and for the following seven years. After that it is assumed that the climate and hydrologic conditions will be similar to the period 1950-1999.

Under each of the above hydrologic scenarios, three project conditions were considered:

a. Without project
b. 300 cubic feet per second (cfs) constrained pumping alternative
c. 480 cfs unconstrained pumping alternative

Specific tasks performed during the study included:

1. Evaluation of historic changes in cross section and planform shapes.
2. Construction of discharge-frequency and discharge-duration curves via statistical analysis for peak and mean daily flows.
3. Field reconnaissance of the study area to observe existing channel conditions.
4. Estimation of historic and future "channel forming discharge" via three separate methods.
5. Determination of "regime channel" dimensions by several different methods.
6. Estimation of project effects for each of the six future scenarios.

1.3 Acknowledgements

Mr. Martin Teal was the WEST Consultants, Inc. (WEST) project manager for this study, led the technical analyses, and wrote the majority of this report. Dr. David Williams, as principal-in-charge, provided overall guidance and quality assurance. Mr. Leo Kreymborg performed the majority of the hydrologic and geomorphic analyses and also

wrote portions of the report. Mr. Iwan Thomas provided the planform and lateral erosion analyses and wrote much of Chapter 6, while Dr. Henry Hu researched regime equations, performed the initial SAM analyses for sediment transport, and wrote part of Chapter 5. Mr. Ramesh Chintala also provided technical assistance for the study, especially in the analysis of vegetation, and wrote the majority of Chapter 8.

Professionals from Saint Paul District managed this study for the U.S. Army Corps of Engineers. Mr. Scott Goodfellow patiently answered our questions and guided us on the field reconnaissance. Mr. Pat Foley coordinated the study efforts and Mr. Dan Reinartz provided the hydrologic traces used in the study. Mr. Terrance Jorgenson provided information on the geology of the Sheyenne River valley. Messrs. Foley and Goodfellow and Ms. Michelle Schneider provided feedback on draft versions of the report.

The assistance and information provided by the following individuals was especially helpful for the vegetation analysis presented in Chapter 8 of this report and is gratefully acknowledged: Mr. Robert A. Anfang (St. Paul District Corps of Engineers), Dr. Michael L. Scott (United States Geological Survey, Midcontinent Ecological Science Center Fort Collins, Colorado), Dr. Bonnie Alexander (Professor of Biology and Plant Science, Valley City State University, Valley City, North Dakota), and Mr. Bryan Stotts (USDA Forest Service, Lisbon, North Dakota).

Chapter 3 (Erosion Reaches) was adopted from an earlier District draft report with only slight modifications.

2 Background

2.1 Basin Description

The Sheyenne River basin lies in eastern North Dakota, as shown in Figure 2-1. The basin covers parts of 16 counties and encompasses approximately 6,900 square miles (excluding the closed Devil's Lake basin) upstream of its confluence with the Red River of the North, which in turn flows into Lake Winnipeg in the Canadian province of Manitoba. The cities of Fargo, Lisbon, Valley City, and Cooperstown lie within the basin, as well as portions of the Sheyenne National Grassland and the Spirit Lake Indian Reservation. At its extremes, the basin extends about 160 miles from north to south and about 175 miles from east to west. The Sheyenne River rises near Krueger Lake in Sheridan County and flows generally eastward about 150 river miles to McVille, where it turns southerly for about 200 miles to the vicinity of Lisbon. There the river forms a loop as it swings northeasterly for about 150 miles to its junction with the Red River, about 10 miles north of Fargo. The study reach for this investigation extends upstream from River Mile (RM) 0 at the Red River of the North to approximately RM 480 at Peterson Coulee.

2.1.1 Topography

The surficial topography and geologic features of Sheyenne River basin are primarily a result of the depositional and erosional effects of continental glaciation. The boundary between the River and Devil's Lake is comprised of a series of recessional moraines (Wiche and Pusc, 1994). Because of the glacial action, many drainage features are not well defined, and runoff collects in numerous closed depressions.

The Sheyenne River basin lies in two distinct topographic areas: the rolling drift prairie, which includes the entire basin upstream from the escarpment of the Sheyenne delta near Kindred; and the flat Red River Valley plain through which the lower 70 miles of the river passes. The Red River of the North valley floor ranges in elevation from 890 feet msl (mean sea level) near the mouth of the Sheyenne River to 950 feet at the margin of the delta near Kindred. The top of the delta escarpment varies between elevations 1000 ft. and 1020 ft. From the fringe of the delta westward, the elevations of the upland areas range from 1020 ft. to 1700 ft. The Sheyenne River valley above Kindred varies in depth from 100 to 200 feet and ranges in width from ¼ to 2 miles. Of the total basin area, about 92 percent is farmland and about 83 percent of the farmland is improved. Timber is limited to a fringe along the Sheyenne River; however, portions of the river valley above Kindred are heavily wooded.

The total length of the meandering Sheyenne River is approximately 542 miles. The source of the river is at an elevation of 1700 feet and the mouth is at elevation 854 feet. Total fall is 846 feet in approximately 542 miles for an average slope of 1.6 feet per mile.

2.1.2 Climate

Weather observations are being obtained from 13 stations in the Sheyenne River basin (USACE, 1999). These stations are listed in Table 2-1. Precipitation records are available for 12 of these stations and temperatures for nine of the stations. Three stations,

INSERT FIGURE 2-1 HERE

Figure 2-1. Location Map

Sheyenne, Hannaford, and Baldhill Dam, have rainfall recording gages. Precipitation is observed at an additional 15 stations adjacent to the basin; nine of these stations also observe temperatures. Streamflow is measured at five of the stations.

Table 2-1. Sheyenne River Basin Weather and Streamflow Stations (after USACE, 1999)

Station	Years of Record		
	Precipitation	Temperature	Streamflow
Maddock Agri. School	81		
Harvey	93	15	
McVille	53	40	
McHenry	74	74	
Courtnay	63		
Warwick			30
Cooperstown	100	100	51
Baldhill Dam	45	45	47
Valley City	92	92	54[1]
Lisbon	92	92	39
McLeod	85	85	
Chaffee	34		
Enderlin	37	37	
Kindred			47

[1]Valley City discharges recorded (1939-1975), stages and annual peak discharges recorded (1979-present).

The annual mean temperature for the Sheyenne River basin is about 40° F. The basin experiences extreme variations in temperature. The normal mean monthly temperature varies from 72° F in July to 0° F in January. National Weather Service records show temperature extremes of 118° F at Cooperstown on 6 July 1936 and 50° F at the Maddock Agricultural School on 7 February 1936.

Normal annual precipitation for the Sheyenne River basin ranges from about 16 inches in the northwestern part of the basin to about 20 inches in the southeastern portion. The greatest annual precipitation observed in the basin was 32.33 inches at Enderlin in 1975. The second greatest annual precipitation was 30.42 inches at Lisbon in 1941, and the least was 7.55 inches at McHenry in 1910. Normal monthly precipitation ranges from maximums of 3.4 inches in the northwest and 3.8 inches in the southeast during the month of June to minimums of 0.3 to 0.5 inch in January and February. Snowfall averages about 36 inches a year throughout the basin.

2.1.3 Geology and Soils

The Sheyenne River flows through glacial till in the upper and middle reaches, through sand deposits in the Sheyenne Delta of the lower basin, and finally through the extremely flat clay deposits of the glacial Lake Agassiz basin. In the upper basin down to Lisbon, the surficial materials are glacial till and outwash. Between Lisbon and Kindred, the Sheyenne River has incised a trench across the Sheyenne Delta, a feature which marks the confluence of the early Sheyenne River with glacial Lake Agassiz. Coarse sands are located at the upstream end of this reach, and become finer as one progresses in the downstream direction. From Kindred to its confluence with the Red River, the Sheyenne River crosses the Red River floodplain that consists mainly of deep clays.

2.1.4 Environmental Setting

More than 70 percent of the land in the Sheyenne Basin is used for agricultural purposes (USACE, 1999). However, even with the predominant agricultural use, it is one of the prime wooded valleys and grassland areas in eastern North Dakota.

The Sheyenne River in the area between Lisbon and Kindred is located in a heavily wooded valley. Extensive grasslands are located in the delta area outside of the river floodplain. The Sheyenne National Grasslands, part of the U.S. Forest Service system, is located here. Domestic livestock grazing and agriculture predominate outside of the valley proper.

Federally listed threatened or endangered species that may be present in the study area include the peregrine falcon (Falco peregrinus anatum), bald eagle (Haliaeetus leucocephalus), whooping crane (Grus americana), gray wolf (Canis lupus), piping plover (Charadrius melodus), and the western prairie fringed orchid (Platanthera praeclara). The peregrine falcon, whooping crane, and gray wolf are endangered while the bald eagle, piping plover, and western prairie fringed orchid are threatened.

2.1.5 Hydrology and Stream Gages

Stream gage data was used extensively in this study as described in later sections. A list of USGS stream gages in the basin having mean daily flow records, flood peak records, or other information utilized in the study are presented in Table 2-2. Gages are listed in the table from upstream to downstream. Gage locations are also shown in Figure 2-1. The drainage areas listed are those from the USGS gage descriptions and do not necessarily reflect non-contributing drainage areas.

Table 2-2. List of Sheyenne River USGS Stream Gages Utilized

Gage Number	Description	Drainage Area Sq. Mi.	Daily Flows Used	Peak Flows Used	Period of Record Available
05055500	Sheyenne River At Sheyenne, ND	1,790	No	Yes	5/1/1929-6/30/1933 and 10/1/1939-9/30/1951
05056000	Sheyenne River Near Warwick, ND	2,070	Yes	Yes	10/1/1949 to 9/30/98 (peaks), 10/1/1949 to 9/30/99 (flows)
05057000	Sheyenne River Near Cooperstown, ND	6,470	Yes	Yes	10/1/1944 to 9/30/98 (peaks), 10/1/1949 to 9/30/99 (flows)
05058000	Sheyenne River Below Baldhill Dam, ND	7,470	Yes	Yes	10/1/1949 to 9/30/98 (peaks), 10/1/1949 to 9/30/99 (flows)
05058500	Sheyenne River at Valley City, ND	7,810	No	Yes	3/1/1919 to 8/31/1919, 3/1/1938 to 6/30/1938, 8/1/1938 to 9/30/1975; 10/1/1979 to 9/30/98 (peaks). Only 1950 – used for analysis.
05058700	Sheyenne River at Lisbon, ND	8,190	Yes	Yes	9/1/1956 to 9/30/98 (peaks), 9/1/1956 to 9/30/99 (flows).
05059000	Sheyenne River Near Kindred, ND	8,800	Yes	Yes	7/1/1949 to 9/30/99 (peaks), 7/1/1949 to 9/30/98 (flows)
05059300	Sheyenne River Above Sheyenne River Diversion Near Horace, ND	8,840	No	No	Used to determine drainage area
05059500	Sheyenne River at West Fargo, ND	8,870	No	Yes	9/1/1929 to 9/30/99 (peaks). Only 1950 – used for analysis.
05060600	Sheyenne River Near Harwood, ND	10,700	No	No	Used to determine drainage area

2.1.6 Dams and Diversions

Lake Ashtabula, formed by Baldhill Dam, is located approximately 16.5 river miles upstream from Valley City, North Dakota. Although several smaller reservoirs exist on the Sheyenne River, only Lake Ashtabula has an appreciable effect on flood flows (USACE, 1999). Baldhill Dam was constructed in 1950. The dam is operated for low flow augmentation to meet downstream water supply and pollution abatement objectives, and to reduce flooding in the Sheyenne River Valley. Recreation, fish, and wildlife enhancement are secondary objectives of the dam operation plan. The dam is currently being raised to provide increased flood control. District investigations (USACE, 1999) have concluded that a) the Sheyenne River has reached a "stable" condition since construction of the dam, and b) the 1.5-year flow in the river below the dam (taken as the dominant discharge) has decreased compared to pre-dam conditions, resulting in lowered erosion rates.

The same Congressional Authorization that approved the raising of Baldhill Dam (WRDA 1986) also provided for a flood diversion scheme that includes levees and flood control channels. One part of this scheme runs from Horace to West Fargo, while another part is located at West Fargo. Construction was finished on these elements in the early 1990's. The diversion begins to take effect when the river flow exceeds approximately 1000 cfs. All subreaches ("erosion reaches") described subsequently in the report are located outside of the influence of the diversion works.

2.2 Project Alternatives

As mentioned in the introduction to this report, six future flow scenarios were defined as part of the scope of work. A list of these scenarios is provided in Table 2-3.

2.2.1 Future Hydrology

Hydrologic traces for the six different future scenarios were provided by the District. These traces (time series data) were provided in DSS format (HEC Data Storage System). A description of the traces is provided in the next section of this report. The simulated flows all covered the time period from 10/1/2000 to 9/30/2050. Traces were provided for the flow locations listed in Table 2-4.

An additional flow location along the Sheyenne called "Into Ashtabula" (Lake Ashtabula formed by Baldhill Dam) was provided in the DSS files, and was within the study area, but was not used. Other flow locations provided in the DSS files (Junction, Halstad, Grand Forks, Oslo, Drayton, and Emerson) were downstream of Kindred, and were apparently on the Red River of the North. These locations were also not used.

Table 2-3. List of Simulated Future Flow Scenarios

Scenario Group	Description	DSS Trace Identifier	Short Identifier
Design Scenario	Moderate future, no pumping but with natural overflow from Stump Lake to Sheyenne	MT1 NOPUMP	Mdnp
	Moderate future, pumping with 300 cfs constrained	MT1 WB300PUMP	Md300
	Moderate future, pumping with 480 cfs unconstrained	MT1 WB480PUMP	Md480
Wet Trace Scenario	Wet future, no pumping but with natural overflow from Stump Lake to Sheyenne	WET NOPUMP	Wtnp
	Wet future, pumping with 300 cfs constrained	WET WB300PUMP	Wt300
	Wet future, pumping with 480 cfs unconstrained	WET WB480PUMP	Wt480

Table 2-4. List of Flow Points Used from the Future Simulated Flows (Listed from Upstream to Downstream)

Flow Point	Description
Peterson Coulee	Where proposed flows are added to the Sheyenne.
Warwick	Location of USGS stream gage.
Cooperstown	Location of USGS stream gage.
Valley City	Location of USGS stream gage.
Lisbon	Location of USGS stream gage.
Kindred	Location of USGS stream gage.

2.2.1.1 Wet Future

The Wet Future (without pumping) is a 50 year trace encompassing the period October 1, 2001 through September 30, 2050. The trace is comprised of flows based on historic data. The first 21 years of the trace contain a seven-year sequence of flows repeated three times. Flows are based on precipitation, evaporation, and inflow data recorded over a recent seven-year period of record (1993 -1999). The seven-year sequence repeats twice until Devils Lake reaches its natural overflow elevation of 1459 in the year 2014. The seven year sequence then repeats once more so that the impacts of the natural overflow through Tolna Coulee can be simulated downstream on the Sheyenne River. Historic data from the years 1981 – 1999, and 1981 – 1990 are then used in the sequence to fill the remaining years for a total trace length of 50 years. Table 2-5 lists the simulation year and the corresponding historic year for this scenario.

Table 2-5. Wet Scenario Simulation Year with Corresponding Historic Year

Simulation Year	Historic Year	Simulation Year	Historic Year
2001	1993	2026	1985
2002	1994	2027	1986
2003	1995	2028	1987
2004	1996	2029	1988
2005	1997	2030	1989
2006	1998	2031	1990
2007	1999	2032	1991
2008	1993	2033	1992
2009	1994	2034	1993
2010	1995	2035	1994
2011	1996	2036	1995
2012	1997	2037	1996
2013	1998	2038	1997
2014	1999	2039	1998
2015	1993	2040	1999
2016	1994	2041	1981
2017	1995	2042	1982
2018	1996	2043	1983
2019	1997	2044	1984
2020	1998	2045	1985
2021	1999	2046	1986
2022	1981	2047	1987
2023	1982	2048	1988
2024	1983	2049	1989
2025	1984	2050	1990

The corresponding in-lake elevation traces for with- and without- project conditions are shown in Figure 2-2. For the without-project condition, the trace shows that the lake will peak in the year 2019 at elevation 1460.6 with a peak outflow of approximately 580 cfs. Natural overflow is shown to end in the year 2024. Figure 2-3 shows the natural overflow hydrograph and Figure 2-4 shows this hydrograph superimposed with the pumping hydrographs for the Wt300 (300 cfs constrained) and the Wt480 (480 cfs unconstrained) alternatives.

For the pumping alternatives, pumping begins May 1, 2005 and occurs throughout the 50-year period. Pumping is terminated when the lake reaches elevation 1441.4 and begins again when the lake rises above this elevation. Hydrographs for with- and without project conditions at the Warwick, Cooperstown, and Kindred flow points are shown in Appendix I.

2.2.1.2 Moderate Future

The Moderate Future 50-year trace is one of the 10,000 stochastic traces generated for Devils Lake (trace number 211). It represents the case where the lake elevation rises to elevation 1450 within the first 15 years of the simulation. This is considered a more moderate trace relative to the wet future and was selected to assess more likely and perhaps more significant water quality impacts. Because conditions in the moderate trace are not as wet as those in the west trace, there is not as much dilution to attenuate water quality impacts.

Flows entering the Sheyenne River were associated with the synthetic trace in Devils Lake by "tagging" each year with a historic year multiplied by a factor. In this way the flows downstream are "in phase" with hydrologic conditions that are being simulated in Devils Lake. In the moderate future scenario the lake reaches a peak elevation of 1450.1 in the year 2014. Following the first 15 years of the trace, conditions tend to be dry and appear to be drier than the average conditions of the last 50 years. The result is that the average conditions of the trace overall are drier than the average conditions of the last 50 years.

Figure 2-5 shows the in-lake elevation trace for Devils Lake for with- and without-project conditions for the moderate future. There is no natural overflow through Tolna Coulee for this scenario. Pumping terminates near the middle of the 50-year period when the lake reaches elevation 1441.4. Hydrographs for with- and without project conditions at the Warwick, Cooperstown, and Kindred flow points are shown in Appendix I.

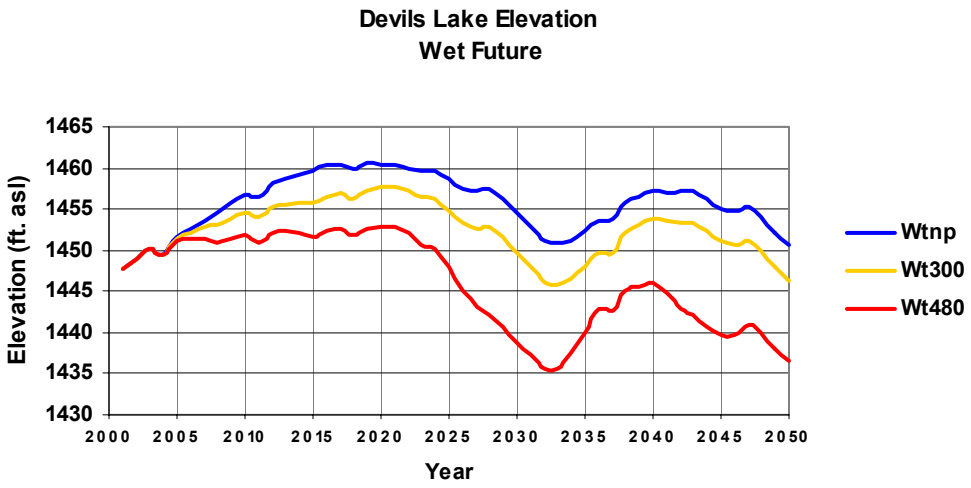

Figure 2-2. Projected Devils Lake Elevation for Wet Future Traces.

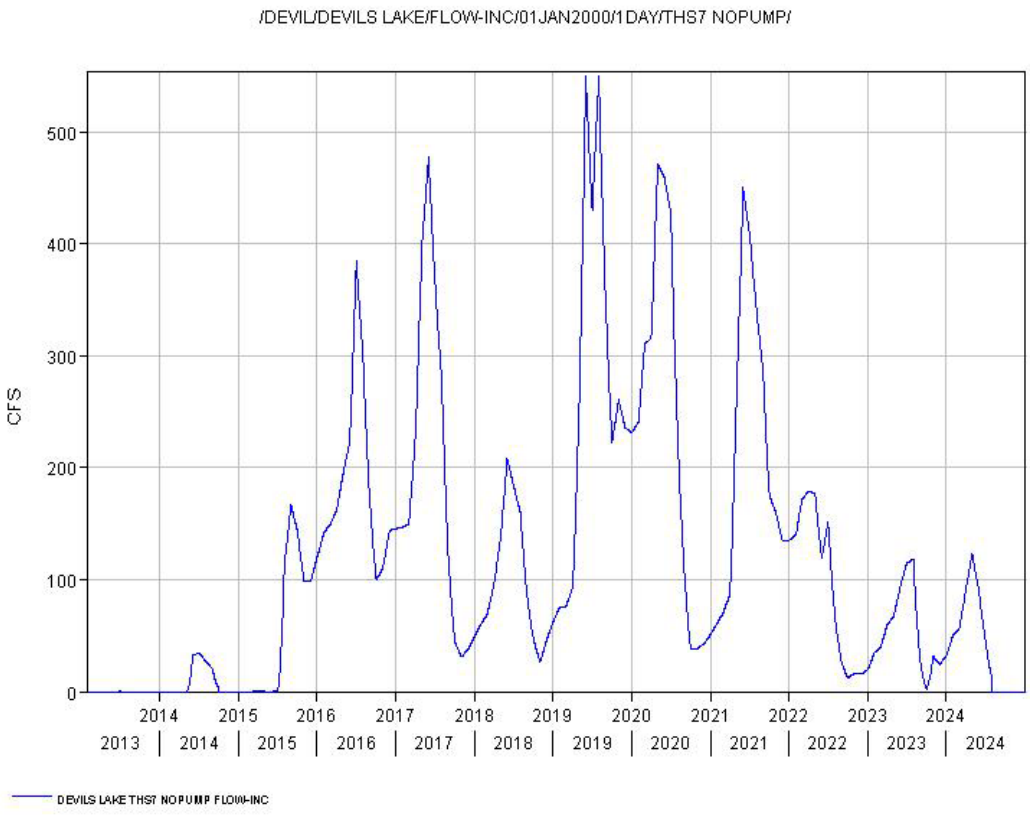

Figure 2-3. Projected Devils Lake Natural Overflow Hydrograph for Wet Future with No Pumping.

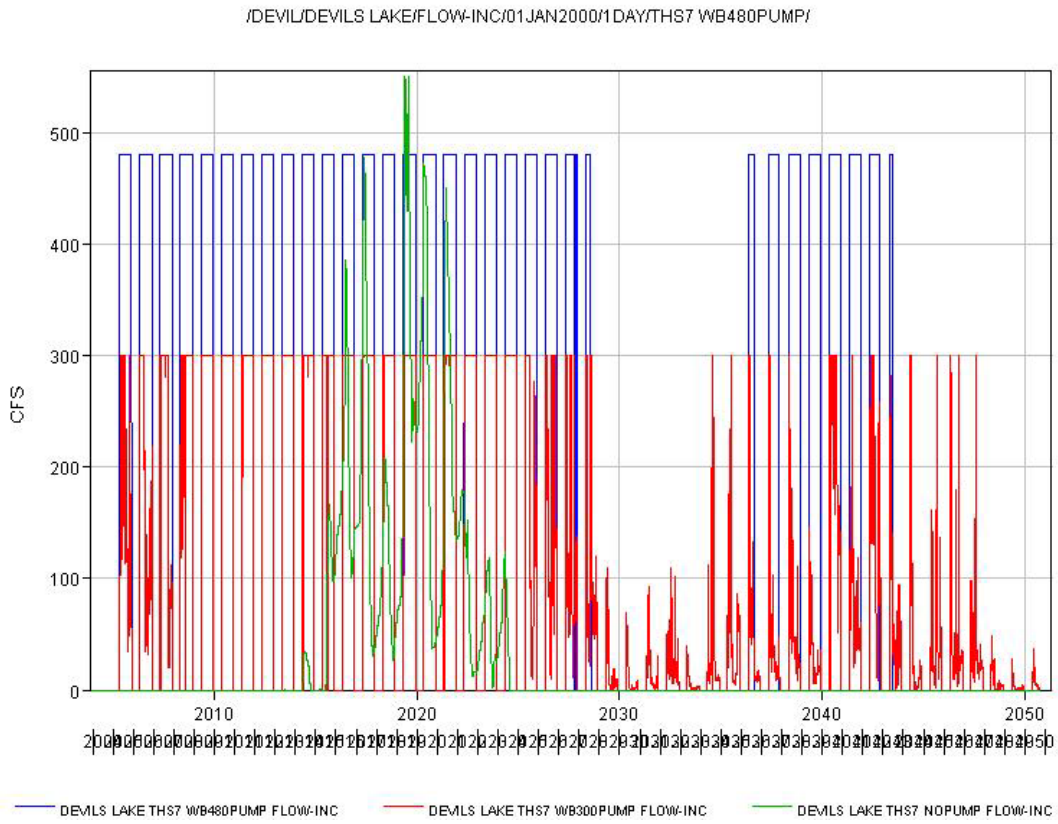

Figure 2-4. Projected Devils Lake Natural Overflow Hydrograph for Wet Future Superimposed on Pumping Hydrographs.

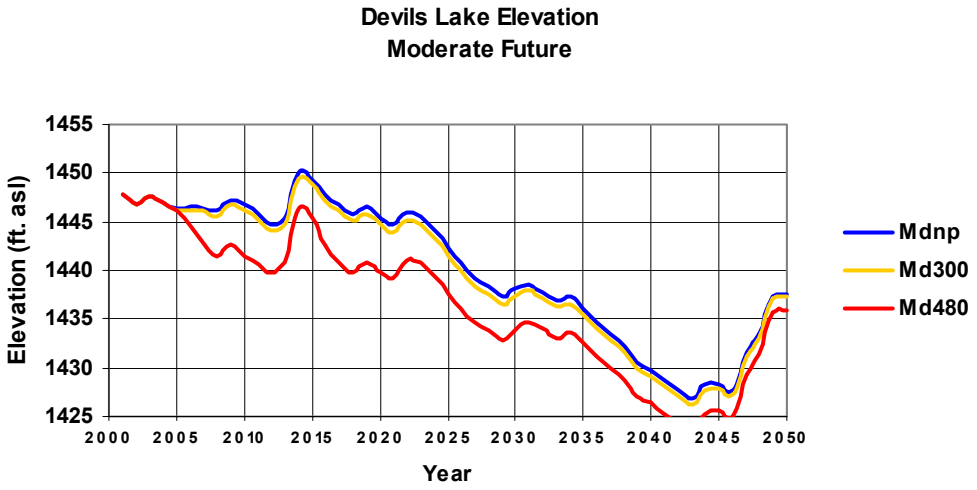

Figure 2-5. Projected Devils Lake Elevation for Moderate Future Traces.

3 Erosion Reach Classification

3.1 General

River characteristics can vary significantly on rivers the length of the Sheyenne. This study was designed to identify important differences in these geomorphic characteristics. The District has performed geomorphic analyses of the Sheyenne River over the last few years, and defined river reaches and monitoring sites. After review of the District methodology, WEST decided to adopt the same reaches for the present study. Information in this chapter relies on previous District studies.

3.2 Definition and Selection of Erosion Reaches

The meander patterns of the river and valley terrain were used to subdivide the river. Visual inspection of digital mapping by District engineers identified areas where meandering patterns changed in general shape, meander width, sinuosity, etc. These areas were then grouped into 12 representative reaches. Figure 2-1 shows the final reaches labeled A through L.

Small reaches (subreaches) were chosen in each of the primary reaches for more detailed analysis. These areas will be labeled erosion study reaches. These reaches were used to:

a. Determine rates of channel migration

b. Provide post-1998 geo-referenced cross section surveys for the present analysis and baseline data for future survey comparison.

c. Obtain bank and bed sediment samples.

Three potential erosion study reaches were identified within each primary reach. These were identified from USGS mapping and were chosen to be reasonably representative of the primary reach. A good road access was necessary. Permission was sought from land owners to allow access for surveyors and others involved in this study. The selection of one of the three possible reaches was accomplished during a field trip by the District in June 1998. Often the availability of access permission was the deciding factor in which area was chosen. If permission was available for multiple areas, the one deemed most representative based on geomorphic characteristics was chosen.

Two erosion study reaches were adopted in study reach H because of the widely different character of the two reaches as observed in the field. Used together they should provide more representative values. Figure 2-1 shows the location of the erosion study reaches.

3.3 Cross Sections

New surveys were conducted to obtain cross section data in these areas. Cross sections were classified as one of three types: Regular, Precision, and Habitat. In each of the adopted erosion study reaches, with the exception of reach G, one or more old cross sections from the 1940's were available. The exact geo-referenced locations of the cross

sections were not available. Only a map showing the cross section placement was available. The digital cartographic technique of warping the old map image to the coordinate system of a USGS 7.5 minute quadrangle map was used to re-locate the old cross section alignments. These re-surveyed cross sections were labeled Precision cross sections. These sections have been used to determine historic changes in the channel.

Regular and Habitat cross sections are newly surveyed cross sections that do not align with historically surveyed locations. Habitat sections have additional field data (velocity and substrate). These habitat sections were used in the construction of a 2-dimensional hydraulic model for the environmental assessment. Figures in Appendix A show the locations of the adopted erosion study areas and the newly surveyed cross sections.

3.4 HEC-RAS Modeling

Many aspects of this study relied on the use of hydraulic data to provide water surface, velocity, and other parameters. A HEC-RAS model of the Sheyenne River (USACE, 1998a) was created by combining various existent HEC-2 models from past studies. Supplemental cross sections were added from cross sections surveyed in the 1940's. The resulting HEC-RAS model started upstream in Sheridan County and continued downstream to the confluence with the Red River of the North. A total of 1098 cross sections describe the 562 river miles modeled.

4 Dominant Discharge Analyses

4.1 General

Concepts of channel equilibrium (or regime) and hydraulic geometry are described in the following chapter. However, all "regime equations" used for prediction of channel characteristics require a discharge to be used as the input variable. This discharge is a single steady representative flow that will theoretically produce (for rivers in regime) the same bankfull dimensions as the natural sequence of flow events. This discharge is called the dominant discharge or the channel-forming discharge. In order to use regime equations to predict channel geometry for future conditions, the dominant discharge must first be identified for each condition. Unfortunately, identification of the dominant discharge is usually not an easy task. Three separate approaches were used to identify the dominant discharge for existing channel conditions, and the results were used to help determine dominant discharge for each of the future scenarios.

4.2 Field Observations

During the field trip of May 14-18, 2001, estimates were made of the physical elevation of the bankfull discharge for each cross section visited. Furthermore, an estimate of the flow in the Sheyenne at the time of the visit was made at each cross section. The estimates were made as follows:

(1) The drainage area at the location of the photograph was estimated by the same method used to estimate the drainage areas of the precision cross sections.

(2) The flows at the upstream and downstream bounding gages at the time the photograph was taken were determined from hourly gage records.

(3) The flow at a section was interpolated based on the flow at the upstream and downstream gages at the time the section was visited. The interpolation was based on the drainage area at the point of the photograph versus the drainage area at the bounding gages.

4.2.1 Single Cross Section SAM Models

Each of the 1998 precision cross sections was modeled using SAM (Hydraulic Design Package for Channels; USACE, 1998b). The roughness coefficients (Manning's "n" values) were taken from the equivalent (or, in the case of one cross section, nearby) cross sections from the HEC-RAS model of the entire river that was provided by the District. Points in the cross sections from the HEC-RAS model where n values changed were projected onto the approximate corresponding locations of the 1998 precision cross sections. The energy slopes were also taken from the corresponding locations in a modified version of the HEC-RAS model provided by the District. The modification consisted of the addition of interpolated cross sections to reduce reach lengths in the original model to 500 feet or less. The approximate 1.5-year discharges were used as the flow values for this model, although it was found that large variations in the discharge had a negligible effect on the energy slopes at the precision cross sections. SAM

provided depth, top width, and cross sectional area versus discharge relationships, as well as sediment rating curves (see Section 4.3.2).

Each of the corresponding precision cross sections from 1940 was also modeled using SAM. For all sections except A2-f, B3-a, and B3-e, the HEC-RAS model provided by the District contained the sections from 1940. Both the geometry and n values were transferred into SAM directly. For the A2-f, B3-a, and B3-e cross sections, the points from the 1940 cross sections were input into SAM, and the n value transitions were estimated using the same method described for the 1998 cross sections. The energy slopes were the same as those used for the 1998 cross sections. These cross sections from 1940 were modeled only to obtain depth, top width and cross sectional area versus discharge relationships.

4.2.2 Bankfull Discharge Based on Field Estimates

For those cross sections visited during the field trip, the flow in cubic feet per second (cfs) and elevation in feet were estimated. Using these flows, HEC-RAS models were developed to estimate the bankfull flow at each cross section. Research has shown that the channel forming discharge is approximated by flows at or about bankfull stage (Biedenharn et al., 2000).

Each precision cross section was input into a separate HEC-RAS model. The n values were taken from the equivalent (or nearby) cross sections from the HEC-RAS model of the entire river provided by the District. The n value transitions from the sections in the model of the entire river were projected onto the approximate corresponding locations on the precision cross sections.

Each of the precision cross sections was input as the most downstream cross section of a model. HEC-RAS requires a minimum of two cross sections per model, so an upstream cross section for was also input into each model. This upstream cross section has no significance.

The downstream boundary condition for each HEC-RAS model was set to normal depth. The energy slope assigned to the normal depth was initially set equal to the energy slope at the same geographic location from the model of the entire river.

The estimated flow value (at the day and time the cross section was visited on the field trip) was interpolated from the gage records. The HEC-RAS model was then calibrated so that the water surface elevation estimated in the field would match the HEC-RAS water surface elevation for that cross section. The calibration was done through adjustments to the energy slopes (and occasionally, the bank station locations) in the single cross section models so that, for the estimated flow, the predicted water surface of a single cross section model would match the observed water surface. Using these "calibrated" single cross section HEC-RAS models, the estimated physical elevation of bankfull yielded a "field estimated" bankfull flow for each cross section.

4.3 Effective Discharge

The procedure outlined in a recent Corps of Engineers Technical Note (Biedenharn et al., 2000) was used to calculate the effective discharge (another estimate of the channel forming discharge) at each precision-cross section for both the historical and future flows. This procedure involves calculation of the flow-duration curve and the sediment rating curve, as described in the following paragraphs.

4.3.1 Flow-Duration Curves

Because historical stream gage records and the simulated future flows were not necessarily located at the precision cross section sites, an interpolation procedure was needed to estimate the future flow-duration curve at each precision cross section. The "flow-duration curve method" outlined by Biedenharn et al. (based on drainage area) was used. The method requires that the drainage areas at all points be known, since the flow-duration curves are built as functions of drainage area. Therefore, the drainage area of each of the precision cross sections needed to be determined.

4.3.1.1 Estimation of Drainage Areas

The drainage area tributary to each precision cross section was estimated from a delineation of the watershed. The delineation was performed using 1:250,000 scale digital elevation models (DEM's) of North Dakota. These digital elevation models were obtained from the USGS at the following web site:
http://edcwww.cr.usgs.gov/glis/hyper/guide/1_dgr_demfig/states/ND.html
The following DEM's were used: Aberdeen (E and W), Devils Lake (E and W), Fargo (E and W), Grand Forks (E and W), Jamestown (E and W), McClusky (E and W), Milbank (E and W), Minot (E and W), New Rockford (E and W), and Thief River Falls (W only). These digital elevation models were converted to ArcView7 GIS format and merged into one DEM.

The USGS DEM's are in units of seconds of latitude (vertical) by seconds of longitude (horizontal) (referred to hereafter to as "second x second DEM"). Therefore, areas measured from these DEM's are in square seconds. Because seconds of longitude become shorter as you mover further north, a square second is not a constant unit of area. However, because the range of latitudes for the study area is small, a "square second" of area on this digital elevation model is approximately constant. For example, if the watershed extends from about 45 to 48 degrees North, the maximum distortion would be Cosine (48°) / Cosine (45°) = 0.95 or about 5% distortion.

Since the drainage area at each stream gage is supplied by the USGS, these drainage areas were compared to the drainage areas in square seconds calculated using the USGS DEM's.

The delineation was performed on the single combined DEM using HEC-GeoHMS (USACE, 2000). The locations of the seven USGS stream gages were transferred into the DEM coordinate system (second x second). All of the stream gages fell very near rivers delineated by HEC-GeoHMS. The "flow accumulation" value at each river point was the

drainage area to the nearest stream gage. Table 4-1 lists the delineation results, with the flow accumulations converted to square seconds.

Table 4-1. DEM Delineation Results for the Seven Stream Gages

USGS Gage Number	Description	Stated Drainage Area, square miles	Delineated flow accumulation value in square seconds
05055500	Sheyenne	1,790	8,769,150
05056000	Warwick	2,070	9,853,749
05057000	Cooperstown	6,470	27,076,059
05058000	Below Baldhill Dam	7,470	30,790,422
05058500	Valley City	7,810	32,088,375
05058700	Lisbon	8,190	34,052,058
05059000	Kindred	8,800	36,396,072

One more gage was available within the study reach, just downstream of Kindred. This was the 05059300 gage (Sheyenne River above Sheyenne River diversion). However, with a drainage area of 8,840 square miles it was so close to the Kindred gage that it was not checked against the DEM delineation.

The USGS supplied drainage areas at these seven stream gages were compared with the "square seconds" predictions from the DEM via a regression analysis. The fit was very good, resulting in an r-squared value of 99.97%. The regression equation was:

Square Miles = -436.04 + (Square Seconds) / 3921.52

The –436.04 term (an adjustment in square miles) probably arose from a large area upstream of all the gage points which was missed in the delineation. Note that the most upstream gage point (the Sheyenne gage) used for the regression analysis was upstream of all the precision cross sections. Because the regression predicts the drainage area within 10 square miles at this gage, the missing 436 squares miles is somewhere upstream of this gage. Therefore, the missing area is also upstream of all the precision cross sections and does not affect the prediction of the drainage areas.

The drainage areas at the locations of the precision cross sections upstream of Kindred (05059000) were also estimated using the DEM. An interpolation was performed between the known drainage areas at the nearest upstream and downstream gages against

the delineated drainage areas in square seconds. This method was used in lieu of the regression equation.

The delineation performed on the DEM incorrectly delineated the portion of the river downstream of the Kindred stream gage (05059000). This was probably due to the poor resolution of the DEM. Therefore drainage areas for points downstream of the Kindred gage could not be determined by the method previously described.

The delineation located the Sheyenne River east of its actual location (closer to the Red River). To correct for this problem, a separate subbasin was delineated for a point on the true river path downstream of Kindred. Using this separate subbasin, it was possible to estimate the drainage area at A2-f, the only precision cross section significantly downstream of Kindred. The B3 reach is also downstream of the Kindred gage, but close enough so that its drainage area was assumed to be identical to that of the gage.

The flow accumulation value from the DEM delineation at the A2-f section was added to the flow accumulation value at the Kindred gage. This value was applied to the regression equation which predicted a drainage area of 10,533 square miles. As a check, this same method was applied to an inactive gage (05060600) which is located immediately downstream of reach A2. The river near this gage had a flow accumulation value of 846,180 x 9 square seconds. The flow accumulation value at this gage was added to that of the Kindred gage. Applying the regression equation yielded a predicted drainage area of 10,787 square miles. The stated drainage area per the USGS for the inactive gage is 10,700 square miles, so this method is proven reasonably accurate.

4.3.1.2 Flow-duration Curves for Historical Stream Gage Records and Future Simulated Flows

Historical flow-duration curves were developed from the records of five USGS stream gages along the Sheyenne. These gages are listed in Table 4-2.

A common period of record from 10/1/1956 to 9/30/1998 was used for all gages. Although some gages had earlier records, because the flow-duration relationships for the precision cross section locations were going to be interpolated a common period of record needed to be used (see following section for an explanation of the interpolation procedure).

The flows for each gage were ranked from high to low. The fractional position for each flow was determined to be n / (m + 1) where n was the flow rank, and m was the total number of flow observations for the period. Then, intervals were chosen for the flow duration curve. The intervals used for the flow duration curves are shown in Table 4-3.

Table 4-2. Stream Gages Used for Historical Flow-duration Curves

USGS Gage Number	Description	Drainage Area, square miles
05056000	Warwick	2,070
05057000	Cooperstown	6,470
05058000	Below Baldhill Dam	7,470
05058700	Lisbon	8,190
05059000	Kindred	8,800

Table 4-3. Intervals Used for Flow-duration Curves

Range	Interval spacing used	Number of Intervals
0% - 0.5%	0.05%	10
0.5% - 1%	0.1%	5
1% - 3%	0.2%	10
3% - 5%	0.5%	4
5% - 15%	1%	10
15%-95%	5%	16

The 99% and 99.999% exceedance flows were also calculated. A total of 57 intervals resulted.

The flows at each of the intervals boundaries were determined by interpolation. The formula shown below was applied to determine the flow rank at an exceedance fraction:

*(Exceedance fraction) * (m + 1)*

where m = total number of observations. For example, one interval is the 0.5% to 0.6% range. At the Kindred gage, there were 15,340 observed flows used, which span the entire range of dates from 10/1/1956 to 9/30/1998. The flow rank is then:

*0.5% exceedance flow rank = 0.005 * (15340 + 1) = 76.705*

Therefore, the 0.5% exceedance point lies between the 76th highest and 77th highest flows. The 76th highest flow was 3,820 cfs. The 77th highest flow was 3,800 cfs. The interpolation point is 70.5%, or 0.705 of the way, from 76th highest flow to the 77th highest flow. The interpolated value is

*(1 – 0.705) * 3820 cfs + 0.705 * 3800 cfs = 3805.9 cfs.*

Therefore, 3,805.9 cfs was taken to be the 0.5% exceedance flow (or 99.5% percentile) for the historical flows at the Kindred gage.

Flow-duration curves were also developed for all the simulated future flows provided by the District. The scenarios are listed in Table 2-3, and the flow points for which these curves were developed are listed in Table 2-4.

4.3.1.3 Flow Duration Curves for Precision Cross Sections

Biedenharn et al., (2000), state that for any particular percentage exceedance, the mean flow at this exceedance should be a function of drainage area. The publication states that the log of mean discharge for any particular percentage exceedance should be a linear function of the log of drainage area, provided there is a regular downstream decrease in discharge per unit area.

This method involves graphing the log of drainage area on the horizontal axis versus the log of daily discharge on the vertical axis. Each percentage exceedance level produces one line. A common period of record is used to develop these lines. This was done with five stream gages along the Sheyenne for which there was a 42-year common period of record. The results are shown in Figure 4-1.

Each plotted line corresponds to one exceedance level. For example, the highest line in Figure 4-1 is for the 1% exceedance level. Each point on this line gives the mean discharge that is exceeded 1% of the time, as a function of drainage area.

As can be seen from the graph, there is a distinct change in slope between the line segment going from Warwick to Cooperstown and those segments upstream of Cooperstown (larger drainage areas). The fact that lines are not straight implies that there is not a regular downstream decrease in discharge per unit area.

A large part of the problem is that beginning at the 05057000 (Cooperstown) gage, the drainage areas include the entire Devils Lake Basin, which is about 3,800 square miles. The gage upstream of the Cooperstown gage is Warwick (05056000), and its drainage area includes none or very little of the Devils Lake Basin. Because the Devils Lake Basin is a closed, non-contributing basin (for the historical record period used), the drainage areas along the Sheyenne are greatly impacted, but the flows are not.

In order to make the drainage area a better predictor of flows, the 3,800 square miles of the Devils Lake Basin was subtracted from the delineated drainage areas for points at or downstream of the Cooperstown gage. This resulted in an "adjusted drainage area."

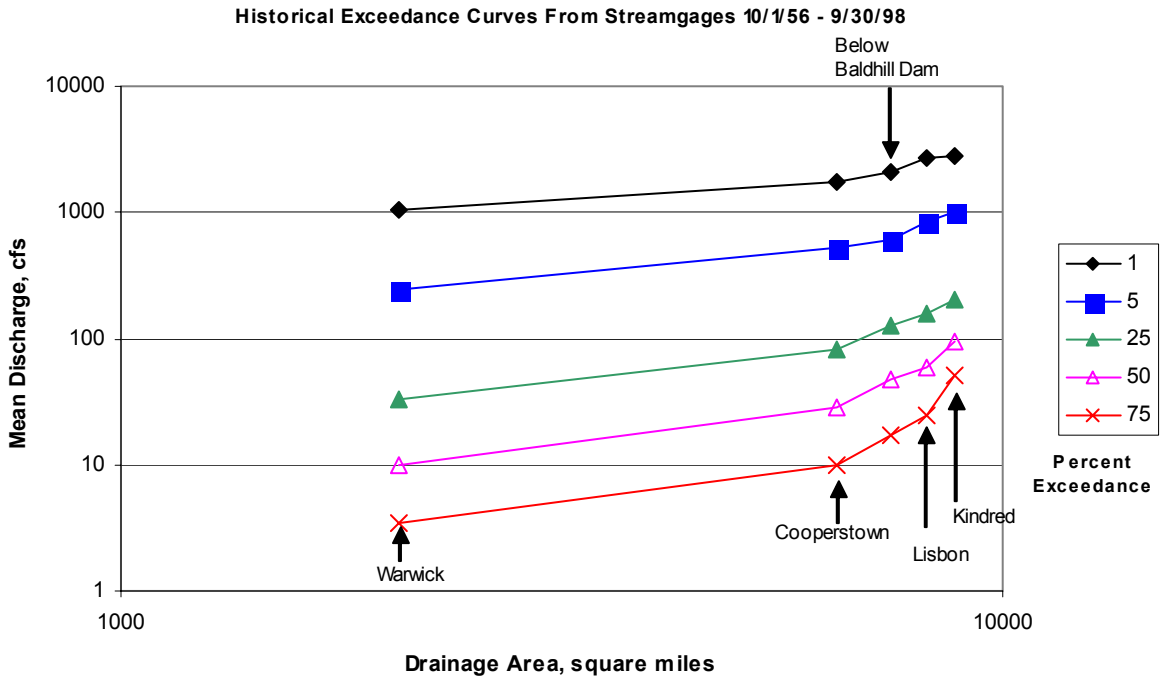

Figure 4-1. Exceedance curves from historical gage records. Each curve represents a constant percent of days that the mean daily discharge is exceeded.

These adjusted drainage areas were used to generate the historical exceedance curves. The exceedance lines using adjusted drainage areas are shown in Figure 4-2.

For each point between Warwick and Kindred, the flow-duration curve was developed by reading the mean discharge for each percent exceedance level at the drainage area of the point. In Figure 4-2, for example, the vertical line represents a point upstream of the Lisbon gage. The flow duration curve for this point would be developed by reading the mean discharge for each percent exceedance line. Figures 4-1 and 4-2 are presented to illustrate the method used in the study. However, all calculations and interpolations were done numerically rather than graphically.

The reach downstream of the Kindred gage (A2), and those reaches upstream of the Warwick Gage (I4, J1, and K3), were beyond the ends of the lines graphed above. A log-log regression equation (of the form Log Q = a + b Log (Adjusted Drainage Area)) was developed for each set of exceedance points. These log-log regression equations were used to calculate the projected exceedance levels, in cfs. For example, the historical regression line for the 5% exceedance level was calculated to be:

$$\text{Log}_e(Q_{5\% \text{ exceedance}}) = -5.403211 + 1.448039 * \text{Log}_e(\text{Adjusted Drainage Area})$$

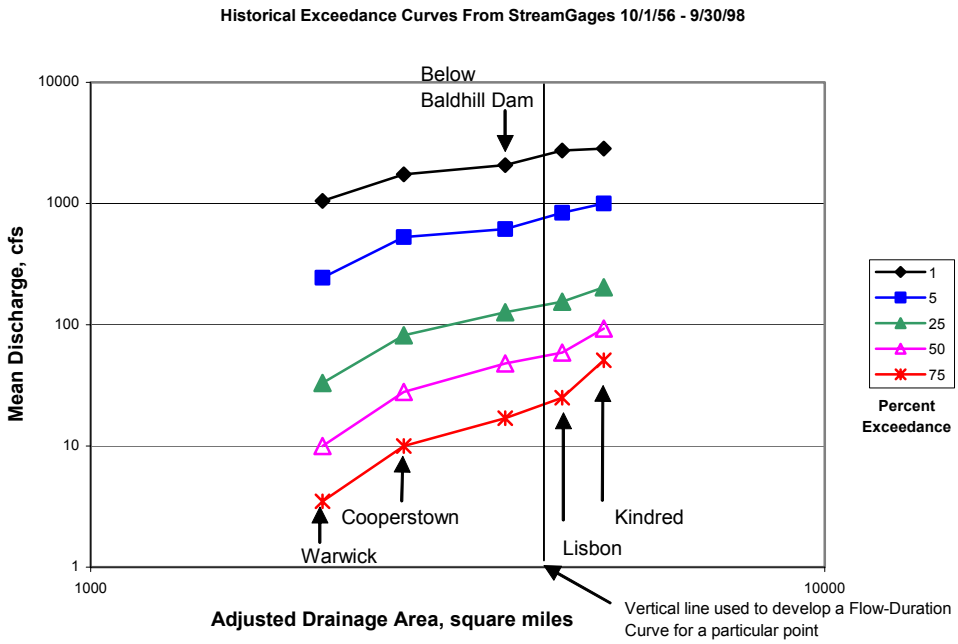

Figure 4-2. Exceedance curves from historical gage records. Adjusted drainage area is without Devils Lake Basin. Each curve represents a constant percent of days that the mean daily discharge is exceeded.

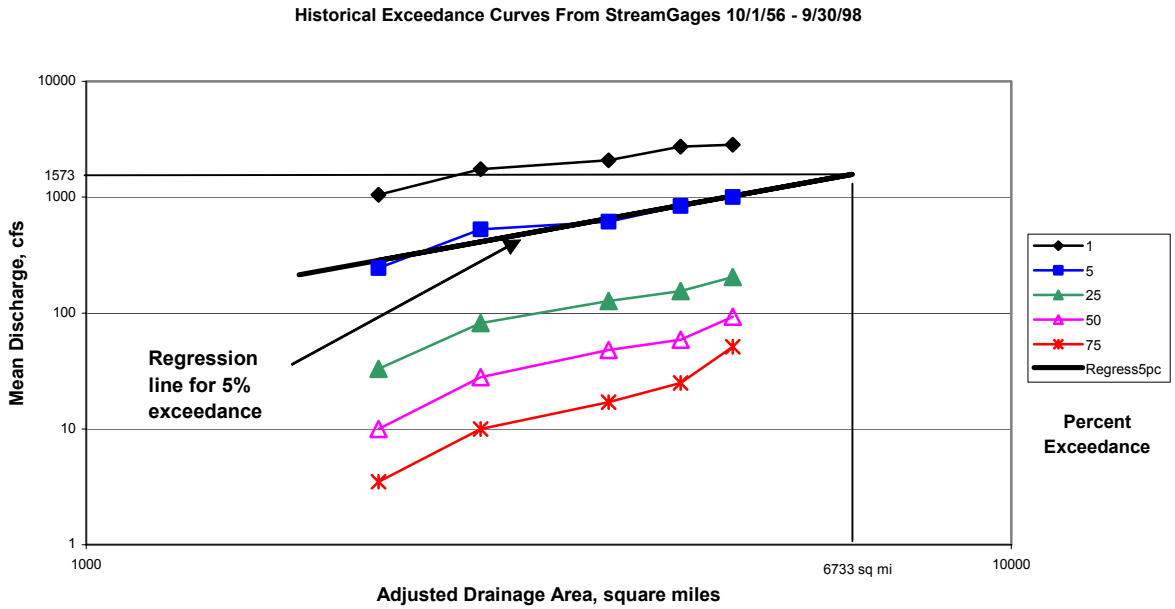

Figure 4-3. Sample regression line used to calculate historical 5% exceedance flow at A2-f cross section. For A2-f, with adjusted drainage area = 6733 square miles, the 5% exceedance flow is 1573 cfs.

For the A2-f cross section, the adjusted drainage area was 6,733 square miles. This results in $Q_{5\% \text{ exceedance}}$ = 1,573.3 cfs. This is illustrated in Figure 4-3, where the heavy black line shows the regression line for 5% exceedance.

Because of the close proximity between exceedance levels (58 different regressions were performed) a few of the extrapolated exceedance lines crossed before they reached the A2-f section. This provides unrealistic results as the higher exceedance level flows (more frequent events) should be smaller than the less frequent events. In these cases, the flows were switched so that the higher flow corresponded to the lower exceedance level. These crossing exceedance curves occurred only at the A2-f cross section, and mostly at very low exceedance levels where the regression lines were tightly spaced (0.05% spacing was used from 0 to 0.5%).

Table 4-4 summarizes the estimated and adjusted drainage areas at each of the precision cross sections. It also provides the bounding upstream and downstream gages for which flow-duration curves were developed (for the historical records), and the bounding upstream and downstream flow points for which flow-duration curves were developed (for the future simulations).

Flow-duration curves were also developed for the future flow scenarios. There were six flow points used in the future simulations (Table 4-5). Five of the flow points correspond to USGS gage locations and the USGS supplied drainage area values were adopted. For the most upstream flow point (Peterson Coulee) the drainage area was estimated with the same procedure used to estimate the precision cross section drainage areas. Using the regression equation developed from the DEM delineation, the estimated drainage area of the confluence of Peterson Coulee with the Sheyenne River was 1,619.4 square miles. As with the flow-duration curves for the historical records, the flow-duration curves for the future simulations are based on interpolation of the flow-exceedance curves. A sample of exceedance curves from a future flow trace is shown as Figure 4-4.

4.3.2 Development of Sediment Transport Relationships for Precision Cross Sections

USGS measured sediment data was available for Kindred (1976-1980) and Lisbon (1976-1980) in the form of tons of sediment transported per day. The measured sediment load was regressed against the flow in cfs, and the following curves were found:

$$\text{Kindred: } \text{Log}_{10}(Q_{\text{sediment}}) = -1.2169 + 0.8790\,(\text{Log}_{10}(Q))^{1.3671} \quad (R^2 = 0.83)$$

$$\text{Lisbon: } \text{Log}_{10}(Q_{\text{sediment}}) = -0.9103 + 0.6045\,(\text{Log}_{10}(Q))^{1.5815} \quad (R^2 = 0.91)$$

Where Q_{sediment} is in tons/day and Q is the average daily flow in cfs.

Table 4-4. Summary of Precision Cross Section Locations, and Bounding Flow Points for Historical Flows and Future Simulated Flows (Listed from Upstream to Downstream)

Section	Estimated Drainage Area, square miles	Adjusted Drainage Area, square miles	Upstream Gage (historical records)	Downstream Gage (historical records)	Upstream flow point (future simulated flows)	Downstream flow point (future simulated flows)
L1-a	1609.8	1609.8	None	5056000	N/A	N/A
K3-j	1631.3	1631.3	None	5056000	Peterson Coulee	Warwick
J1-e	1822.7	1822.7	None	5056000	Peterson Coulee	Warwick
J1-a	1822.7	1822.7	None	5056000	Peterson Coulee	Warwick
I4-a	1883.7	1883.7	None	5056000	Peterson Coulee	Warwick
H3-f	5975.3	2175.3	5056000	5057000	Warwick	Cooperstown
H2-I	5977.1	2177.1	5056000	5057000	Warwick	Cooperstown
F2-a	6457.7	2657.7	5056000	5057000	Warwick	Cooperstown
E2-j	7926.7	4126.7	5058000	5058700	Valley City	Lisbon
E2-f	7926.7	4126.7	5058000	5058700	Valley City	Lisbon
E2-a	7926.7	4126.7	5058000	5058700	Valley City	Lisbon
D3-l	8078.3	4278.3	5058000	5058700	Valley City	Lisbon
D3-k	8078.3	4278.3	5058000	5058700	Valley City	Lisbon
D3-h	8078.3	4278.3	5058000	5058700	Valley City	Lisbon
D3-f	8078.3	4278.3	5058000	5058700	Valley City	Lisbon
D3-d	8078.3	4278.3	5058000	5058700	Valley City	Lisbon
D3-a	8078.3	4278.3	5058000	5058700	Valley City	Lisbon
C2-j	8572.5	4772.5	5058700	5059000	Lisbon	Kindred
C2-d	8572.5	4772.5	5058700	5059000	Lisbon	Kindred
B3-e	8800	5000	5059000	None	Kindred	None
B3-a	8800	5000	5059000	None	Kindred	None
A2-f	10533	6733	5059000	None	Kindred	None

Table 4-5. Flow Points Used for Future Simulations

Point Name	USGS Gage Number	Drainage Area (DA), Sq. Mi.	Source of drainage area	Adjusted DA, Sq. Mi.
Peterson Coulee	None	1,619.4	DEM delineation	1,619.4
Warwick	05056000	2,070	USGS gage description	2,070
Cooperstown	05057000	6,470	USGS gage description	2,670
Valley City	05058500	7,470	USGS gage description	3,670
Lisbon	05058700	8,190	USGS gage description	4,390
Kindred	05059000	8,800	USGS gage description	5,000

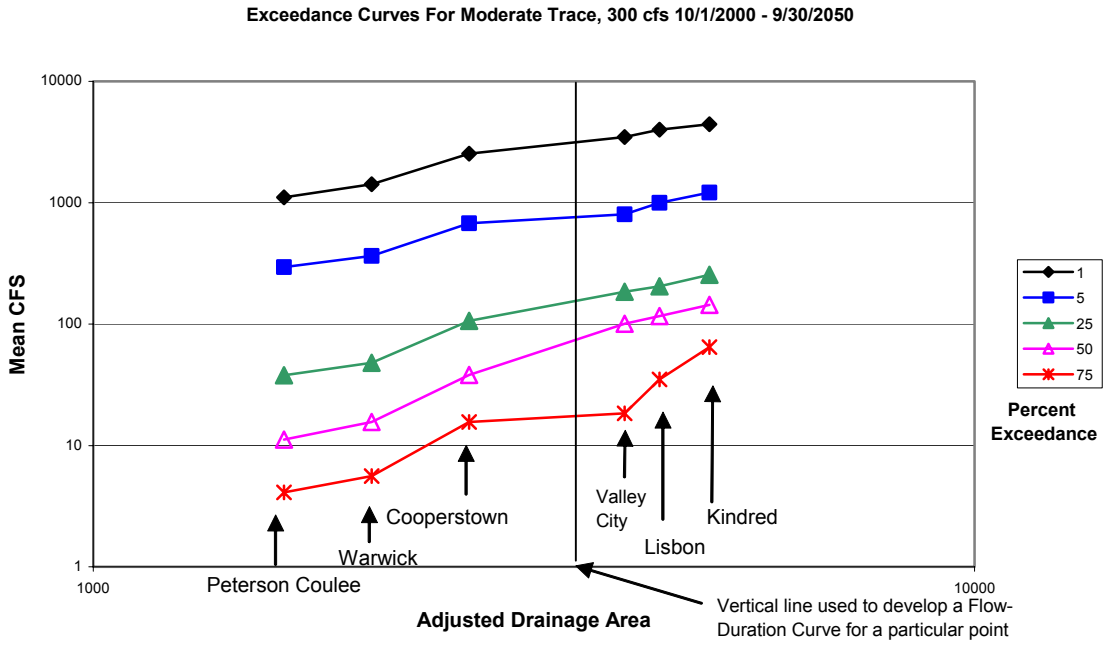

Figure 4-4. Sample exceedance curves from a future flow trace. Trace is Moderate, 300 cfs.

Using these curves, measured data was compared with computed sediment transport values obtained from the single cross section models.

For the Kindred gage, the measured fines (passing through the 0.062 sieve) averaged 17%, and ranged from 4% to 25% in 11 sediment samples taken by the USGS during the gaged period. For the Lisbon gage, the measured fines averaged 5%, and ranged from 1% to 14% in 4 sediment samples taken by the USGS during the gaged period. Because these fines are assumed to be wash load, predictive sediment transport models/methods will not take them into account. Therefore, the wash load should theoretically be deducted from the measured sediment transport before comparing it to the predicted results from a sediment transport model which uses a bed material transport equation (bed load plus suspended load). However, an estimate of bedload transport would need to be added to the measured sediment transport before comparing it to a sediment transport results as only suspended material is measured. Because these two effects tend to cancel each other out, and are expected to be of the same order of magnitude, no adjustments were made for this analysis.

The precision cross sections nearest to the gages where sediment samples were collected were used to compare computed and measured sediment amounts. The geometry of the precision sections (B2-a and B2-e, roughly 4-5 miles downstream of Kindred, and the six D3 sections roughly 40 miles upstream of Lisbon) and the grain size distributions (provided by the District for each cross section) were entered into SAM (USACE, 1998b). Energy slopes from the HEC-RAS single cross section models were also input data. Twenty-seven flows ranging from 100 cfs to about 17,000 cfs were input into SAM. The hydraulic module of SAM then generated, for each of the flows, the water surface elevation and other parameters needed for input into the SAM sediment transport module.

Within the SAM sediment transport module, all 20 sediment transport methods available were selected, so that SAM would generate sediment rating relationships, in tons per day for each level of flow, for each of the cross sections (Table 4-6).

The sediment rating curves developed by each of the 20 methods were compared to the measured sediment transport data. The SAM predicted sediment transport at sections B2-a and B2-e was compared to the Kindred sediment transport regression curve generated from the sediment gage. The sediment transport predicted by SAM at sections D3-a, d, f, h, k, and l were compared to the Lisbon sediment transport regression curve generated from the sediment gage.

The method found to best match computed to observed sediment transport was the Brownlie D_{50} method. In the case of the B3-a and B3-e cross sections, the magnitude of the sediment curve from the Brownlie D_{50} method matched the Kindred observed data well (Figure 4-5). In the case of the D3 sections, there was a wide variety of energy slopes, and thus a wide range of sediment transport rates. The Brownlie D_{50} curve generated by SAM provided the best match with the observed results (in the form of the regression curves), especially in the shape of the curve (Figure 4-6).

Table 4-6. The Twenty Sediment Transport Methods Available in SAM

Ackers- White, D50
Ackers-White (HEC-6)
Brownlie, D50
Colby (HEC-6)
Einstein bed load
Einstein total load
Engelund Hansen
Laursen (Copeland)
Laursen (Madden), 85
MPM(1948) (HEC-6)
MPM(1948), D50
Parker
Profitt Sutherland
Schoklitsch
Toffaleti- MPM
Toffaleti
Toffaleti-Schoklitsch
Van Rijn
Yang,D50
Yang (HEC-6)

It should be noted that at high flows, the computed water surface from the SAM modeled cross sections was sometimes higher than the limits of the surveyed cross sections. When this happens, SAM extends the end(s) of the cross section as vertical walls. This may cause the water surface to be higher, and/or the velocity to be greater, than would actually be the case if the modeled cross section extended out farther to the left and/or right. This effect causes sediment transport to be over-predicted at the higher flows. Therefore the SAM curves might be steeper than they should be. However, as can be seen from Figure 4-5 and Figure 4-6, the measured sediment curves are actually steeper than the SAM results.

The Yang (HEC-6) method also yielded reasonably good results. Therefore, sediment rating curves were developed in SAM for all the precision cross sections using both the Brownlie D_{50} and the Yang methods.

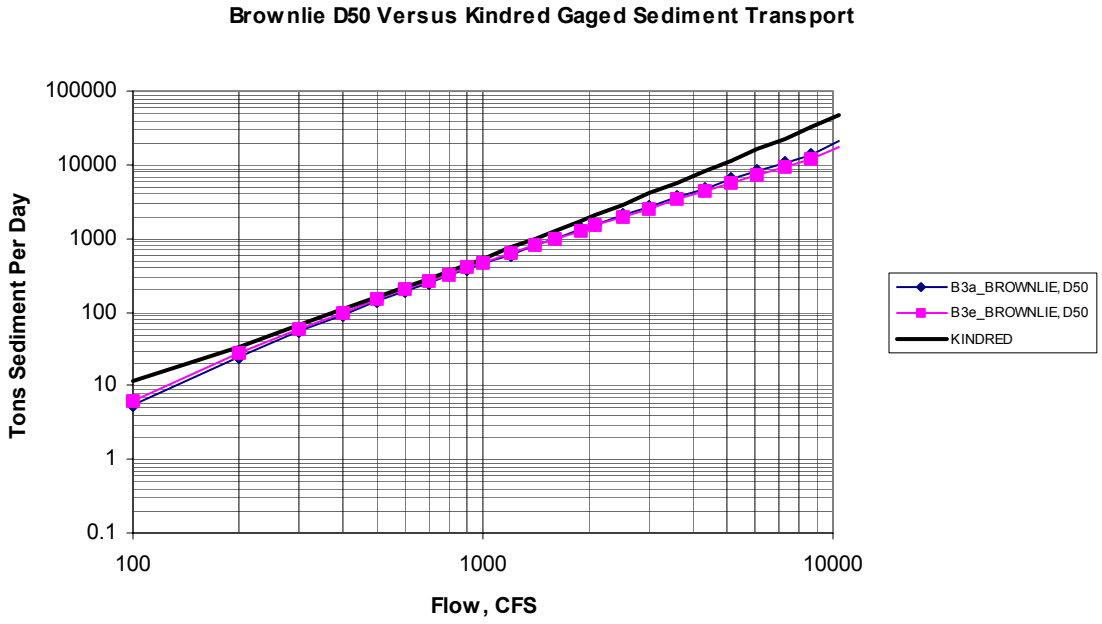

Figure 4-5. Brownlie D_{50} method results versus regression line for Kindred measured sediment transport

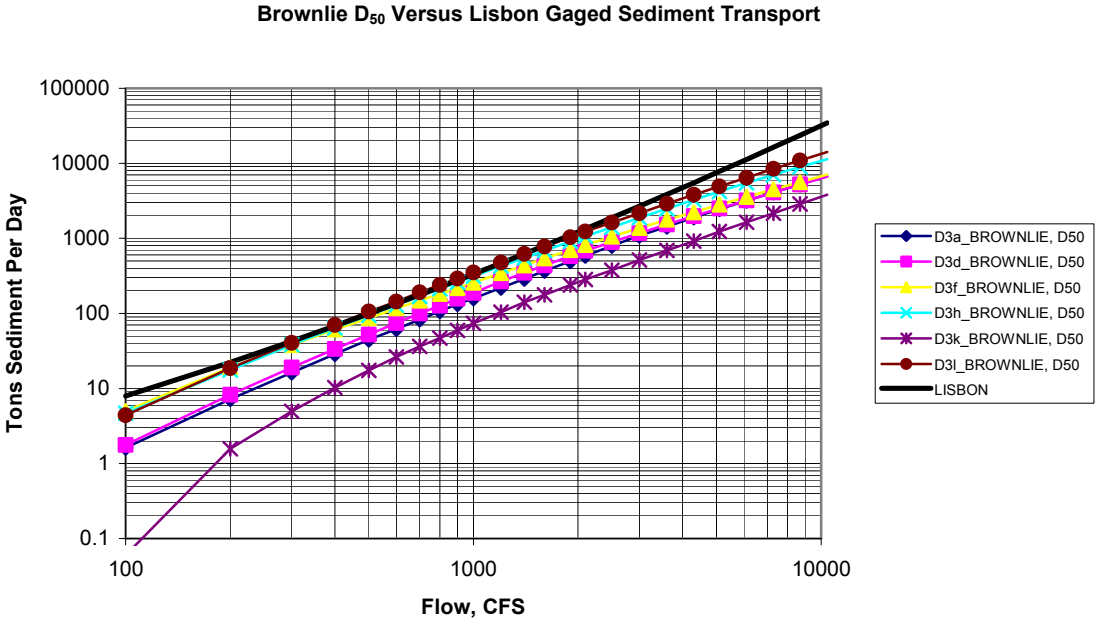

Figure 4-6. Brownlie D_{50} method versus regression line for Lisbon measured sediment transport

4.3.3 Estimate of Effective Discharge by Maximum Sediment Transport

The guidelines in "Effective Discharge Calculation: A Practical Guide" (Biedenharn et al., 2000) were used to estimate effective discharge at each of the precision cross sections. This method involves generating a sediment-transport histogram, where the sediment transported at various flows is plotted. The flow that appears to have the peak sediment transport is identified as the effective discharge. The flow-duration curves developed for each precision cross section were divided in 100 cfs intervals. The first interval was 50-150 cfs, for which 100 cfs is the center of the interval. The next interval was 150-250 cfs, for which 250 is the center of the interval. Flows below 50 cfs were not considered for the chart. Each of these intervals had a specific duration, in percent. This is the expected number of days as a percentage of all days that the average daily flow will be in each range. The interval duration is simply the exceedance percentage at the low end of the flow interval minus the exceedance percentage at the high end of the flow interval. Since the flow duration curve is made up of line segments, the exceedance percentage for each flow amount was interpolated. This interval duration for each of the 100 cfs intervals was then multiplied by the Brownlie D_{50} sediment transport at the center of the interval, as predicted by SAM. This yielded a sediment transport histogram.

A sample histogram, for the historical flows at section C2-d, is shown in Figure 4-7. All histograms are presented in Appendix B.

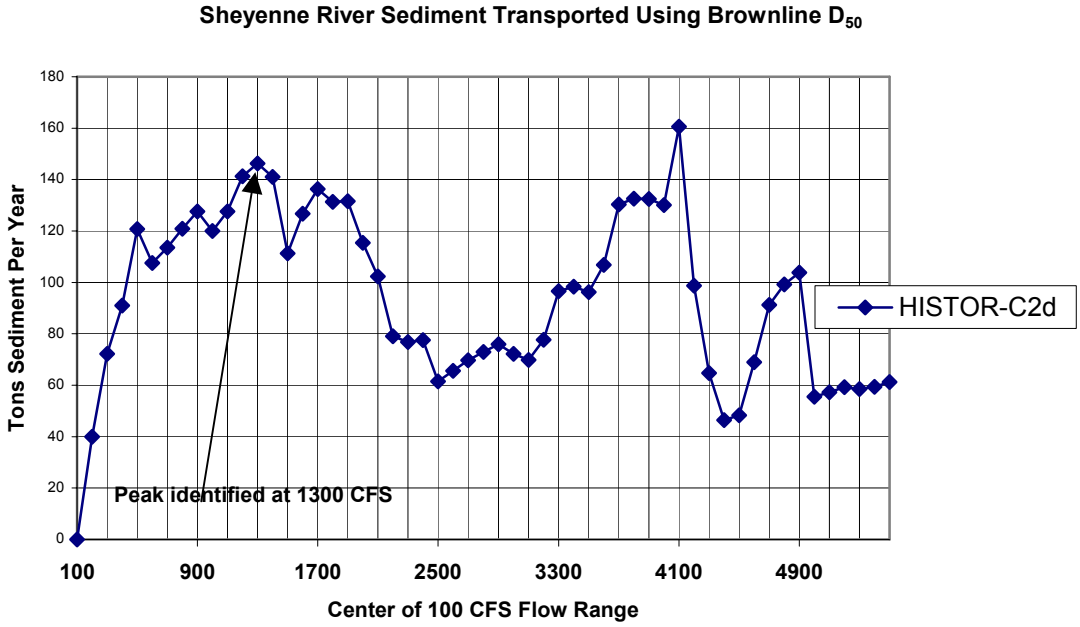

Figure 4-7. Sample sediment transport histogram

For the sample histogram, the apparent peak is at 1300 cfs. There is an additional peak at about 4100 cfs, but this secondary peak is well beyond the expected range in which the bankfull discharge should occur.

4.4 Frequency Analysis

Another method for estimation of bankfull discharge is through the use of annual maximum flood series. The annual maximum flood is the highest peak flow recorded during a water year. Many investigators have found that the 1.5-year flood (the annual flood that occurs on average in 1 / 1.5 = 66.7% of the years) is a good approximation of bankfull discharge (e.g., Dunne and Leopold, 1978, p. 621).

An analysis of flood recurrence intervals was therefore conducted using both the historical and future simulated flows to provide estimates of bankfull discharge. Because the flow locations available for the historical flow series (USGS stream gages) and the locations provided by the District for the future flows did not coincide with the locations of the precision cross sections, a series of calculations had to be conducted in order to interpolate the flood recurrence intervals at the precision cross section locations.

4.4.1 Determination of Flood Recurrence Interval Flows

Flood recurrence interval flows were determined for the stream gage sites and for the points at which simulated future flows were provided. An interpolation procedure was used to develop both historical and future flood recurrence interval flows for the 1.5-year flood and for the 2-year flood at the precision cross section locations. The following sections outline the procedures used.

4.4.1.1 Historical Flood Recurrence Interval Flows at Stream Gages

The historical annual flood exceedance frequencies were calculated for numerous gages along the Sheyenne River, using HEC-FFA (USACE, 1992). Table 4-7 summarizes the gages that were used, and the 1.5-year and 2-year flood frequency results. Graphical results are shown in Appendix C.

A regional skew coefficient of –0.2 was used in HEC-FFA. This value was based on a chart included in the report "Guidelines for Determining Flood Flow Frequency" (USGS, March 1982). Water years from 1950 through 1999 were used for the gages downstream of Baldhill Dam (Valley City, Lisbon, Kindred, and Fargo).

4.4.1.2 Flood Recurrence Intervals for Simulated Future Flows

The flow series (traces) supplied by the District were in the form of mean daily flows, not the instantaneous peak flows that need to be used as input to HEC-FFA. Therefore, the flood frequency analysis for the simulated future flows could not be calculated directly from the data supplied by the District.

The procedure followed was to (1) use HEC-FFA to perform a flood frequency analysis using the maximum mean daily flow from each year, and (2) estimate flood recurrence interval flows based on instantaneous annual peak flows from the first step.

Table 4-7. Estimated Historical Flood Frequencies at Stream Gages

Gage Number	Description	Years of record used to calculate flood frequencies	1.5 Year Flood, CFS	2 Year Flood, CFS
05056000	Sheyenne River near Warwick	1950-1999	520	890
05057000	Sheyenne River near Cooperstown	1945-1999	760	1240
05058500	Sheyenne River at Valley City	1950-1975, 1980-1999	880	1360
05058700	Sheyenne River at Lisbon	1957-1999	980	1490
05059000	Sheyenne River near Kindred	1950-1999	920	1370
05059500	Sheyenne River at West Fargo	1950-1994, 1996-1999	910	1350

To complete the second part of the procedure, a relationship needed to be developed between the peak floods that result from using the maximum annual mean daily flows and the peak floods that result from using peak annual instantaneous flows. To establish this relationship, HEC-FFA was used to analyze both mean daily and peak flows for four historical gage records. For each comparison, the period of record for the data used was the same in order to establish a consistent relationship. Although peak flows at all gages analyzed were available through water year 1999, the mean daily flows were available only through water year 1998. Therefore, only the peak flows through water year 1998 were used for this comparative FFA analysis. As a result, the flood frequencies based on this shortened period of record are slightly different than the flood frequencies given in Table 4-7. The 1.25-year, 1.5-year, 2-year, and 2.5-year floods were compared. The results are summarized in Table 4-8 and Table 4-9.

A regression between the two data sets yielded the following equation:

Flood recurrence from peak flows =

25.206 cfs + 1.0341 * (Flood recurrence from mean daily flows)

For example, to predict the 2-year flood for Cooperstown, start with the peak flood based on the daily means, or 1,150 cfs.

Table 4-8. Flood Recurrence Flows Based on Maximum Annual Mean Daily Flows

		Annual exceedance in percent / Flood recurrence in years			
Gage	Water Years	80% / 1.25-year flood, cfs	67% / 1.5-year flood, cfs	50% / 2-year flood, cfs	40% / 2.5-year flood, cfs
Warwick (05056000)	1950-98	270	460	800	1080
Cooperstown (05057000)	1945-1998	435	700	1150	1500
Lisbon (05058700)	1957-1998	580	890	1380	1750
Kindred (05059000)	1950-1998	590	870	1310	1650

Table 4-9. Flood Recurrence Flows Based on Peak Annual Instantaneous Flows

		Annual exceedance in percent / Flood recurrence in years			
Gage	Water Years	80% / 1.25-year flood, cfs	67% / 1.5-year flood, cfs	50% / 2-year flood, cfs	40% / 2.5-year flood, cfs
Warwick (05056000)	1950-98	300	500	860	1170
Cooperstown (05057000)	1945-1998	465	750	1200	1590
Lisbon (05058700)	1957-1998	650	970	1470	1860
Kindred (05059000)	1950-1998	620	900	1350	1690

Then the predicted peak flow exceedance is

= 25.206 cfs + 1.0341 * 1,150 cfs

= 1,241 cfs.

The actual value from the HEC-FFA results based on instantaneous peak flows is 1,200 cfs. Overall, the predicted flows using the above regression equation were within -4% to +3% of the actual values.

Table 4-10 through Table 4-12 summarize the frequency flows for the historical and simulated future records.

Table 4-10. 1.5-year and 2-year Flows for Historical Flow Series (Gages are Listed from Upstream to Downstream)

Gage	Water Years in Record	1.5-Year Flow, CFS	2-Year Flow, CFS
Warwick (05056000)	1950-1999	520	890
Cooperstown (05057000)	1945-1999	760	1240
Below Baldhill Dam (05058000)	1950-1999	670	1170
Valley City (05058500)	1950-1975, 1980-1999	880	1360
Lisbon (05058700)	1957-1999	980	1490
Kindred (05059000)	1950-1999	920	1370
West Fargo (05059500)	1950-1994, 1996-1999	910	1350

Table 4-11. 1.5-year Flows for Simulated Future Flow Series (Listed from Upstream to Downstream)

	Future Flow Trace					
Flow Point	Moderate, 300 CFS	Moderate, 480 CFS	Moderate, No Pump	Wet, 300 CFS	Wet, 480 CFS	Wet, No Pump
Peterson Coulee	346	356	346	935	852	946
Warwick	408	413	397	925	977	966
Cooperstown	625	635	615	1421	1452	1421
Valley City	790	801	790	1421	1452	1421
Lisbon	842	852	842	1494	1525	1494
Kindred	925	946	915	1597	1680	1576

Table 4-12. 2-year Flows for Simulated Future Flow Series (Listed from Upstream to Downstream)

	Future Flow Trace					
Flow Point	**Moderate, 300 CFS**	**Moderate, 480 CFS**	**Moderate, No Pump**	**Wet, 300 CFS**	**Wet, 480 CFS**	**Wet, No Pump**
Peterson Coulee	625	635	615	1214	1276	1256
Warwick	728	749	708	1401	1473	1473
Cooperstown	1080	1111	1059	2145	2176	2145
Valley City	1245	1245	1245	2093	2114	2093
Lisbon	1318	1349	1318	2300	2300	2300
Kindred	1463	1473	1452	2424	2507	2424

4.4.1.3 Interpolation of Flood Events at Precision Cross Sections

To find the flood events for each precision cross section, for both the historical and simulated future flows, interpolations were performed. It was assumed that the following equation holds true between two gage points (for the historical flows) or two flow points (for the future simulated flows provided by the District):

$$\text{Log}\,(Q_{\text{N-year flood event}}) = A_N + B_N * \text{Log}\,(\text{Drainage Area})$$

where the constants A_N and B_N are chosen such that the equation holds for the two bounding gages or flow points. The value of $Q_{\text{N-year flood event}}$ (for example, $Q_{1.5\text{ year flood}}$) for each gage or flow point was determined through a flood-frequency analysis. This follows a similar methodology outlined in Chapter 10 of Dunne and Leopold (1978), where the same log-log relationship is used to relate annual flood to drainage area.

Except for the A2-f precision cross section, all frequency flows were interpolated for the future scenarios. Figure 4-8 is an example showing the lines used in the interpolation. This figure also illustrates how the flood-frequency for the A2-f section was extrapolated.

For the historical flow scenarios, the A2-f frequency flows also needed to be extrapolated. However, instead of using a sloped line, the A2-f frequency flows were assumed identical to those at the Kindred gage. This was done because for historical flows, the frequency flows did not increase for gages downstream of Kindred. The frequency flows at the I4, J1, and K3 sections were extrapolated from a line going through the flows at the Warwick and Cooperstown gages, as illustrated in Figure 4-9.

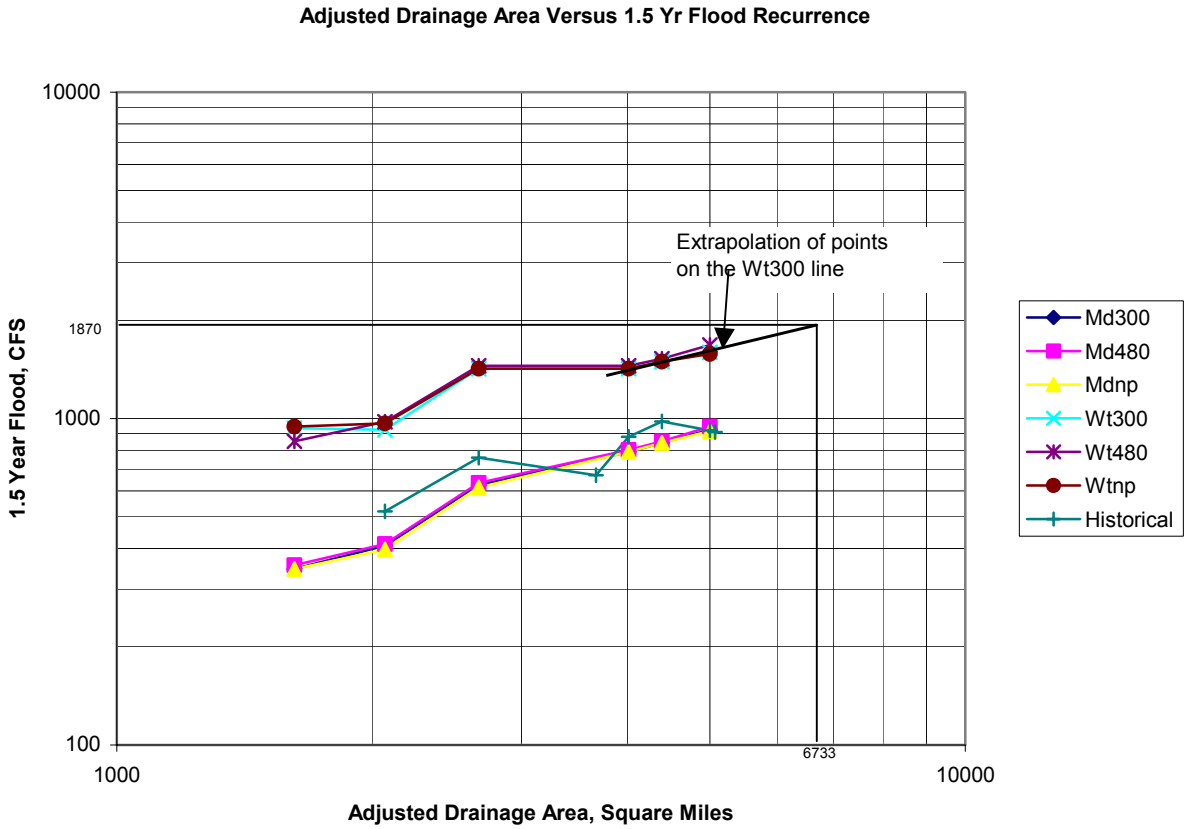

Figure 4-8. Extrapolation showing flow of 1870 cfs for the 1.5-year flood at precision cross section A2-f.

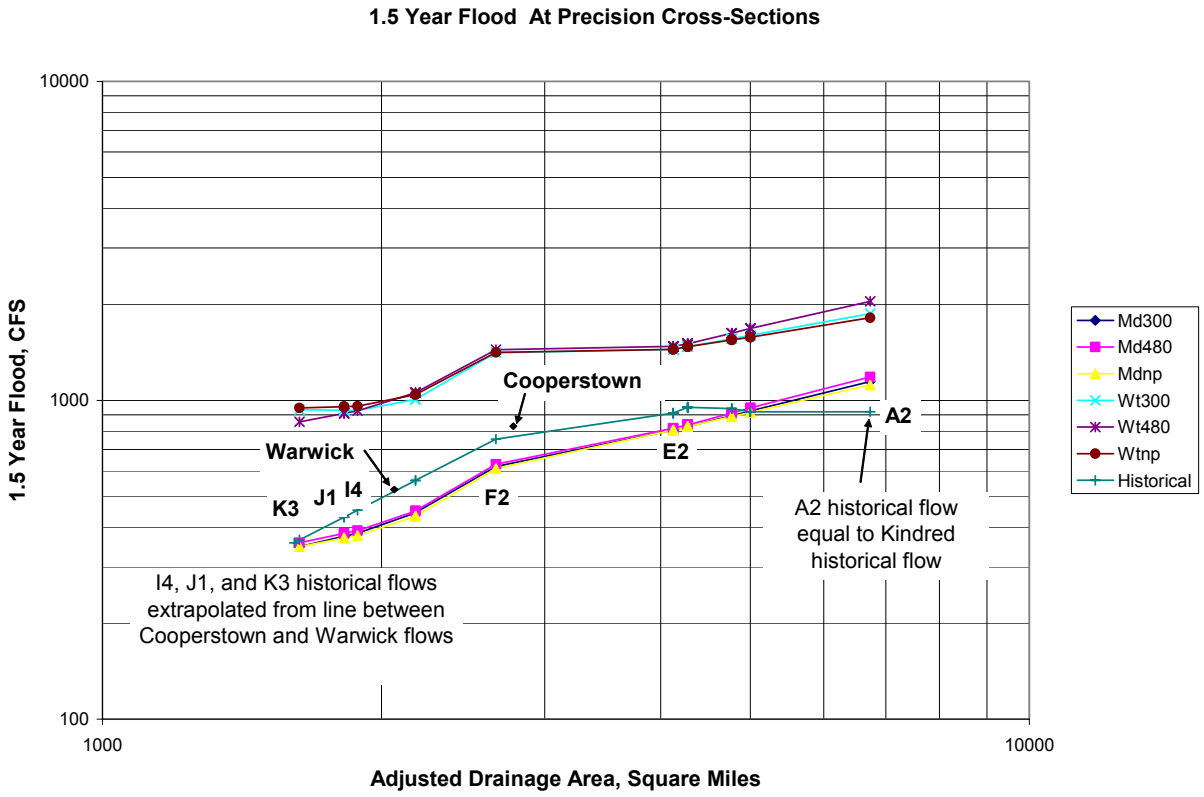

Figure 4-9. Illustration of how I4, J1, K3, and A2 historical flood frequencies were estimated.

4.5 Adopted Values

Results for channel forming (alternatively called effective or bankfull) discharge from the three different methods described in this chapter were compared. Based on a weighting of the results and professional judgment, an adopted channel forming discharge was selected for historical and each of the six future conditions. A summary of these results is presented in Table 4-13.

Table 4-13. Summary of Computed and Adopted Channel Forming Discharges (cfs)

Reach	Section	Trace	Field Estimated Bankfull	1.5-Year Flood	2-Year Flood	Peak of Sediment Histogram	Grading of Sediment Histogram Peak	Adopted Bankfull
A2	f	HISTOR	1600	920	1370	700	G	1400
A2	f	Mdnp	0	1116	1785	400	F	1460
A2	f	Md300	0	1144	1817	400	F	1500
A2	f	Md480	0	1183	1850	900	F	1530
A2	f	Wtnp	0	1814	2966	500	F	1900
A2	f	Wt300	0	1870	2966	600	G	2000
A2	f	Wt480	0	2043	3160	800	G	2100

Reach	Section	Trace	Field Estimated Bankfull	1.5-Year Flood	2-Year Flood	Peak of Sediment Histogram	Grading of Sediment Histogram Peak	Adopted Bankfull
B3	a	HISTOR	1400	920	1370	500	P	1200
B3	a	Mdnp	0	915	1452	200	P	1200
B3	a	Md300	0	925	1463	200	P	1200
B3	a	Md480	0	946	1473	700	G	1220
B3	a	Wtnp	0	1576	2424	700	F	1880
B3	a	Wt300	0	1597	2424	600	G	1900
B3	a	Wt480	0	1680	2507	700	G	1980
B3	e	HISTOR	1200	920	1370	500	F	1200
B3	e	Mdnp	0	915	1452	200	P	1200
B3	e	Md300	0	925	1463	200	P	1210
B3	e	Md480	0	946	1473	700	F	1230
B3	e	Wtnp	0	1576	2424	700	F	1880
B3	e	Wt300	0	1597	2424	600	G	1900
B3	e	Wt480	0	1680	2507	700	G	1980
C2	d	HISTOR	900	941	1412	1300	G	1100
C2	d	Mdnp	0	888	1403	1300	P	1050
C2	d	Md300	0	894	1409	1500	P	1050
C2	d	Md480	0	911	1427	700	G	1070
C2	d	Wtnp	0	1546	2379	1100	F	1680
C2	d	Wt300	0	1559	2379	600	F	1700
C2	d	Wt480	0	1623	2431	700	G	1750
C2	j	HISTOR	1300	941	1412	1300	P	1100
C2	j	Mdnp	0	888	1403	200	P	1050
C2	j	Md300	0	894	1409	1500	P	1050
C2	j	Md480	0	911	1427	700	P	1070
C2	j	Wtnp	0	1546	2379	700	P	1680
C2	j	Wt300	0	1559	2379	500	F	1700
C2	j	Wt480	0	1623	2431	700	GF	1750
D3	a	HISTOR	1000	950	1452	1300	F	1100
D3	a	Mdnp	0	827	1297	1100	P	1000
D3	a	Md300	0	827	1297	1300	P	1000
D3	a	Md480	0	837	1319	600	F	1010
D3	a	Wtnp	0	1473	2239	600	F	1700
D3	a	Wt300	0	1473	2239	500	F	1700
D3	a	Wt480	0	1504	2245	700	G	1720
D3	d	HISTOR	900	950	1452	1300	F	1100
D3	d	Mdnp	0	827	1297	200	P	1000
D3	d	Md300	0	827	1297	200	P	1000
D3	d	Md480	0	837	1319	600	F	1020
D3	d	Wtnp	0	1473	2239	600	F	1600
D3	d	Wt300	0	1473	2239	500	F	1600
D3	d	Wt480	0	1504	2245	700	F	1620
D3	f	HISTOR	900	950	1452	1300	P	1100
D3	f	Mdnp	0	827	1297	200	P	1000

Reach	Section	Trace	Field Estimated Bankfull	1.5-Year Flood	2-Year Flood	Peak of Sediment Histogram	Grading of Sediment Histogram Peak	Adopted Bankfull
D3	f	Md300	0	827	1297	900	P	1000
D3	f	Md480	0	837	1319	600	F	1020
D3	f	Wtnp	0	1473	2239	600	P	1600
D3	f	Wt300	0	1473	2239	500	F	1600
D3	f	Wt480	0	1504	2245	700	G	1620
D3	h	HISTOR	900	950	1452	1300	P	1100
D3	h	Mdnp	0	827	1297	200	P	1000
D3	h	Md300	0	827	1297	200	P	1000
D3	h	Md480	0	837	1319	600	F	1020
D3	h	Wtnp	0	1473	2239	600	P	1600
D3	h	Wt300	0	1473	2239	600	F	1600
D3	h	Wt480	0	1504	2245	700	F	1620
D3	k	HISTOR	1000	950	1452	1300	G	1100
D3	k	Mdnp	0	827	1297	1600	P	1000
D3	k	Md300	0	827	1297	1300	P	1000
D3	k	Md480	0	837	1319	600	G	1020
D3	k	Wtnp	0	1473	2239	900	F	1600
D3	k	Wt300	0	1473	2239	500	F	1600
D3	k	Wt480	0	1504	2245	700	G	1620
D3	l	HISTOR	1200	950	1452	1300	G	1100
D3	l	Mdnp	0	827	1297	1500	P	1000
D3	l	Md300	0	827	1297	1300	P	1000
D3	l	Md480	0	837	1319	600	F	1020
D3	l	Wtnp	0	1473	2239	600	F	1700
D3	l	Wt300	0	1473	2239	500	F	1700
D3	l	Wt480	0	1504	2245	700	G	1720
E2	a	HISTOR	1300	911	1400	1200	F	1200
E2	a	Mdnp	0	806	1268	0	P	1100
E2	a	Md300	0	806	1268	1100	P	1100
E2	a	Md480	0	817	1277	600	F	1110
E2	a	Wtnp	0	1444	2156	600	P	1680
E2	a	Wt300	0	1444	2156	500	F	1700
E2	a	Wt480	0	1475	2171	700	F	1725
E2	f	HISTOR	1200	911	1400	1200	G	1200
E2	f	Mdnp	0	806	1268	0	P	1100
E2	f	Md300	0	806	1268	0	P	1100
E2	f	Md480	0	817	1277	600	F	1110
E2	f	Wtnp	0	1444	2156	800	F	1680
E2	f	Wt300	0	1444	2156	500	F	1700
E2	f	Wt480	0	1475	2171	700	G	1725
E2	j	HISTOR	1200	911	1400	1200	F	1200
E2	j	Mdnp	0	806	1268	200	P	1100
E2	j	Md300	0	806	1268	200	P	1100
E2	j	Md480	0	817	1277	600	F	1110

Reach	Section	Trace	Field Estimated Bankfull	1.5-Year Flood	2-Year Flood	Peak of Sediment Histogram	Grading of Sediment Histogram Peak	Adopted Bankfull
E2	j	Wtnp	0	1444	2156	600	F	1680
E2	j	Wt300	0	1444	2156	500	F	1700
E2	j	Wt480	0	1475	2171	700	F	1725
F2	a	HISTOR	1200	755	1233	1600	F	900
F2	a	Mdnp	0	610	1051	1400	F	770
F2	a	Md300	0	620	1072	800	F	780
F2	a	Md480	0	630	1103	500	F	800
F2	a	Wtnp	0	1411	2130	600	P	1600
F2	a	Wt300	0	1410	2128	400	G	1600
F2	a	Wt480	0	1442	2161	500	G	1630
H2	i	HISTOR	900	561	950	1500	F	700
H2	i	Mdnp	0	433	767	1800	F	550
H2	i	Md300	0	444	787	1800	F	570
H2	i	Md480	0	450	810	1800	F	580
H2	i	Wtnp	0	1043	1587	1700	FG	1150
H2	i	Wt300	0	1007	1524	1600	P	1150
H2	i	Wt480	0	1057	1591	1500	P	1200
H3	f	HISTOR	600	560	949	1500	G	600
H3	f	Mdnp	0	432	766	1000	F	480
H3	f	Md300	0	443	786	700	GF	500
H3	f	Md480	0	449	809	500	FG	510
H3	f	Wtnp	0	1041	1585	600	G	1100
H3	f	Wt300	0	1006	1522	400	F	1100
H3	f	Wt480	0	1055	1589	500	F	1150
I4	a	HISTOR	500	452	787	900	F	500
I4	a	Mdnp	0	377	671	1400	P	420
I4	a	Md300	0	383	687	600	F	430
I4	a	Md480	0	390	703	500	F	440
I4	a	Wtnp	0	958	1386	600	G	1000
I4	a	Wt300	0	929	1326	300	G	1000
I4	a	Wt480	0	927	1394	500	G	1020
J1	a	HISTOR	1000	430	754	900	F	500
J1	a	Mdnp	0	370	658	1400	F	440
J1	a	Md300	0	375	673	700	F	450
J1	a	Md480	0	382	688	500	FG	460
J1	a	Wtnp	0	956	1356	600	G	1000
J1	a	Wt300	0	930	1301	300	F	1000
J1	a	Wt480	0	910	1367	500	FG	1010
J1	e	HISTOR	1000	430	754	900	F	500
J1	e	Mdnp	0	370	658	1400	FG	440
J1	e	Md300	0	375	673	700	PF	450
J1	e	Md480	0	382	688	500	FG	460
J1	e	Wtnp	0	956	1356	600	G	1050
J1	e	Wt300	0	930	1301	400	FG	1050

Reach	Section	Trace	Field Estimated Bankfull	1.5-Year Flood	2-Year Flood	Peak of Sediment Histogram	Grading of Sediment Histogram Peak	Adopted Bankfull
J1	e	Wt480	0	910	1367	500	FG	1060
K3	j	HISTOR	800	365	653	1200	P	400
K3	j	Mdnp	0	347	618	1200	P	380
K3	j	Md300	0	348	628	600	P	380
K3	j	Md480	0	358	638	500	G	390
K3	j	Wtnp	0	947	1262	700	G	985
K3	j	Wt300	0	935	1219	600	F	985
K3	j	Wt480	0	855	1281	500	G	990
L1	a	HISTOR	600	357	641	1200	F	400

4.5.1 Check of Effective Discharge Using Duration Exceeded Versus Drainage Area Relationship

Biedenharn et al. (2000) provide an approximate relationship between flow duration of effective discharge and drainage area. A scatter plot in the document shows that the percent duration equaled or exceeded for the effective discharge tends to increase with drainage area. For example, for a drainage area of 1,000 square kilometers (386 square miles), the daily flows exceed the effective discharge from about 0.7% to 2% of the time. For a larger drainage area of 20,000 square kilometers (7,722 square miles), the daily flows exceed the effective discharge about 2%-5% of the time.

For each of the precision cross sections, the drainage area was compared against the Biedenharn scatter plot. The range of exceedance percentages appropriate to each drainage area was compared to the exceedance percentage of the adopted historical bankfull discharge. As shown in Table 4-14, the exceedance percentages of the adopted bankfull discharges generally increased with drainage area. The adopted bankfull exceedance percentages were also found to be within the ranges shown on the Biedenharn scatter plot, lending credibility to the bankfull values chosen.

4.6 Discharge-Duration and Elevation-Duration Curves

Discharge-frequency relationships as described previously provide information about changes between flow traces, but do not describe the distribution of flow rates over a typical year. The discharge-duration curve shows what percent of the time a given flow is equaled or exceeded under a certain hydrologic regime. Discharge-duration curves have also been used as tool by some to check bankfull discharge estimates (Biedenharn et al., 2000). Given an elevation versus discharge relationship for a cross section, an elevation-duration curve may be constructed from a discharge-duration curve. This curve shows the percent of time that the water level is at or above any given elevation in the cross section for a given flow scenario. This type of curve can be useful for estimating the effect of water levels on plant communities.

Table 4-14. Comparison of Adjusted Drainage Area versus Exceedance Percentages for Adopted Historical Bankfull Flows

Reach & section	Adjusted drainage area, square miles	Adopted bankfull discharge, CFS	Percent of days bankfull flow was exceeded or equaled
A2-f	6,733	1,400	5.7%
B3-a	5,000	1,200	4.0%
B3-e	5,000	1,200	4.0%
C2-d	4,773	1,100	4.2%
C2-j	4,773	1,100	4.2%
D3-a	4,278	1,100	3.6%
D3-d	4,278	1,100	3.6%
D3-f	4,278	1,100	3.6%
D3-h	4,278	1,100	3.6%
D3-k	4,278	1,100	3.6%
D3-l	4,278	1,100	3.6%
E2-a	4,127	1,200	3.0%
E2-f	4,127	1,200	3.0%
E2-j	4,127	1,200	3.0%
F2-a	2,658	900	2.8%
H2-i	2,177	700	2.0%
H3-f	2,175	600	2.4%
I4-a	1,884	500	2.6%
J1-a	1,823	500	2.5%
J1-e	1,823	500	2.5%
K3-j	1,631	400	2.7%
L1-a	1,610	400	2.7%

Discharge-duration curves were constructed for each cross section for the historical and each of the future scenarios. These plots are shown in Appendix D. Based on the hydraulic rating curves developed for each cross section, elevation-duration curves were also produced for each cross section for each of the hydrologic scenarios. These plots are presented in Appendix E.

5 Regime Channel Analyses

5.1 General/Background

Regime theory was developed about a century ago by British engineers working on irrigation canals in what is now India and Pakistan. Canals that required little maintenance were said to be "in regime", meaning that they conveyed the imposed water and sediment loads in a state of dynamic equilibrium, with width, depth, and slope varying about some long-term average. These engineers developed empirical formulas linking low-maintenance canal geometry and design discharge by fitting data from relatively straight canals carrying near-constant discharge.

Fifty years later, hydraulic geometry formulas similar to regime relationships were developed by geomorphologists studying stable, natural rivers. In this way, the concept of regime theory or a regime channel has been extended to natural alluvial channels. An alluvial channel is considered to be in regime when there is no net change in its discharge capacity or morphology over a period of years. A regime channel essentially represents a stable channel in equilibrium conditions under which the channel has adjusted its slope, width, depth, and velocity to achieve stable conditions given a supply of water and sediment over a period of time.

Regime theory continues to be the subject of considerable research and is of great practical interest. It has been used extensively in river engineering to design stable channels and to assess channel stability for existing channels. The theory has been applied to river systems subject to hydrologic and hydraulic condition changes in order to predict channel response (e.g., USACE, 1994).

For this study, an extensive literature search was conducted to identify appropriate regime equations or methods for calculating the regime channel dimensions (channel width, depth, and slope). Three methods were selected for application. Each of these methods is applicable to the whole or a portion of the study reach given the particular hydrologic and hydraulic conditions and sediment characteristics of the Sheyenne River.

The regime channel analysis began with the determination of the regime channel dimensions corresponding to the historical and existing water and sediment conditions. The regime channel dimensions were compared to the channel width, depth, and slope values obtained from surveyed cross sections (1940 and 1998) to assess the historical channel response trend (towards or away from the equilibrium condition). The prediction of regime channel dimensions for the different future project scenarios was then performed.

5.2 Methods

There are numerous channel regime relations and methods available for calculating the regime channel dimensions. The various approaches generally fall into three broad categories: the regime, semi-analytical, and analytical methods. The regime method is an empirical method that relies on available data and attempts to determine appropriate

relationships from the data. The usefulness of this method depends on the quality of the data and the validity of the assumed form of the relationships. It has always been acknowledged that the various coefficients derived may not be truly constant but may vary slightly. Furthermore, the equations should only be applied in situations similar to those for which the data were collected.

The semi-analytical method either relies on a dimensional analysis or on combining some fundamental relationships, such as flow rate, resistance to flow, bank stability, particle mobility, and secondary flow, to derive a set of regime equations with physical support. The exponents and coefficients in hydraulic geometry formulas are generally determined through regression analysis using measured data. Because formula coefficients vary, applying a given set of hydraulic geometry relationships should be limited to channels similar to the calibration sites.

The analytical method relies on finding a theoretical description of the fluvial processes. Some of the analytical approaches to the design of stable channels utilize the combination of a sediment transport equation, a flow resistance equation, and an extremal hypothesis, such as minimum stream power, minimum unit stream power, or sediment transport maximization. This approach can only be successful if the dominant processes are correctly identified and appropriate equations exist to describe them adequately.

The use of channel regime relations requires the watershed and stream channel characteristics of the reach in question to be similar to the data set or consistent with the implied assumptions used to develop the channel regime relations. For the Sheyenne River, based on the sediment samples collected on channel bed point bars and on the bank, the river can be characterized as a fine sand-bed channel with cohesive bank materials (except for reach C2, where both the channel and bank are composed of sands). The suspended sediment concentration in the Sheyenne River is low and the bed load transport is negligible. This channel bed and bank condition excludes the majority of the regime relations available because they were primarily developed for non-cohesive, coarse sand-bed or gravel-bed alluvial rivers.

In this study, three different methods were selected for the determination of the channel regime dimensions for both the existing and future conditions: Simons and Albertson's method, Julien and Wargadalam's method, and Copeland's procedure.

5.2.1 Simons and Albertson's (SA) Method

To remedy the deficiencies of the Lacey and Blench regime equations, Simons and Albertson (1963) made a collection of field data from Indian and North American sources and developed a set of equations to calculate the hydraulic parameters. The SA method is based purely on field data. The exponents and coefficients in the formulas are dependent on the type of canals. This allows the calculation of the regime channel dimensions for channels with different bed and bank composition and sediment concentrations, including channels with sand beds, cohesive or non-cohesive banks, and sediment concentrations less than 500 ppm. The input requirements of the Simons and Albertson equations include the channel forming discharge, type of channel bed and bank, and the water

temperature. Appendix F includes the equations and the associated coefficients and exponents for different channel types as well as a sample calculation.

5.2.2 Julien and Wargadalam's (JW) Method

Julien and Wargadalam's method (Julien and Wargadalam, 1998) is a semi-analytical approach. The method is based on four theoretical hydraulic equations for alluvial channels, including flow continuity, flow resistance, longitudinal shear stress, and radial shear stress to account for natural channel bends. The longitudinal and radial shear stresses are combined into one term expressed as a Shield's parameter for sediment mobility. The governing equations are solved to analytically define the downstream hydraulic geometry of noncohesive alluvial channels as a function of water discharge, sediment size, and shields number. The equations are written as:

$$h = 0.133 Q^{1/(3m+2)} d_{50}^{(6m-1)/(6m+4)} \tau_\theta^{*-1/(6m+4)} \tag{5-1}$$

$$W = 0.512 Q^{(2m+1)/(3m+2)} d_{50}^{(-4m-1)/(6m+4)} \tau_\theta^{*(-2m-1)/(6m+4)} \tag{5-2}$$

$$S = 12.4 Q^{-1/(3m+2)} d_{50}^{5/(6m+4)} \tau_\theta^{*(6m+5)/(6m+4)} \tag{5-3}$$

where

Q = channel forming discharge in m^3/s,

h = average water depth in meters,

W = water surface width in meters,

S = channel slope,

d_{50} = bed material median grain size in meters,

τ_θ^* = Shields number = $hS/[(\gamma_s - \gamma)/\gamma \times d_{50}]$.

The Shields number, τ_θ^*, for the incipient motion of bed material is 0.047. This is reasonable for gravel-bed rivers. For sand-bed channels, τ_θ^* = 1.0 was suggested to account for the effects of sediment transport on the hydraulic geometry of the channel. The exponent, m, in the equations is calculated from

$$m = \frac{1}{\ln(12.2h/d_{50})} \tag{5-4}$$

From Equations (5-1) and (5-4), a trial and error solution can be obtained for h.

Julien and Wargadalam's formulas are applicable only to non-cohesive alluvial channels. The formulas were tested with a comprehensive data set covering a wide range of flow conditions from meandering to braided, sand-bed, and gravel-bed rivers. For this study,

these equations are used to determine the regime channel dimensions for the reach with sand bed and banks.

Julien and Wargadalam's formulas require the input of the median particle size, D_{50}. The sediment gradation curves supplied by the District (Appendix H) were used to compute the D_{50} for each reach. For each reach, curves from two samples appear in the sediment gradation chart. The sample that corresponded to the bed or to a point bar was used to represent the bed grain sediment. The D_{50} values were then interpolated from these sediment gradation curves. The sediment samples used to calculate the D_{50} values are summarized in Table 5-1.

Table 5-1. Sediment Samples and Median Grain Sizes (D_{50}) used for Julien and Wargadalam's Method

Precision Cross Sections	Location Description	Sample Number	D_{50}, mm
A2-f	Crossing Bar	A2-1	0.109
B3-a, e	Bed at Point Bar (Clay above Sample)	B3-1	0.093
C2-d, j	Point Bar	C2-1	0.193
D3-a, d, f, h, k, l	Bed, Downstream	D3-1	0.032*
E2-a, j	Point Bar Near Rapid Upstream of Bridge	E2-2	0.032*
F2-a	Point Bar	F2-2	0.087
H2-i	Point Bar on Bank Downstream of Downstream High Cut Bank	H2	3.657
H3-f	Sand Bar	H3-1	0.188
I4-a	Upstream, Emerging Point Bar	I4-2	0.185
J1-a,e	Bed	J1-1	0.032*
K3-j	Bed	K3-1	0.187
L1-a	Riffle Bed	L1-2	2.197

Note: * = extrapolated

For the D3, E2, and J1 sections, the D_{50} was extrapolated. This was done because the amount of fines in the sample was so great that more than 50 percent of the sample by weight was finer than smaller sieve size (all three sections were classified on the soil gradation charts as "sandy lean clay"). Because the JW method requires a median size, one had to be extrapolated. However, it should be noted that the JW method is not intended for use on cohesive materials.

5.2.3 Copeland's Procedure

The approach described by Copeland (1994) features the use of the Brownlie (1981) flow-resistance and sediment transport relations. This stable channel analytical method is included in the U.S. Army Corps of Engineers' hydraulic design package SAM (USACE, 1998b) as one of the hydraulic design routines. The method is based on a typical trapezoidal cross section and assumes steady uniform flow. SAM determines the stable channel dimensions based on a particular user-defined effective discharge. SAM will

also calculate the bed material sediment concentration from hydraulic parameters for an upstream "supply reach," or this value may be input by the user. If a supply reach is used, it is represented by a bed slope, a trapezoidal cross section, a bed material gradation, and a discharge. Regardless of how the sediment concentration is specified, bank and bed roughness are composited using the equal velocity method (Chow, 1959) to obtain total roughness for a cross section. A family of slope-width solutions that satisfy the flow resistance and sediment transport relations is then computed. The designer selects any combination of channel properties that are represented by a point on the slope-width curve (any point on the curve will theoretically yield a stable channel solution). Selection may be based on minimum stream power, maximum possible slope, width constraint due to right-of-way, or maximum allowable depth. Effects of bank vegetation are considered in the assigned roughness coefficient. For this study, the minimum stream power solution provided by SAM was considered to be the most stable channel configuration and was used in the analyses. The reader is referred to the SAM User's Manual for more details regarding this stable channel analytical method.

Copeland's method is especially applicable to sand bed streams because it accounts for sediment transport, bed form and grain roughness, and bank roughness. The cohesive bank effect can be considered by assigning an appropriate bank roughness. The required inputs include the channel forming discharge, the bank roughness, the bank slopes, the bed material size distribution, and the geometry for the supply reach if the required inflow sediment concentration is calculated by the program. For this study, the Manning's bank roughness coefficient was taken as n = 0.045 for all banks. The bed material size distribution was taken from the gradation curves referenced in Table 5-1. The side slopes of the banks were based on the 1998 precision cross sections. These side slopes are presented in Table 5-2.

For this study, the sediment concentrations were entered directly. Two different sediment concentrations were tried: (1) the sediment concentration based on the Brownlie D_{50} method (using the SAM sediment transport module, as discussed in Chapter 4), and (2) the sediment concentration based on the Yang (HEC-6) method (USACE, 1993b; Yang, 1984, 1973). At each cross section, the sediment concentration for each flow value was calculated as the sediment transport rate in tons per day (from the sediment rating curve developed in SAM), divided by the flow expressed in tons of water per day.

5.3 Historical Versus Regime Conditions

The regime methods described in Section 5.2 were applied to the twenty-one precision cross sections in the study reach. For each cross section, calculations provided a prediction of the stable channel top width, average depth, and energy slope. In addition, the adopted historical bankfull flows listed in Section 4.5 were applied to the single-cross section models of the 1940 and 1998 cross sections, as described in section 4.2.1. These 1940 and 1998 single cross section models were executed using adopted historical bankfull discharges, providing a top width and average depth for each cross section. Results from the regime methods and historical information are shown in Figures 5-1, 5-2, and 5-3 for the top widths, average depths, and energy slopes, respectively.

Table 5-2. Side Slopes Used For SAM (Copeland's) Stable Channel Procedure

Precision Cross Section	Left Bank Side Slope	Right Bank Side Slope
A2-f	1.66	2.93
B3-a	2.48	2.62
B3-e	1.16	1.85
C2-d	2.89	2.59
C2-j	1.65	4.27
D3-a	1.25	0.8
D3-d	0.47	1.69
D3-f	4.22	2.09
D3-h	1.09	1.99
D3-k	0.47	1.94
D3-l	0.18	2.1
E2-a	0.46	2.11
E2-f	0.39	2.68
E2-j	0.54	1.9
F2-a	0.31	3.14
H2-i	3.06	1.86
H3-f	1.48	6.99
I4-a	3.52	0.13
J1-a	8.31	6.88
J1-e	4.59	7.61
K3-j	2.17	1.66
L1-a	3.32	1.97

Both the Julien and Wargadalam method and the Simons and Albertson method yielded very poor agreement. Neither the magnitudes nor the shapes of the curves seemed to match the historical (1998) cross sections for top width, average depth, or energy slope.

The Copeland procedure in SAM, using the Yang sediment transport relationship to develop sediment concentrations (lines labeled SAM-Yang in the figures), were in better agreement. In most cases, however, the best agreement was obtained using the Copeland procedure in SAM with sediment concentrations derived from the Brownlie D_{50} sediment rating curves. These regime predictions are labeled "SAM-Brownlie D_{50}" in the figures. The "SAM-Brownlie D_{50}" method generally agreed with the existing conditions better than any other regime method for top width, average depth, and energy slope alike. Predicted top widths and depths were nearly evenly split between the number of over and under predictions compared to the 1998 bankfull values. Slightly more predictions were made that gave wider top widths than the bankfull values (12 of the 21 cross sections) and shallower depths (11 of the 21 cross sections). However, this would be expected as a

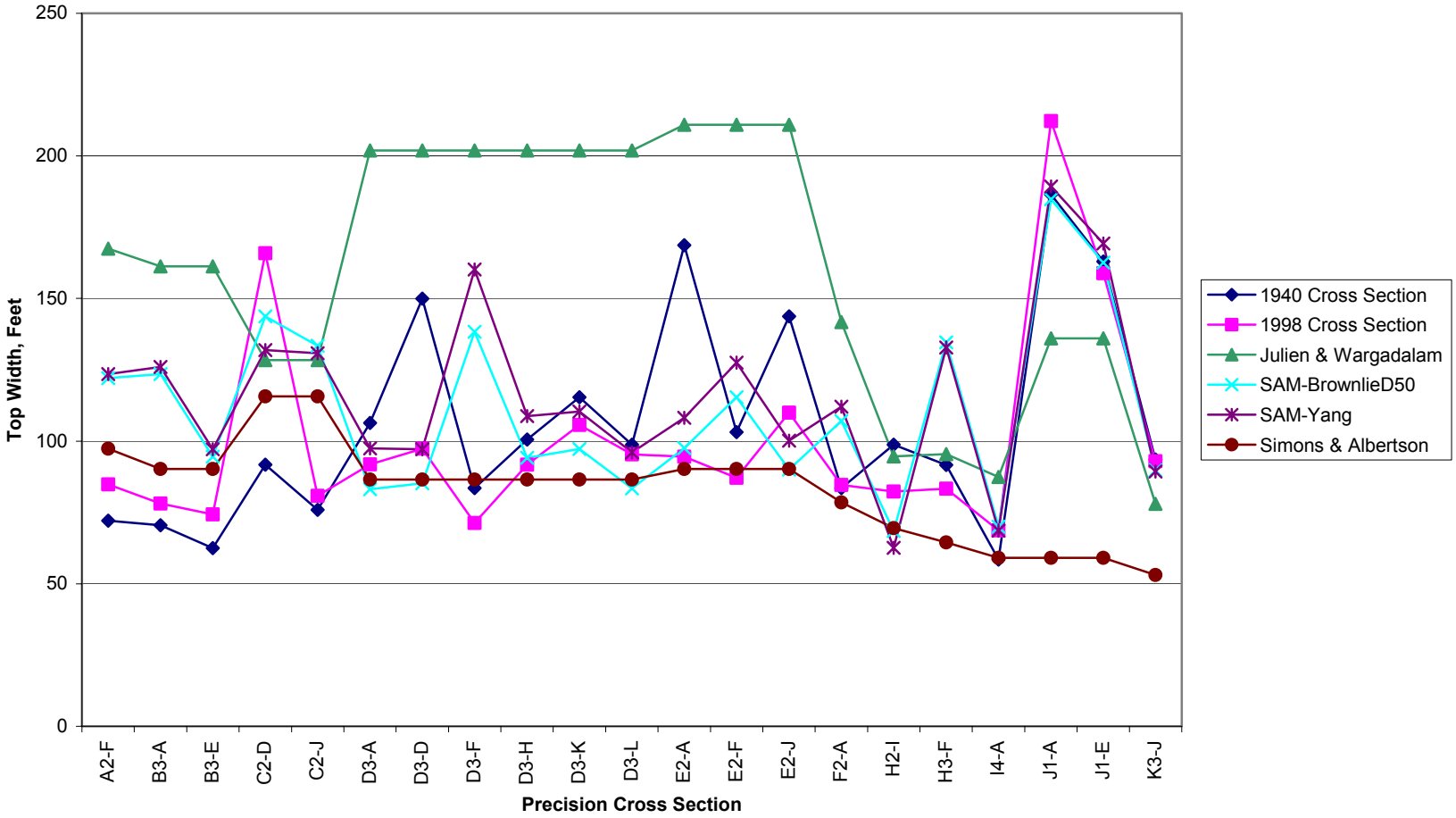

Figure 5-1. Top width at historical adopted bankfull flows: Cross section models for 1940, 1998, and regime predictions.

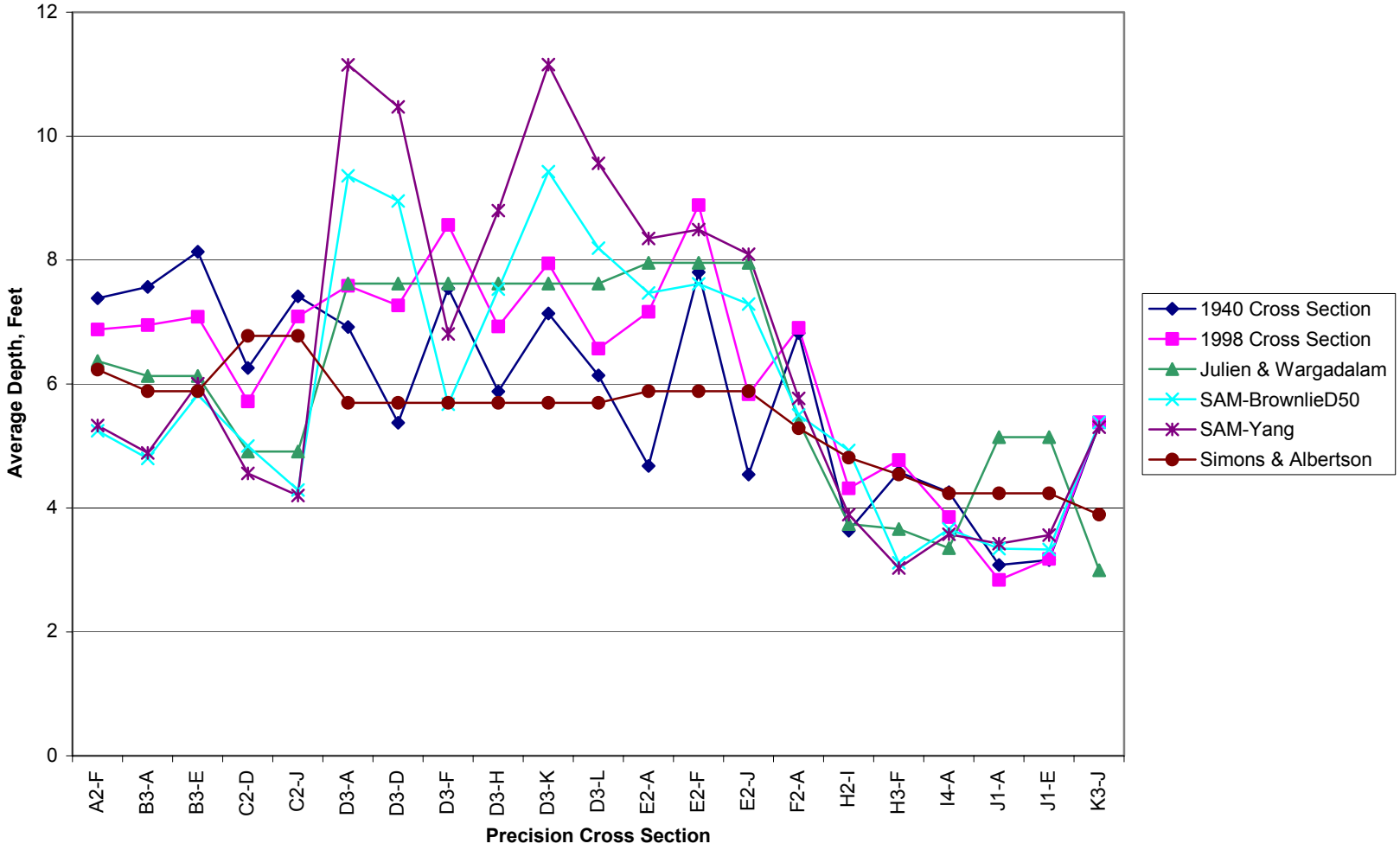

Figure 5-2. Average depth at historical adopted bankfull flows: Cross section models for 1940, 1998, and regime predictions.

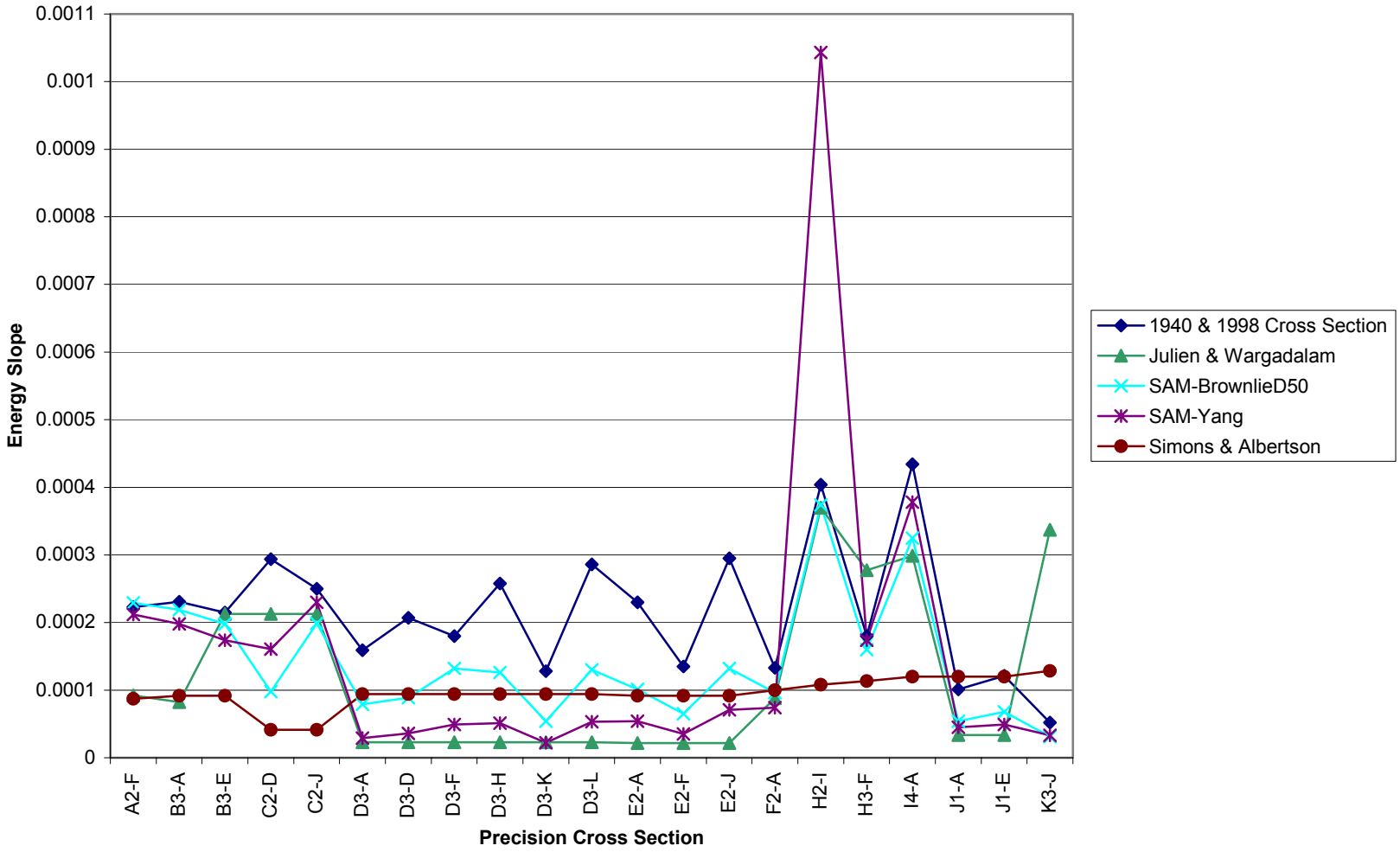

Figure 5-3. Energy slope at historical adopted bankfull flows: Cross section models for 1940, 1998, and regime predictions.

regime theory based on non-cohesive material should predict wider and shallower channel shapes than would be realized in cohesive or semi-cohesive systems where the channels tend to be narrower and deeper.

All regime methods under predicted the bankfull energy slope from HEC-RAS at nearly every cross section. However, the SAM-Brownlie D_{50} method again gave the best results. It should be noted that the energy slopes from the HEC-RAS model are dependent on hydraulic conditions downstream from their location while the regime methods yield theoretical uniform flow values.

Because the SAM-Brownlie D_{50} method gave the best results, it was selected to be the regime method used for all subsequent analyses presented in this report.

5.3.1 Cross Section Shape Trends

By observing the changes in top width from 1940 to 1998 for a constant discharge in Figure 5-1 it can be seen that, for most of the cross sections, the river is either relatively stable or top widths are moving closer to the values predicted by the regime method (the SAM-Brownlie D_{50} method, described previously). Several trends in cross section width changes were observed:

- Cross sections that had little change in top width from 1940 to 1998, and also appeared to be stable per the regime equation: D3-a, D3-d, D3-h, E2-a (see comment in Table 5-3), F2-a, I4-a, J1-e, and K3-j.
- Cross sections that have been widening from 1940 to 1998, and are narrower than the regime predicted top width (implying that they will continue to widen): A2-f, B3-a, B3-e, and C2-j.
- Cross sections that have been narrowing from 1940 to 1998, and are wider than the regime predicted top width (implying that they will continue to narrow): D3-k, D3-l, E2-j, and H2-i.

Section C2-d widened considerably, changing from much narrower than regime width in 1940 to slightly wider than regime width in 1998 — although the adopted bankfull flow water surface does occupy the left overbank in the 1998 single cross section model (see Appendix G for cross section plots). If only the main channel is considered, the channel width (about 113 feet) is still narrower than regime width. The main channel will probably continue to widen. In any case, the obvious difference between the 1940 and 1998 cross section shapes raises concerns over the survey location for these sections (i.e., were both cross sections surveyed at the same location).

For section H3-f, the single cross section models and Figure 5-1 indicate that the bankfull flow in the 1998 section has a lower top width than bankfull top width for the 1940 section, while the regime method indicates the channel should be widening. An inspection of the cross section, however, reveals that the 1998 cross section is wider at depths of up to 3 feet, narrower at depths from 3-5 feet, and about the same width at higher depths. The channel appears approximately stable, though the regime method indicates it should be widening.

For sections J1-a, D3-f, and E2-f, the 1940 to 1998 trend is contrary to the predicted regime trend. Section J1-a was at the predicted regime width in 1940, but has widened slightly, moving away from regime conditions. Sections D3-f and E2-f are narrower than regime width and should be widening per the regime predictions, but the 1940 to 1998 trend shows that they are narrowing. The long-term trend is therefore uncertain for sections J1-a, D3-f, and E2-f.

Table 5-3 summarizes the comparison of top widths from 1940 to 1998, as well as the predicted future changes in top width.

Table 5-3. Summary of Cross Section Trends from 1940 to 1998 and Regime Trends

Precision Cross Section	1998 Top Width Compared to Regime Width	Is 1998 Top Width Closer to Regime Width Than 1940 Top Width?	Comments and Predictions
A2-f	Much narrower	Yes	River has been widening, will continue to do so.
B3-a	Much narrower	Yes	River has been widening, will continue to do so.
B3-e	Much narrower	Yes	River has been widening, will continue to do so.
C2-d	Wider	Yes	River may be stable. The 1940 width was well below regime, and the river has widened considerably. Main channel is probably continuing to widen.
C2-j	Much narrower	Slightly	River has been widening, should continue to do so.
D3-a	Slightly wider	Yes, much closer	River has been narrowing, now very near regime; may be stable now.
D3-d	Slightly wider	Yes, much closer	River narrowing, now very near regime. May be stable now. 1940 top width is exaggerated in Figure 5-1 due to low possibly ineffective area on right overbank.
D3-f	Much narrower	No	1940 to 1998 trend is slightly narrowing but regime predicts it should widen. Trend is uncertain.
D3-h	Almost the same	Yes	1940 to 1998 trend is slightly narrowing, but now at regime. May be stable.

Precision Cross Section	1998 Top Width Compared to Regime Width	Is 1998 Top Width Closer to Regime Width Than 1940 Top Width?	Comments and Predictions
D3-k	Wider	Yes	River narrowing, will continue to do so.
D3-l	Wider	Yes	River narrowing, will continue to do so.
E2-a	Almost the same	Yes	River narrowing slightly, 1940 top width is exaggerated on Figure 5-1 due to flow entering possibly ineffective low area on left overbank. Probably stable now.
E2-f	Narrower	No, 1940 was wider, and closer to regime	River narrowed very slightly from 1940 to 1998, but regime predicts it should widen; cannot determine trend.
E2-j	Wider	Much closer	Has been narrowing, should continue to do so.
F2-a	Same	Same	At regime, stable.
H2-i	Wider	Yes	River narrowing, will continue to do so.
H3-f	Narrower	No	River should be widening per regime, but appears to be widening only at shallow depths of less than 3 feet. Has narrowed at depths of 3-5 ft., approximately stable historically above this depth. Top width may be approximately stable.
I4-a	Same	Yes	1940 was slightly narrower than regime, 1998 is at regime. Stable.
J1-a	Higher	No	River has widened from 1940 to 1998, but was at regime in 1940. Future trend uncertain.
J1-e	Almost the same	Both near regime	Stable.
K3-j	Almost the same	Both near regime	Stable.

From Figure 5-3, it can be seen that the predicted regime energy slopes are almost all lower than the actual energy slopes (derived from the HEC-RAS river model provided by the District). This is true not only for the adopted regime method, but also for every regime method that was tried, and at almost every cross section. This implies that energy

slopes should be decreasing over time. The two mechanisms through which this could occur are (1) the river slope will rotate downwards around a fixed point (e.g., the confluence with the Red River of the North), resulting in incising of the upper river reaches, or (2) the river will become longer, that is, more sinuous. However, there is no evidence from field and office studies that the river has incised significantly. Nor was evidence found of increased sinuosity over the last 40 years (see Chapter 6). More likely, the channel has found a quasi-equilibrium state at a slope other than the minimum stream power solution (see Section 5.2.3).

5.4 Future Conditions

The future conditions analysis involves determining the effect of pumping on channel shape and slope. Therefore, the future without project (no pump) condition is the point against which the future scenarios are compared. The predictions of the SAM regime calculations were applied to each adopted bankfull discharge for the future scenarios. Results from the 300 cubic feet per second (cfs) pumping condition or 480 cfs pumping condition are compared to the no pump condition for both moderate and wet climatic scenarios.

5.4.1 Predicted Changes in Top Width

The predicted changes in top width from the no pump condition are tabulated in Table 5-4 for the moderate future and Table 5-5 for the wet future. Because of the limited accuracy of the methods, the changes are reported to the nearest half foot. The results are plotted in Figure 5-4 (moderate future) and Figure 5-5 (wet future). Generally, the changes from the no pump condition are minor. For the moderate future, most sections show no change for the Md300 scenario, and a few show modest widening, up to a maximum of 3 feet. For the Md480 scenario, most cross sections widen, up to a maximum of 4 feet wider than the no pump scenario.

The wet future results are similar to those from the moderate future. For the Wt300 scenario, most sections showed no change, and the maximum predicted change in width from the no pump (Wtnp) scenario of 2.5 feet. With increased amounts of pumping (Wt480 scenario), most sections showed some width increase above the no pump condition, with a maximum predicted increase of 5 feet.

Table 5-4. Predicted Changes in Top Width from No Pump Condition, Moderate Future

Cross Section	Regime Top Width, (ft) Mdnp	Regime Top Width, (ft) Md300	Change from Mdnp to Md300 (ft)	Regime Top Width, Feet, Md480 (ft)	Change from Mdnp to Md480 (ft)
A2-f	123.54	125.00	1.5	126.00	2.5
B3-a	123.54	123.54	-	124.54	1.0
B3-e	94.57	94.87	0.5	95.87	1.5
C2-d	142.14	142.14	-	141.14	-1.0
C2-j	131.82	131.82	-	131.82	-
D3-a	80.32	80.32	-	81.53	1.0
D3-d	82.60	82.60	-	82.82	-
D3-f	134.02	134.02	-	135.65	1.5
D3-h	91.18	91.18	-	92.49	1.5
D3-k	93.55	93.55	-	94.79	1.0
D3-l	80.75	80.75	-	81.98	1.0
E2-a	95.07	95.07	-	95.07	-
E2-f	111.48	111.48	-	112.48	1.0
E2-j	87.28	87.28	-	87.52	-
F2-a	100.67	101.01	0.5	102.36	1.5
H2-i	62.52	63.01	0.5	63.01	0.5
H3-f	123.10	125.95	3.0	126.95	4.0
I4-a	67.24	67.60	0.5	68.60	1.5
J1-a	175.72	177.24	1.5	176.72	1.0
J1-e	155.36	155.36	-	155.14	-
K3-j	86.98	86.98	-	88.36	1.5

Table 5-5. Predicted Changes in Top Width from No Pump Condition, Wet Future

Cross Section	Regime Top Width, (ft) Wtnp	Regime Top Width, (ft) Wt300	Change from Wtnp to Wt300 (ft)	Regime Top Width, (ft) Wt480	Change from Wtnp to Wt480 (ft)
A2-f	136.75	139.21	2.5	141.67	5.0
B3-a	144.13	145.64	1.5	147.15	3.0
B3-e	111.48	111.48	-	113.78	2.5
C2-d	167.62	169.17	1.5	169.17	1.5
C2-j	156.74	157.74	1.0	157.74	1.0
D3-a	97.83	97.83	-	98.04	-
D3-d	97.70	97.70	-	97.70	-
D3-f	160.22	160.22	-	161.22	1.0
D3-h	108.11	108.11	-	108.11	-
D3-k	111.13	111.13	-	111.37	-
D3-l	97.31	97.31	-	97.54	-
E2-a	109.42	110.67	1.5	111.93	2.5
E2-f	129.78	130.78	1.0	132.09	2.3
E2-j	102.94	102.94	-	104.18	1.0
F2-a	132.22	132.22	-	133.57	1.5
H2-i	84.42	84.42	-	86.41	2.0
H3-f	170.42	170.42	-	172.27	2.0
I4-a	89.71	89.71	-	90.71	1.0
J1-a	246.47	246.47	-	248.47	2.0
J1-e	222.22	222.22	-	220.00	-2.0
K3-j	125.41	125.41	-	125.79	0.5

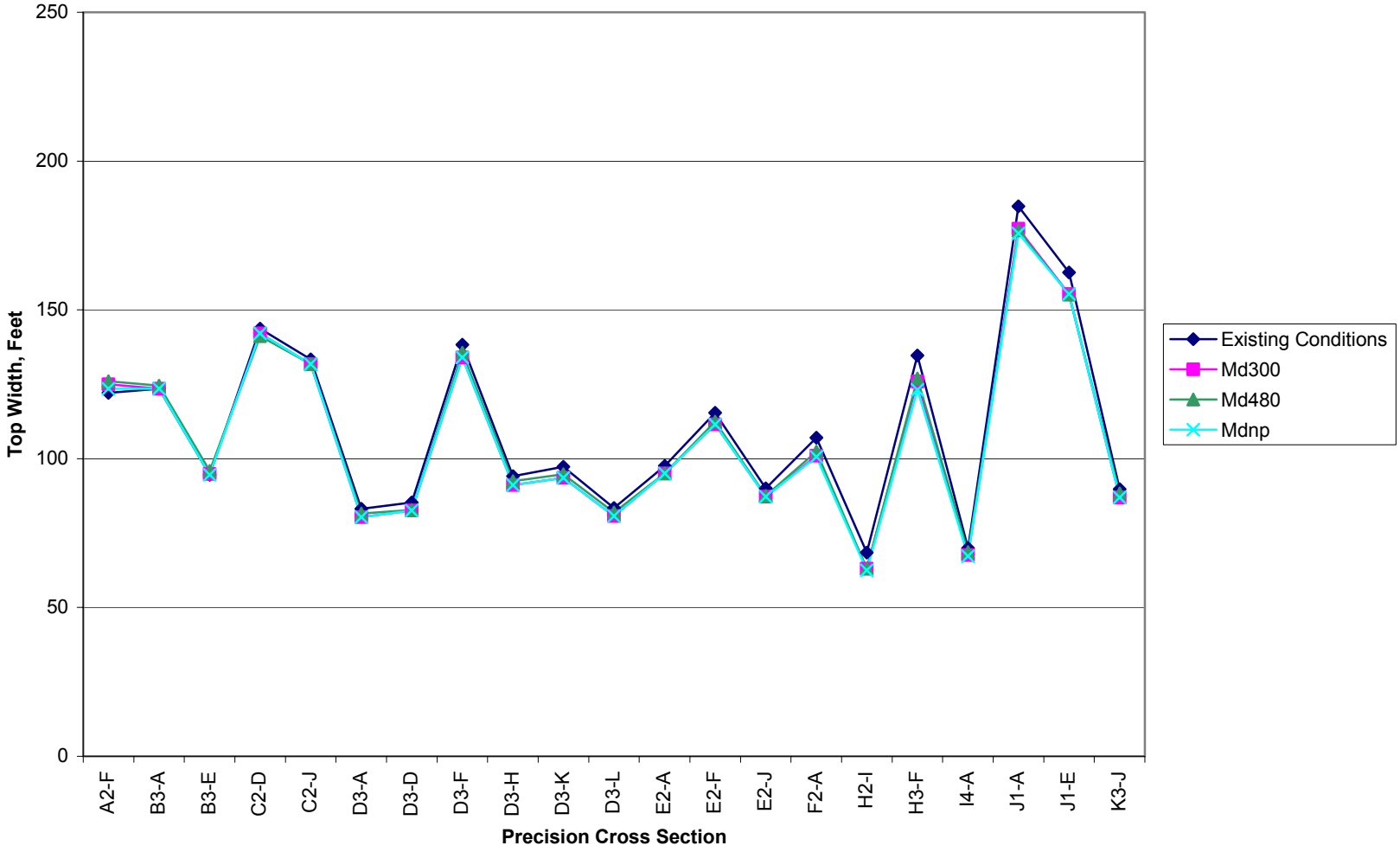

Figure 5-4. Top width at bankfull, predicted by SAM regime for existing conditions and moderate future.

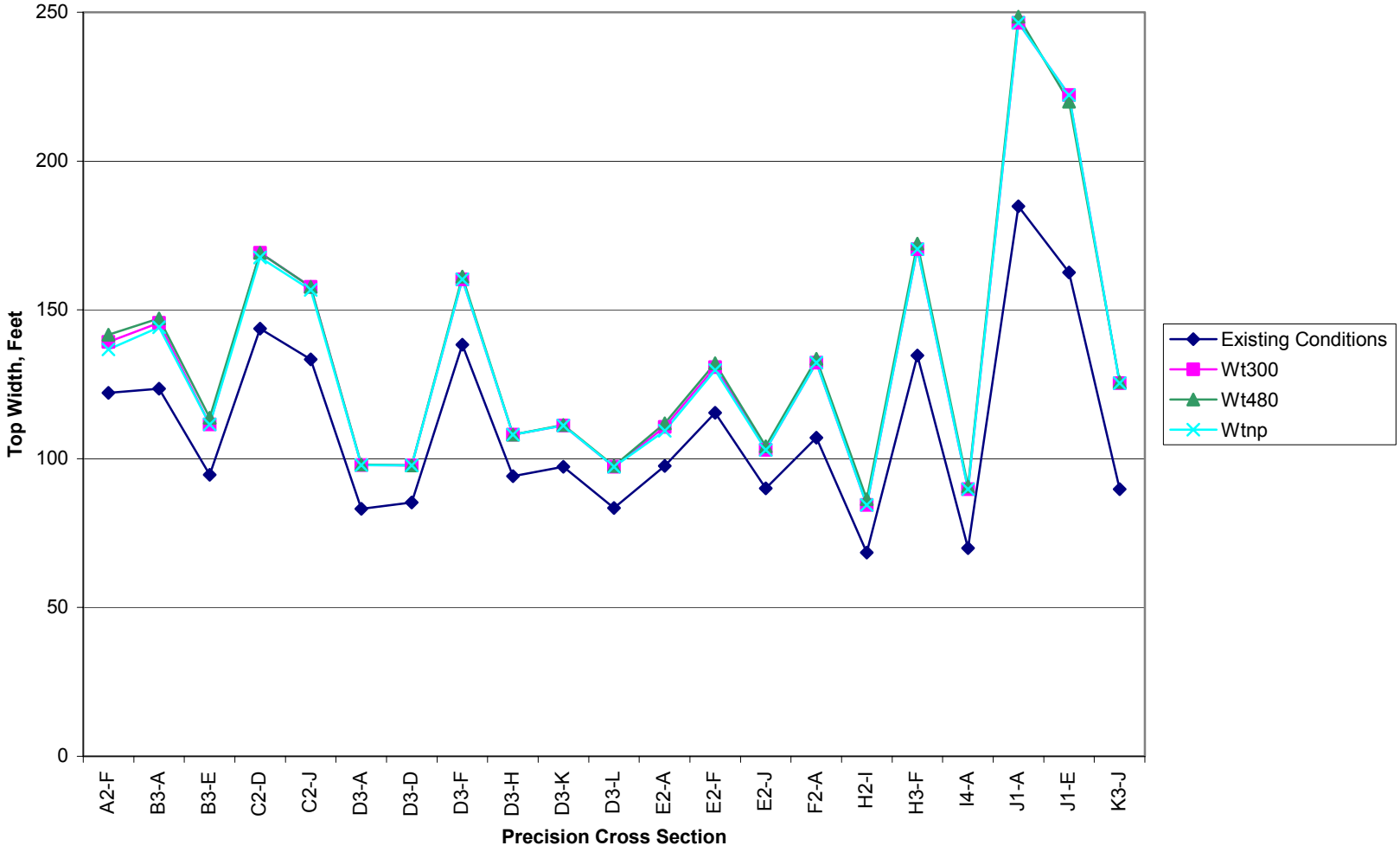

Figure 5-5. Top width at bankfull, predicted by SAM regime for existing conditions and wet future.

5.4.2 Predicted Changes in Average Depth

The predicted changes in average depth, versus the base no pump condition, are tabulated in Table 5-6 for the moderate future, and Table 5-7 for the wet future. The results are plotted in Figure 5-6 and Figure 5-7. The predicted changes from the no pump condition are very small. The maximum increase in average depth versus the no pump condition is 0.09 feet (1 inch) for the moderate future, and 0.18 feet (2 inches) for the wet future. As these predicted changes are within the expected accuracy of the methods, the expected changes in average depth are essentially nil.

Table 5-6. Predicted Changes in Average Depth from No Pump Condition, Moderate Future

Reach	Regime Average Depth, (ft) Mdnp	Regime Average Depth, (ft) Md300	Change from Mdnp to Md300 (ft)	Regime Average Depth, (ft) Md480	Change from Mdnp to Md480 (ft)
A2-f	5.33	5.42	0.09	5.42	0.09
B3-a	4.80	4.80	-	4.80	-
B3-e	5.83	5.91	0.08	5.92	0.09
C2-d	4.92	4.92	-	4.91	-
C2-j	4.20	4.20	-	4.20	-
D3-a	9.02	9.02	-	9.11	0.09
D3-d	8.69	8.69	-	8.77	0.08
D3-f	5.51	5.51	-	5.59	0.08
D3-h	7.28	7.28	-	7.37	0.09
D3-k	9.15	9.15	-	9.24	0.09
D3-l	7.93	7.93	-	8.02	0.09
E2-a	7.29	7.29	-	7.29	-
E2-f	7.35	7.35	-	7.36	0.01
E2-j	7.03	7.03	-	7.11	0.08
F2-a	5.14	5.23	0.08	5.31	0.17
H2-i	4.58	4.65	0.06	4.65	0.06
H3-f	2.85	2.93	0.09	2.94	0.09
I4-a	3.49	3.57	0.08	3.57	0.09
J1-a	3.18	3.25	0.07	3.18	-
J1-e	3.23	3.23	-	3.16	-0.07
K3-j	5.21	5.21	-	5.29	0.09

Table 5-7. Predicted Changes in Average Depth from No Pump Condition, Wet Future

Reach	Regime Average Depth, (ft) Wtnp	Regime Average Depth, (ft) Wt300	Change from Wtnp to Wt300 (ft)	Regime Average Depth, (ft) Wt480	Change from Mdnp to Wt480 (ft)
A2-f	5.95	6.04	0.09	6.13	0.18
B3-a	5.60	5.68	0.09	5.77	0.17
B3-e	6.98	6.98	-	7.07	0.10
C2-d	5.81	5.89	0.09	5.89	0.09
C2-j	5.09	5.09	-	5.09	-
D3-a	10.94	10.94	-	11.01	0.08
D3-d	10.33	10.33	-	10.33	-
D3-f	6.60	6.60	-	6.61	0.01
D3-h	8.65	8.65	-	8.65	-
D3-k	10.81	10.81	-	10.88	0.08
D3-l	9.66	9.66	-	9.73	0.08
E2-a	8.44	8.53	0.09	8.62	0.18
E2-f	8.59	8.60	0.01	8.68	0.10
E2-j	8.35	8.35	-	8.44	0.09
F2-a	6.85	6.85	-	6.93	0.09
H2-i	5.69	5.69	-	5.84	0.15
H3-f	3.84	3.84	-	3.92	0.08
I4-a	4.81	4.81	-	4.81	0.01
J1-a	4.30	4.30	-	4.30	0.01
J1-e	4.39	4.39	-	4.31	-0.08
K3-j	7.17	7.17	-	7.25	0.08

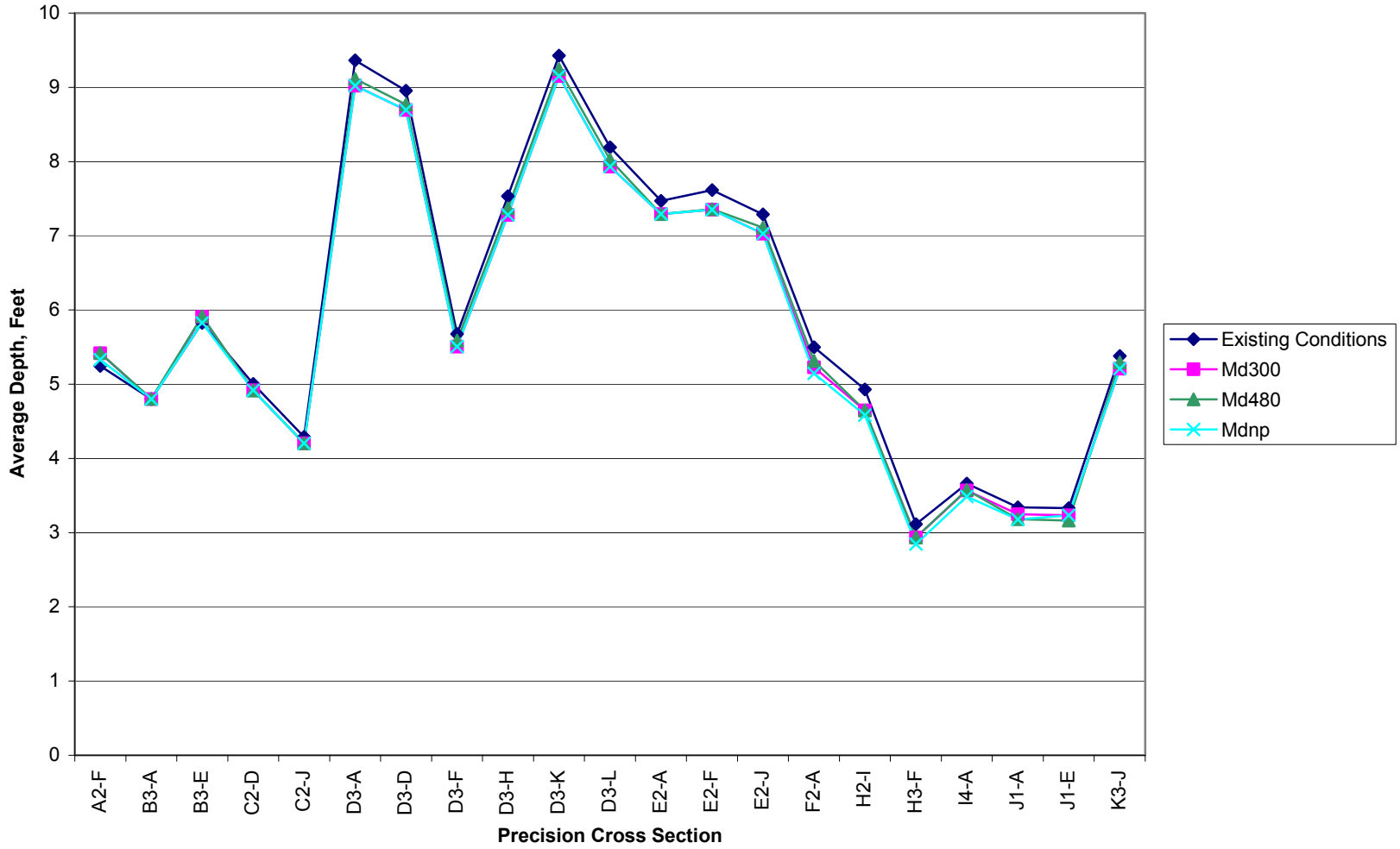

Figure 5-6. Average depth at bankfull, predicted by SAM regime for existing conditions and moderate future.

Figure 5-7. Average depth at bankfull, predicted by SAM regime for existing conditions and wet future.

5.4.3 Predicted Changes in Energy Slope

The predicted changes in energy slope, versus the no pump condition, are tabulated in Table 5-8 for the moderate future and Table 5-9 for the wet future. The results are plotted in Figure 5-8 and in Figure 5-9. The results are rounded to the fifth decimal place. The changes are quite small on an absolute basis, though on a percentage basis, they may be as large as 10%. For the Md300 scenario, there was no increase in energy slope at any section, and two sections had slightly lower energy slopes. For the Md480 scenario, the maximum increase in energy slope was 0.00002, an increase in slope of about 10%. Some sections decreased in slope. For the wet future, there was virtually no increase in energy slope, except that one section in the Wt480 condition had a predicted increase of 0.00001 and two sections had a predicted decrease of 0.00001.

Table 5-8 Predicted Changes in Energy Slope from No Pump Condition, Moderate Future

Reach	Regime Energy Slope, Mdnp (no pump based condition)	Regime Energy Slope, Md300	Change from Mdnp to Md300 condition	Regime Energy Slope, Md480	Change from Mdnp to Md480 condition
A2-f	0.00024	0.00023	-	0.00023	-0.00001
B3-a	0.00022	0.00022	-	0.00022	-
B3-e	0.00020	0.00020	-	0.00019	-
C2-d	0.00009	0.00009	-	0.00010	0.00001
C2-j	0.00019	0.00019	-	0.00020	0.00002
D3-a	0.00008	0.00008	-	0.00008	-
D3-d	0.00009	0.00009	-	0.00009	-
D3-f	0.00013	0.00013	-	0.00013	-
D3-h	0.00012	0.00012	-	0.00012	-
D3-k	0.00005	0.00005	-	0.00005	-
D3-l	0.00013	0.00013	-	0.00013	-
E2-a	0.00010	0.00010	-	0.00010	-
E2-f	0.00007	0.00007	-	0.00006	-
E2-j	0.00013	0.00013	-	0.00013	-
F2-a	0.00010	0.00010	-	0.00009	-
H2-i	0.00038	0.00037	-0.00001	0.00037	-0.00001
H3-f	0.00016	0.00015	-	0.00015	-0.00001
I4-a	0.00030	0.00030	-0.00001	0.00029	-0.00001
J1-a	0.00005	0.00005	-	0.00006	0.00001
J1-e	0.00007	0.00006	-	0.00007	0.00001
K3-j	0.00003	0.00003	-	0.00003	-

Table 5-9. Predicted Changes in Energy Slope from No Pump Condition, Wet Future

Reach	Regime Energy Slope, Wtnp (no pump based condition)	Regime Energy Slope, Wt300	Change from Wtnp to Wt300 condition	Regime Energy Slope, Wt480	Change from Wtnp to Wt480 condition
A2-f	0.00023	0.00023	-	0.00023	-
B3-a	0.00023	0.00023	-	0.00024	-
B3-e	0.00021	0.00021	-	0.00021	-
C2-d	0.00010	0.00010	-	0.00010	-
C2-j	0.00020	0.00020	-	0.00021	-
D3-a	0.00009	0.00009	-	0.00008	-
D3-d	0.00010	0.00010	-	0.00009	-
D3-f	0.00014	0.00014	-	0.00013	-
D3-h	0.00013	0.00013	-	0.00013	-
D3-k	0.00006	0.00006	-	0.00006	-
D3-l	0.00014	0.00014	-	0.00014	-
E2-a	0.00011	0.00011	-	0.00010	-
E2-f	0.00007	0.00007	-	0.00007	-
E2-j	0.00013	0.00013	-	0.00013	-
F2-a	0.00010	0.00010	-	0.00010	-
H2-i	0.00044	0.00044	-	0.00042	-0.00001
H3-f	0.00017	0.00017	-	0.00017	0.00001
I4-a	0.00036	0.00036	-	0.00036	-0.00001
J1-a	0.00005	0.00005	-	0.00005	-
J1-e	0.00007	0.00007	-	0.00007	-
K3-j	0.00004	0.00004	-	0.00004	-

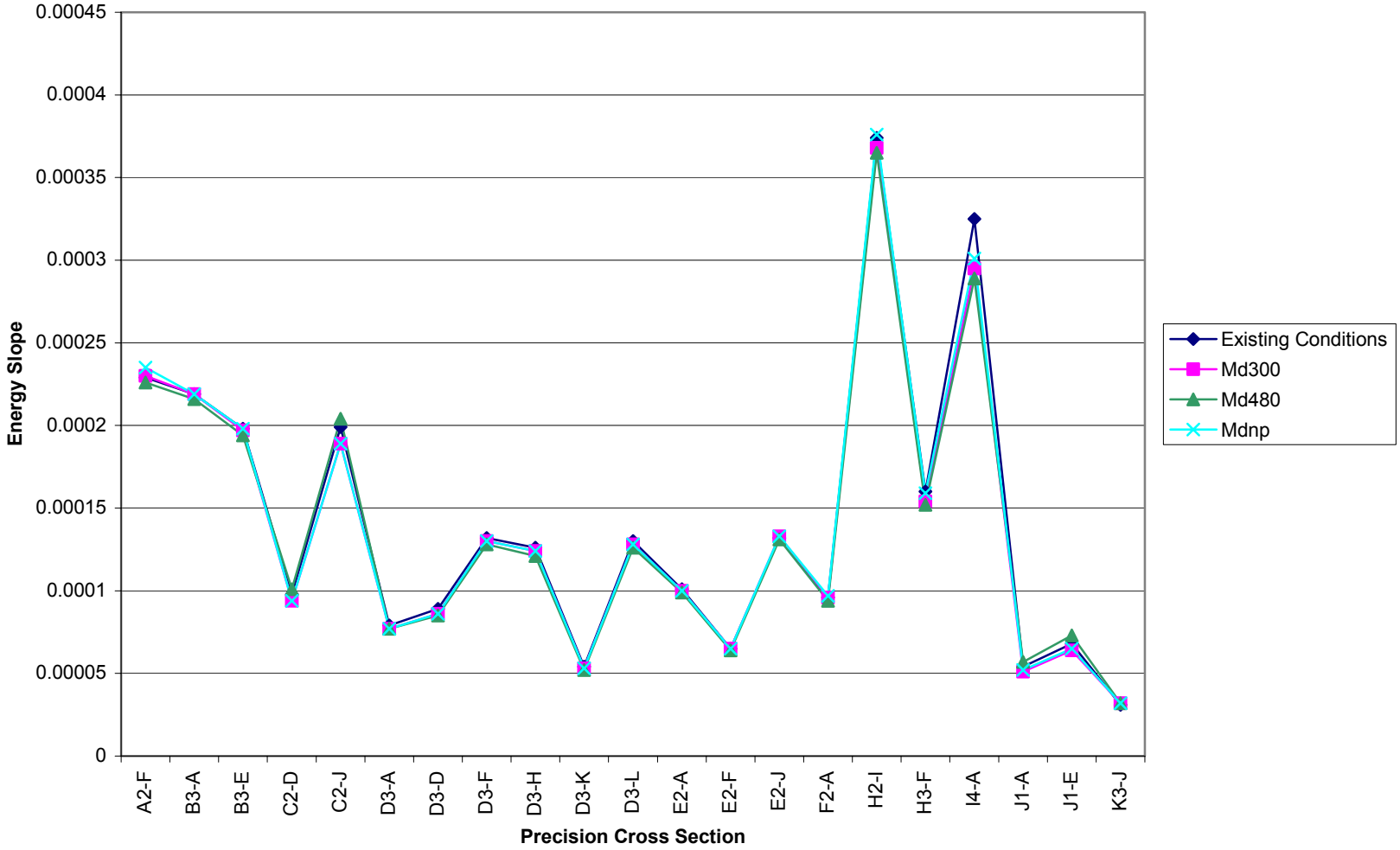

Figure 5-8. Energy slope at bankfull, predicted by SAM regime for existing conditions and moderate future.

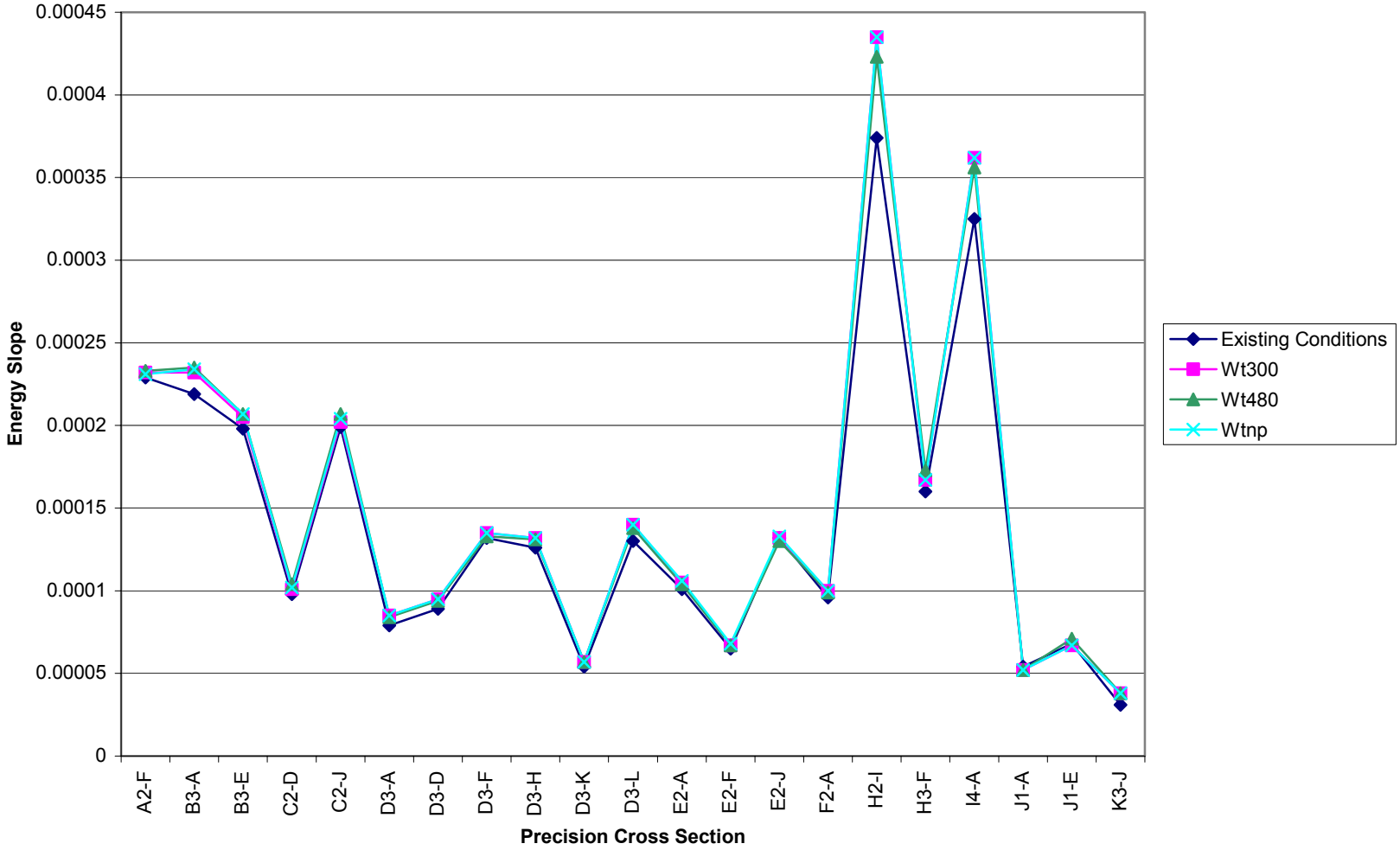

Figure 5-9. Energy slope at bankfull, predicted by SAM regime for existing conditions and wet future.

6 Channel Planform and Erosion Rates

6.1 General

The channel planform of the Sheyenne River was analyzed for the twelve erosion reaches described previously in this report. Each of these reaches has an orthophotograph taken in 1998 associated with it. These photographs were compared to USGS 7.5 minute quadrangle topographic maps for changes in the channel planform. The USGS maps were produced between 47 and 31 years prior to the photographs being taken. Comparison was made between the photographs and the maps for the following parameters: channel area (in plan view), sinuosity, meander amplitude, and meander length. The rate of erosion was also calculated for each detailed section and then extrapolated for each river reach.

6.2 Historical Conditions

Channel area (in plan view) was calculated for both the 1998 photographs and the USGS topographic maps using ArcView7 GIS. Polygons were created for each erosion reach, covering the area of the river marked as water on the topographic maps and areas that appeared to be water on the orthophotographs. The orthophotographs were black and white and in some instances it was difficult to determine the exact location of the banks of the river. Additionally, some of these photos did not seem to be located properly. Tests were conducted on each photo by tracing roads, which were then converted to NAVD 27 coordinates and compared to the digital topographic maps. Each orthophotograph was evaluated as good, questionable, or unusable. Photographs were characterized as good if the location and size of features appeared correct. Questionable evaluations were given to photos in which the location of features seemed to be incorrect while their size appeared accurate. If both the location and size of features appeared incorrect then photos were classified as unusable.

The area of the channel, more specifically, the width of the channel, varied between the topographic maps and the photographs. However, the general channel location was relatively unchanged. The centerline of the channel appeared to retain the same general shape on both the topographic maps and photographs, definitely within the margin of error that could be expected when placing the photographs digitally and making the necessary coordinate conversions. As a result, it was concluded that variations of the parameters related to the stream centerline (sinuosity, meander length, and meander amplitude) between the photographs and topographic maps would be within the margin of error expected in their calculation. That is, although differences were computed for these parameters, it is just as likely that the differences are due to measurement errors as to physical processes.

Sinuosity, meander length, and meander amplitude were all calculated based on the stream centerline as determined from the 1998 orthophotographs. Inflection points were identified. The distance between inflection points along a smooth line was measured, this distance being equal to one half of the meander length. The largest distance between the line connecting inflection points and the river centerline was calculated and assumed to

be equal to one half of the meander amplitude. These numbers were then averaged for each erosion reach. This method of determining the planform parameters is illustrated in Figure 6-1. Sinuosity was also determined by dividing the length of the stream centerline by the valley length, determined from the aerial photographs using ArcView, for each of the study reaches. The average sinuosity for the study reaches was calculated to be 2.02; rivers having a sinuosity of 1.5 or greater are classified as meandering (Leopold, Wolman, & Miller, 1964). Table 6-1 shows the sinuosity calculated for each reach.

Table 6-1. Sinuosity Calculated from 1998 Orthophotographs

Reach	Valley Length (m)	River Length (m)	Sinuosity
A2	551	871	1.58
B3	605	2080	3.44
C2	1001	2384	2.38
D3	1550	3172	2.05
E2	986	1950	1.98
F2	896	1992	2.22
G3	664	1421	2.14
H2	1091	1884	1.73
H3	979	2064	2.11
I1	623	1233	1.98
J1	2624	2723	1.04
K3	895	1618	1.81
L1	953	1748	1.83

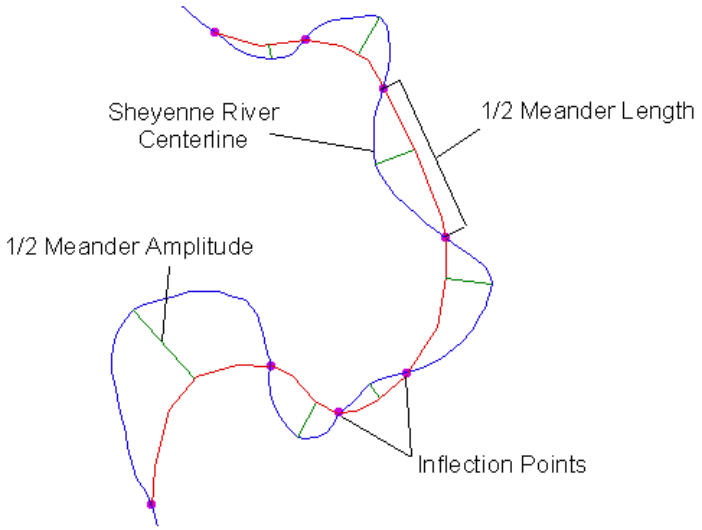

Figure 6-1. Parameters calculated based on stream centerline.

6.2.1 Predicted and Observed Planform Parameters

Empirical relations were used to compute planform variables (meander length and amplitude) using channel width as input. Comparisons were made between observed values and computed theoretical values in order to judge the applicability of the equations for prediction of future conditions. The equations used were:

Meander Length: $\lambda = 10.9w^{1.01}$ (Leopold and Wolman, 1960)

Meander Amplitude: $A = 2.7w^{1.1}$ (Leopold and Wolman, 1960)

where w is the channel width. The theoretical (regime) channel width determined by SAM using the Brownlie D_{50} sediment transport option (see Chapter 5) was used in the equations to determine theoretical meander length and meander amplitude for comparison with the observed values. These relationships provided the most accurate results when comparing theoretical to observed values (two other equations proposed by Inglis (Leopold et al., 1964) were also considered but provided worse results).

The average channel width from the 1998 photographs was determined by dividing the plan view area of the stream by the reach length, based on the assumption that the stream is a rectangle in plan view. The bankfull channel width is determined by applying the adopted bankfull flow for historical conditions to cross sections taken in 1998. These are presented in Table 6-2. The values from the 1998 photographs are also included in the table for reference. However, because the flow is not known at the time the photograph was taken, it cannot be determined if the river is at bankfull conditions (in almost all instances it appears that the flow was less than bankfull when the photos were taken). The SAM channel width was computed using the adopted bankfull flow for historical conditions and the Brownlie D_{50} sediment transport equation to solve for stable channel dimensions. The average difference between the SAM and bankfull widths for all erosion reaches was 15 feet. This shows that the SAM stable channel widths agree very well with the "actual" widths determined by applying the bankfull flow to the cross section geometry. Table 6-2 shows the SAM predicted channel width based on historical flows, the channel width calculated from the 1998 photographs, the bankfull channel width, and the difference between the SAM and bankfull channel widths for the detailed study reaches.

The theoretical meander length and amplitude for each of the reaches are based on the above equations using the SAM widths listed in Table 6-2. The computed meander length and amplitude using these widths are shown in Table 6-3 where they are also compared to the values measured from the 1998 orthophotographs.

Large discrepancies were observed between the computed theoretical values and the average of those measured from the 1998 orthophotographs (when the river was probably not at bankfull conditions). In order to present a consistent comparison, theoretical parameters for future conditions should not be compared to values based on the photos. Rather, predicted future values (based on the equations) should be compared to the

theoretical existing conditions results (also based on the equations). Predictions for future conditions are presented in the following section.

Table 6-2. Channel Width Comparison

Channel Width					
Reach	No. of Values Averaged	SAM (feet)	1998 Photographs (feet)	Bankfull (feet)	SAM –Bankfull (feet)
A2	1	122	68	85	37
B3	2	109	81	76	33
C2	2	139	77	123	15
D3	6	97	84	92	5
E2	3	101	55	97	4
F2	1	107	64	85	22
H2	1	94	55	82	11
H3	1	135	62	83	51
I1	1	70	57	69	1
J1	2	174	71	186	-12
K3	1	90	85	93	-3

Table 6-3. Meander Lengths and Amplitudes

		Meander Length			Meander Amplitude		
Reach	No. of Values Averaged	Average SAM (feet)	1998 Photographs (feet)	SAM - Photos (feet)	Average SAM (feet)	1998 Photographs (feet)	SAM - Photos (feet)
A2	1	1396	1357	39	533	653	-120
B3	2	1246	1508	-262	471	571	-99
C2	2	1587	703	883	613	315	298
D3	6	1106	1371	-265	414	412	2
E2	3	1153	874	279	433	266	167
F2	1	1223	800	423	461	323	138
H2	1	1068	530	539	398	188	211
H3	1	1541	1077	465	594	471	122
I1	1	796	1121	-326	289	469	-180
J1	2	1993	976	1018	786	61	724
K3	1	1023	693	330	380	174	206

The erosion rate for the time period between the creation of the topographic maps and the creation of the orthophotographs was calculated to provide a baseline for "normal" erosion in the study area. This baseline is established under the assumption that the channel is in a state of relative stability. Based on cross sections taken in 1940 and again in 1998 the water surface top width decreased an average of 4 feet for the adopted

bankfull flows, lending credence to the quasi-stable assumption. Despite the decrease in channel width, approximately 27 acres per year are lost to erosion due to local changes in width and the downstream movement of meanders. This rate was calculated in the following way. First, the polygon of the river traced from the topographic maps was subtracted from the polygon of the river traced from the orthophotographs in the detailed study areas. This produced a third set of small polygons whose areas were summed to compute the total area lost in the reach (Figure 6-2). The area lost was then divided by the length of the particular erosion reach to provide an erosion area per unit of stream length. This area was then divided by the number of years between the collection of the two sets of data. The erosion rates were determined for all of the study reaches in which the orthophotographs were classified as good (Table 6-4). These rates were then averaged and used to estimate the amount of erosion that would occur over the other river reaches (classified as questionable or unusable). The erosion rate for each reach was then multiplied by the reach length, and all of the rates were then totaled to give the erosion rate for the entire study reach of the Sheyenne River.

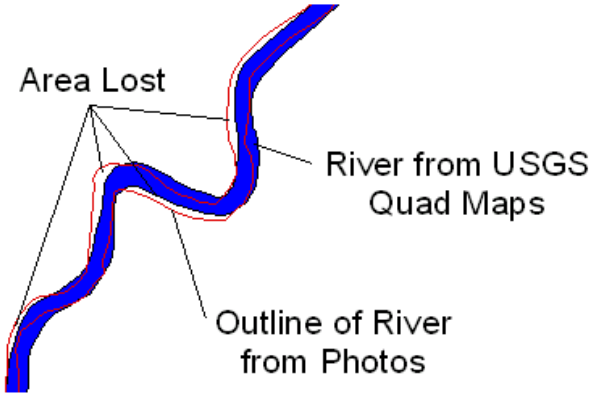

Figure 6-2. Representative reach showing calculation of the area lost due to erosion between the time when the USGS topographic map was created and the orthophotograph was taken.

6.3 Future Conditions

Using SAM with the Brownlie D_{50} sediment transport option, new theoretical channel widths were predicted for each of the six future conditions. Using these theoretical channel widths, meander length and meander amplitude were computed according to the previously presented equations. As mentioned, because of the discrepancy between the computed parameters for the current conditions and those actually measured, parameter values for future scenarios should be viewed with some caution. For a more accurate comparison, one should consider the differences in predicted theoretical values between future and existing conditions results. This comparison was performed for channel width, meander length and meander amplitude. The results (rounded to the nearest whole foot) are presented in Tables 6-5, 6-6, and 6-7. Also, emphasis should be given to comparing

the differences between with and without project scenarios for each hydrologic trace (moderate or wet future), as this will indicate the overall project effects.

Table 6-4. Calculation of Historical Erosion Rates

A	B	C	D	E	F	G	H	I
Study Sub-reach	**Sub-reach Length (m)**	**Total Reach Length (mi)**	**Area Lost in Sub-reach (m^2)**	**Area Lost in Total Reach (m^2)**	**Time Period (years)**	**Area Lost in Reach per Year (m^2)**	**Acres Lost per Year**	**Acres Lost per Year per Mile of River**
A2	870.70	43	5854.18	465181.09	39	11927.72	2.947	0.0685
B3	2079.91	29	20569.83	461466.42	39	11832.47	2.924	0.1008
C2	2384.36	70	N/A	N/A	N/A	N/A	N/A	N/A
D3	3172.19	59	16224.73	485541.56	31	15662.63	3.870	0.0656
E2	1949.89	69	4570.61	260237.34	31	8394.75	2.074	0.0301
F2	1992.02	43	5984.66	207859.75	37	5617.83	1.388	0.0323
G2	1421.07	32	N/A	N/A	N/A	N/A	N/A	N/A
H2	1883.99	17.5	N/A	N/A	N/A	N/A	N/A	N/A
H3	2063.86	17.5	N/A	N/A	N/A	N/A	N/A	N/A
I4	1232.61	43	N/A	N/A	N/A	N/A	N/A	N/A
J1	2722.75	19	36789.13	413067.82	48	8605.58	2.126	0.1119
K3	1617.60	11	5461.55	59757.66	47	1271.44	0.314	0.0286
Reaches		Total					Total	Average
A, B, D, E, F, J, and K		273	Reaches classified as “good”				15.644	0.0625
C, G, H2, H3, and I		180	Reaches classified as “questionable” or “unusable”				11.257*	
Sum		**453**					**27**	

*Total acres lost per year for Reaches C, G, H2, H3, and I calculated from average acres lost per year per mile of river for “good” reaches multiplied by reach length.

Notes: 1) Column E = Column D (Column C / Column B)
2) Column I = Column H / Column C

Table 6-5. Change in Average Theoretical Channel Width in Feet by Trace

Reach	No. of Values Averaged	Mdnp	Md300	Md480	Wtnp	Wt300	Wt480
A2	1	1	3	4	15	17	20
B3	2	0	0	1	19	20	21
C2	2	-2	-2	-2	24	25	25
D3	6	-3	-3	-2	15	15	15
E2	3	-3	-3	-3	13	14	15
F2	1	-6	-6	-5	25	25	27
H2	1	-6	-5	-5	16	16	18
H3	1	-12	-9	-8	36	36	38
I4	1	-3	-2	-1	20	20	21
J1	2	-8	-7	-8	61	61	61
K3	1	-3	-3	-1	36	36	36

Table 6-6. Change in Average Theoretical Meander Length in Feet by Trace

Reach	No. of Values Averaged	Mdnp	Md300	Md480	Wtnp	Wt300	Wt480
A2	1	17	34	45	170	198	226
B3	2	0	2	13	217	225	247
C2	2	-18	-18	-24	274	288	288
D3	6	-37	-37	-23	175	175	178
E2	3	-35	-35	-30	150	159	174
F2	1	-74	-70	-54	291	291	306
H2	1	-69	-63	-63	183	183	206
H3	1	-133	-100	-89	414	414	436
I4	1	-31	-27	-16	227	227	239
J1	2	-94	-85	-90	704	704	703
K3	1	-32	-32	-16	411	411	416

Table 6-7. Change in Average Theoretical Meander Amplitude in Feet by Trace

Reach	No. of Values Averaged	Mdnp	Md300	Md480	Wtnp	Wt300	Wt480
A2	1	7	14	19	71	83	95
B3	2	0	1	5	90	94	103
C2	2	-8	-8	-10	116	122	122
D3	6	-15	-15	-10	72	72	73
E2	3	-14	-14	-12	62	65	72
F2	1	-30	-29	-22	121	121	127
H2	1	-27	-25	-25	73	73	82
H3	1	-56	-42	-37	176	176	185
I4	1	-12	-11	-6	91	91	96
J1	2	-40	-37	-38	307	307	306
K3	1	-13	-13	-6	169	169	171

From Table 6-5 it can be seen that the average channel widths are predicted to decrease for nearly all reaches for the moderate climate scenario with or without pumping. This is due to the overall drier than average conditions for the moderate future trace over the 50-year time span (a description of the traces was given in Chapter 2). The largest predicted increase in channel width is 4 feet for the most downstream reach (A), an amount 3 feet greater than the future without pumping scenario. For the wet climate future, predicted widening is much greater, up to 61 feet. However, because widening is also predicted for the no pump scenario, the differences between with and without project are relatively small: up to 2 feet for the Wt300 scenario and up to 5 feet for the Wt480 scenario.

Because the predicted meander lengths and amplitudes are a function of the channel width, the results in Table 6-6 and Table 6-7 follow the same pattern as those in Table 6-5. Changes in the predicted meander length between the with and without pumping futures are relatively small for the moderate climate scenarios. Maximum changes of 33 feet and 44 feet were predicted for the Md300 and Md480 scenarios, respectively. Note

that the change would be applied over the entire meander length, between 500 and 1,500 feet for existing conditions. The results for the wet climate scenarios follow a similar pattern, with a predicted maximum increase in meander length of 28 feet and 57 feet for the Wt300 and Wt480 scenarios, respectively.

The predicted change in meander amplitude between with and without project conditions is also small, with maximum values of 14 feet and 19 feet for the Md300 and Md480 scenarios, respectively. Maximum predicted changes between with and without project conditions are 12 feet and 24 feet for the Wt300 and Wt480 scenarios, respectively. These predicted changes would be applied to existing meander amplitudes, measuring 60 to 650 feet under current conditions.

6.3.1 Erosion Magnitude

The effects of the changes in meander amplitude and meander length on erosion rates are very difficult to quantify. The change in theoretical channel width can be used to calculate the area lost along the river. This was done by multiplying the increase in theoretical channel width by the length of the reach represented. If the theoretical channel width was less than the historical condition width, then no area was calculated. Area created due to deposition is typically unusable for long periods of time and was thus not included in the calculations. Calculation of area lost due to increase in channel width is shown in Table 6-8. Note that the predicted area lost due to widening would be in addition to the area lost due to planform shifts (a total of 27 acres per year if historical rates continue) described in Section 6.2.1.

The proposed project would cause an increase in the total area eroded due to predicted increases in average channel width. The minimum predicted increase due to the project is 8 acres for the Md300 scenario (difference between the Md300 and Mdnp results) while the maximum predicted increase is 85 acres under Wt480 scenario (difference between the Wt480 and Wtnp results). Note that the effect of the proposed project was calculated by comparing the amount of erosion predicted with and without pumping from Devils Lake. The minimum change due to the project occurs during the moderate hydrologic scenario when 300 cubic feet per second (cfs) is pumped from the lake (Md300). The maximum change due to the project occurs during the wet hydrologic scenario when 480 cfs is pumped from the lake (Wt480). It should also be noted that the future climatic conditions (moderate or wet) have a far greater impact on predicted erosion rates than any of the proposed pumping scenarios.

The magnitude of the increase in erosion due to planform changes caused by pumping may be estimated by assuming that one half of a complete meander loop takes the form of an ellipse. The area lost due to increases in the meander length and/or amplitude is then defined as the area between two ellipses (Figure 6-3). Assuming that each half meander loop changes the average amount over the entire length of a reach will provide an estimate of the quantity of land eroded. Table 6-9 provides a summary of these calculations. A conservative assumption (that is, one yielding *higher* eroded land results) would be to assume that the planform erosion given in Table 6-9 (due to flow changes) and the historical average (27 acres per year, based on meander migration) are additive.

Table 6-8. Acres Eroded due to Increase in Average Channel Width by Trace

Reach	Mdnp	Md300	Md480	Wtnp	Wt300	Wt480
A	7.6	15.2	20.4	76.5	89.3	102.1
B	0.0	0.5	4.0	65.9	68.6	75.3
C	0.0	0.0	0.0	200.5	211.3	211.3
D	0.0	0.0	0.0	108.3	108.3	110.3
E	0.0	0.0	0.0	109.1	115.4	126.0
F	0.0	0.0	0.0	131.2	131.2	138.2
H2	0.0	0.0	0.0	33.8	33.8	38.0
H3	0.0	0.0	0.0	75.9	75.9	79.8
I	0.0	0.0	0.0	102.9	102.9	108.1
J	0.0	0.0	0.0	139.7	139.7	139.5
K	0.0	0.0	0.0	47.6	47.6	48.1
Total	**7.6**	**15.7**	**24.5**	**1091.3**	**1123.9**	**1176.6**

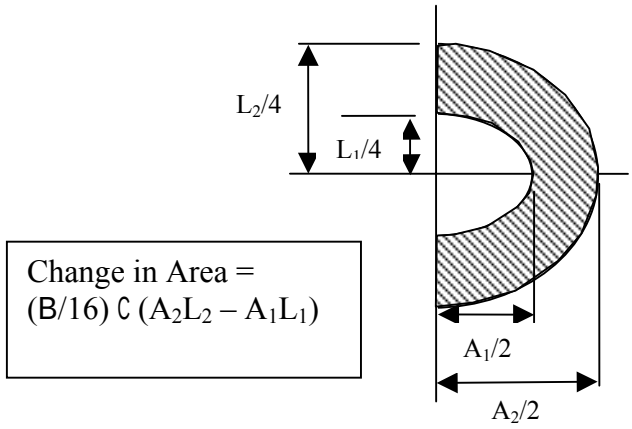

Figure 6-3. Schematic for Computing Change in Area due to Planform Changes.

Table 6-9. Acres Eroded due to Planform Changes Caused by Pumping

Reach	Md300-Mdnp	Md480- Mdnp	Wt300- Wtnp	Wt480- Wtnp
A	19.6	32.9	33.1	65.7
B	1.2	10.1	7.9	24.5
C	0.0	0.0	28.6	28.6
D	0.0	21.6	0	6.4
E	0.0	9.7	16.9	44.0
F	4.6	22.3	0	18.2
H2	2.6	2.6	0	10.5
H3	15.5	20.8	0	10.3
I	4.7	17.5	0	13.1
J	4.9	3.3	0	0.1
K	0.0	4.6	0	1.3
Total	**53.1**	**145.4**	**86.5**	**229.1**

6.3.2 Erosion Rates

The rate at which the present channel will adjust and reach a new quasi-equilibrium state is extremely difficult to predict. Variations in bank material, vegetation, bank failure mechanisms, and sediment supply to a reach (among other factors) increase the uncertainty of any predictions (effects of vegetation are treated in more detail in Chapter 8). However, it can be assumed that increased erosion would occur due to increased discharges until a new state of stability is reached. It is anticipated, based upon experience and the available literature, that the changes in width would occur relatively quickly compared to changes in planform (meander length and amplitude).

6.3.2.1 Width Adjustment

In order to estimate a maximum probable lateral erosion rate, channel bends were analyzed in each of the reaches from the 7.5 minute USGS topographic maps and the 1998 orthophoto data sets. Channel bends are under direct attack from the current and will experience more lateral movement over time than straighter reaches of the river. The observed lateral movement of channel bends ranged from a minimum of zero (i.e., the bend did not move appreciably during the time period) to a maximum of 27 meters over a period of 38 years for a bend in reach C2. The maximum computed lateral erosion rate was therefore 27/38 = 0.7 m/yr or 2.3 ft/yr. Applied to Table 6-5, this rate would yield adjustment times shown in Table 6-10 (note that times are not provided for reaches predicted to narrow).

Table 6-10. Adjustment Time (Years) for Change in Average Theoretical Channel Width by Trace

Reach	No. of Values Averaged	Mdnp	Md300	Md480	Wtnp	Wt300	Wt480
A2	1	0.4	1.3	1.7	6.4	7.3	8.6
B3	2			0.4	8.1	8.6	9
C2	2				10.3	10.7	10.7
D3	6				6.4	6.4	6.4
E2	3				5.6	6	6.4
F2	1				10.7	10.7	11.6
H2	1				6.9	6.9	7.7
H3	1				15.4	15.4	16.3
I4	1				8.6	8.6	9
J1	2				26.2	26.2	26.2
K3	1				15.4	15.4	15.4

The times in Table 6-10 are conservative because the actual adjustment time will probably take longer than the values shown. Because the average adjustment rate for a reach will most probably be slower that the maximum observed bend erosion rate, the adjustment time is expected to be greater than the values shown. However, even if the actual erosion rates are assumed to be one-half of the maximum rate, the changes predicted to occur will happen within a normal expected project life of 50 to 100 years.

Comparison of the top widths of the 1940 and 1998 cross sections for the adopted bankfull flows at a constant energy slope showed some sections becoming narrower while others became wider. The average rate of widening is about 0.5 ft/year. As this rate is approximately 5 times less than the maximum rate used to develop Table 6-10, the adjustment time would be about 5 times longer. Looking at the highest value in the table (Reach J1) and multiplying by 5 gives an adjustment time of 125 years. All other sections would adjust more quickly, again showing that the width adjustment should be expected within the life of the project.

6.3.2.2 System-Wide Adjustment

System-wide adjustment will occur when the channel width, meander length and amplitude, and channel slope have all reached quasi-equilibrium conditions. As mentioned, this process is expected to take much longer than the initial changes in width. Scientific prediction of the adjustment time is not possible given the state of the art. Rough calculations were performed assuming that the material removed from a given reach as the channel moves towards equilibrium is transported entirely by the increased flows. These calculations give conservative estimates of the time needed to reach system-wide equilibrium. One such calculation is given below:

Assumptions:

- The study reach is 500 miles in length, and is cut in two 250 mile segments by Baldhill Dam.
- A bottom width of 88 feet (average of the SAM-Brownlie D_{50} regime bottom widths)
- A change in slope of 0.00001 (see Tables 5-8 and 5-9)
- An average sediment weight of 130 pounds per cubic foot

The amount of material scoured is:

250 miles*5280 ft/mile*(250 miles * 5280 ft/mile*0.00001)*0.5*88 feet

$= 766 * 10^6$ cubic feet of sediment
$= 99.7 * 10^9$ pounds of sediment
$= 49.8* 10^6$ tons of sediment

Average annual sediment transport rates for each precision cross section were computed with SAM for all of the hydrologic scenarios using the full 50-year trace. Using a high average annual sediment transport rate from the Wt480 scenario (which gives a conservatively low estimate of time to equilibrium) of 150,000 tons per year yields:

49.8* 10^6 tons of sediment/150,000 tons/year = 332 years

This estimate of time to equilibrium is much greater than the width adjustment time. Actual adjustment time could actually be many hundreds of years, well beyond a normal project lifetime.

7 Morphologic Classification

7.1 General

The Rosgen Stream Classification System (Rosgen, 1996) is intended to classify rivers and to predict their behavior. The Rosgen classification system is based on morphological characteristics such as degree of incision, sinuosity, water surface slope, and other features. For each stream classification type, the Rosgen system provides qualitative predictions of the sensitivity to a disturbance (such as a long-term change in flows), the lateral and vertical stability, and other characteristics such as the tendency to form point bars. The predictive ability of the classification in determining channel response is subject to debate and is not widely accepted. Furthermore, even assuming that the classification system provides valid predictions, it is difficult to draw firm conclusions due to the qualitative nature of the predictions.

Each one of the precision cross sections was classified using the Rosgen system for two purposes: 1) to aid in communication when discussing the channel reaches and, 2) to predict approximate rates at which the morphology of the sections might change in response to the future pumping scenarios. In spite of possible limitations in the predictive capability of the Rosgen system, it was believed that the results would still be valuable when viewed in conjunction with the regime channel and planform analysis results described in Chapters 5 and 6.

7.2 Existing Conditions

The precision cross sections were classified using the existing conditions geometry (based on the 1998 survey). The Rosgen classifications are based on five parameters:

(1) Entrenchment ratio. The top width when the stream is flowing at twice bankfull depth divided by the top width at bankfull. The top widths at twice bankfull depth (used to establish the Rosgen entrenchment ratio) often exceeded the boundaries of the 1998 cross sections. In these cases, visual inspection and comparisons with the 1940 cross sections were made to estimate a top width at twice bankfull depth.

(2) Width/depth ratio. The ratio of the top width at bankfull divided by the mean or average depth. The SAM single cross section models of the 1998 sections, described in Chapter 4, supplied the width/depth ratios.

(3) Sinuosity. The ratio of stream length to valley length. The sinuosities from Chapter 6 were used.

(4) Slope. The slope of the water surface. The slopes used for the Rosgen classifications were the energy slopes from the HEC-RAS model, and were less than 0.001 (the lowest threshold for slope used by the Rosgen system) for all cross sections.

(5) Channel material (silt/clay, sand, gravel, etc.). The sediment gradation curves are described in Chapter 5. The median grain size (D_{50}) from these gradations was used to categorize the channel material.

Table 7-1 provides a summary of the Rosgen stream classifications for the precision cross sections.

Table 7-1. Rosgen Classification for 1998 Precision Cross Sections

Reach and section	HEC-RAS section number	Entrench-ment*	Width/depth category**	Sinuosity	Bed material	Rosgen class
A2-f	48	Moderate / Slight	Moderate to High / Low	Very High	Sand	B5c
B3-a	Between 275 & 276	Moderate	Low / Moderate to High	Very High	Sand	B5c
B3-e	276	Moderate	Low / Moderate to High	Very High	Sand	B5c
C2-d	371	Entrenched	Moderate to High	Very High	Sand	G5c
C2-j	372	Moderate	Low / Moderate to High	Very High	Sand	B5c
D3-a	594	Moderate / Entrenched	Moderate to High / Low	Very High	Silt/Clay	B6c
D3-d	595	Slight	Moderate to High / Low	Very High	Silt/Clay	C6c
D3-f	596	Slight	Low	Very High	Silt/Clay	E6
D3-h	597	Slight	Moderate to High / Low	Very High	Silt/Clay	C6c
D3-k	598	Moderate	Moderate to High / Low	Very High	Silt/Clay	B6c
D3-l	599	Moderate	Moderate to High	Very High	Silt/Clay	B6c
E2-a	685	Slight	Moderate to High / Low	Very High	Silt/Clay	C6c
E2-f	686	Slight	Low	Very High	Silt/Clay	E6
E2-j	687	Slight	Moderate to High	Very High	Silt/Clay	C6c
F2-a	952	Slight	Moderate to High / Low	Very High	Sand	C5c
H2-i	980	Slight	Moderate to High	Very High	Gravel	C4c
H3-f	982	Slight	Moderate to High	Very High	Sand	C5c
I4-a	1019	Moderate	Moderate to High	Very High	Sand	B5c
J1-a	1026	Slight	Moderate to High	Low	Silt/Clay	C6c
J1-e	1027	Slight	Moderate to High	Low	Silt/Clay	C6c
K3-j	1045	Slight	Moderate to High	Very High	Sand	C5c
L1-a	1047	Entrenched / Moderate	Moderate to High	Very High	Sand***	F5

* Entrenchment ratios from 1 to 1.4 are "entrenched," those from 1.4 to 2.2 are "moderate," and those greater than 2.2 are "slight." The Rosgen system allows for entrenchments to vary +/- 0.2 from the classification boundaries of 1.4 and 2.2. Therefore, some entrenchment ratios are "borderline," that is, not definitely in any one category. In these cases, the category where the entrenchment ratio lies appears before the slash, and the category that the entrenchment ratio is near appears after the slash.

** The Rosgen system allows for width/depth ratios to vary +/- 2.0 from the boundary of 12. Therefore, some width/depth ratios are not definitely in any one category. Ratios less than 10 are "Low." Those greater than 14 are "Moderate to High." Those ratios from 10 to 12 are classified as "Low / Moderate to High," while those widths over depths from 12 to 14 are classified as "Moderate to High / Low."

*** The D50 channel material of 2.2 mm is very fine gravel, but very near the border with very coarse sand. Based on field trip observations, the channel material was classified as sand.

According to Rosgen (1996), the B5, B6, and E6 channel types are fairly stable, the C4, C5, and C6 channel types are susceptible to changes in river conditions (such as a changes in flow or sediment), and the G5 channel type is very susceptible to disturbances. A more detailed description of the various channel types is given in the following section.

The Rosgen characterizations of the sensitivity of these channel types to disturbances are summarized in Section 7.4.

7.3 Description of Channel Types

The book *Applied River Morphology* (Rosgen, 1996) should be consulted for a more detailed description of the classification types. Below are a few excerpts from this book describing the channel types found in the Sheyenne River:

B5 Stream Type

> The B5 stream types are moderately entrenched systems with channel gradients of 2-4%. The channel bed morphology is dominated by sand-sized materials and characterized as a series of rapids with irregular spaced scour pools. The average pool-to-pool spacing for the B5 stream type is 3-4 bankfull channel widths. Pool to pool spacing for the B5c (<2% slope) is generally 4-5 bankfull widths. Pool to pool spacing adjusts inversely with stream gradient. The B5 stream type has a moderate width/depth ratio and a sinuosity greater than 1.2. The channel materials are composed predominantly of sand and small gravel with occasional amounts of silt/clay. The B5 stream type is relatively stable where the presence of dense riparian vegetation is noted.

B6 Stream Type

> The B6 stream type is a moderately entrenched system, incised in cohesive materials, with channel slopes less than 4%. The width/depth ratio of the B6 stream type is generally the lowest of all of the B stream types due to the cohesive nature of the silt/clay stream banks. B6 stream types are generally stable due to the effects of moderate entrenchment and lower width/depth ratios. Additionally, riparian vegetation associated with the B6 type is generally very dense, except in arid environments and plays an important role in maintaining channel stability and lower width/depth ratios. These stream types are washload rather than bedload streams, and thus have a characteristically low sediment supply and an infrequent occurrence of sediment deposition.

C4 Stream Type

> The C4 stream type is a slightly entrenched, meandering, gravel dominated, riffle/pool channel with a well-developed floodplain. The stream banks are generally composed of unconsolidated, heterogeneous, non-cohesive, alluvial materials that are finer than gravel-dominated bed material. Consequently, the stream is susceptible to accelerated bank erosion. Rates of lateral adjustment are influenced by the presence and condition of riparian vegetation. Sediment supply is moderate to high, unless stream banks are in a very low erodibility condition. The C4

stream type, characterized by the presence of point bars and other depositional features, is very susceptible to shifts in both lateral and vertical stability caused by direct channel disturbance and changes in the flow and sediment regimes of the contributing watershed

C5 Stream Type

The C5 stream type is a slightly entrenched, meandering, sand dominated, Riffle/pool channel with a well-developed floodplain. Generally, C5 stream channels have gentle gradients of less than 2%. Gradients less than 0.001 are denoted as a C5c- to indicate the slope condition of many C5 stream types. The riffle/pool sequence for the C5 stream type averages 5-7 bankfull channel widths in length. Bed forms such as ripples, dunes, and anti-dunes are prevalent. The stream banks are generally composed of sandy material with stream beds exhibiting little difference in pavement and sub-pavement material composition. Rates of lateral adjustment are influenced by the presence and condition of riparian vegetation. Sediment supply is high to very high, unless stream banks are in very low erodibility condition. The C5 stream type, characterized by the presence of point bars and other depositional features, is very susceptible to shifts in both lateral and vertical stability caused by direct channel disturbance and changes in the flow and sediment regimes of the contributing watershed.

C6 Stream Type

The C6 stream type is slightly entrenched, meandering, silt-clay dominated, riffle pool channel with a well-developed floodplain. Generally, C6 stream channel have gentle gradients of less than 2%. Gradients less than 0.001 are denoted as a C6c- to indicate the very low gradients of many C6 stream types. The C6 stream channel displays a lower width/depth ratio than all of the other C stream types due to the cohesive nature of stream bank materials. The riffle/pool sequence for the C6 stream type is, on average 5-7 bankfull channel widths in length. The stream banks are generally composed of silt-clay and organic materials, with the stream beds exhibiting little difference in pavement and sub-pavement material composition. Rates of lateral adjustment are influenced by the presence and condition of riparian vegetation. Sediment supply is moderate to high, unless stream banks are in a very high erodibility condition. Bedload sediment yields for the stream types are typically low, reflecting the presence of fine bed and bank materials and gentle channel slopes. The C6 stream type is very susceptible to shifts in both lateral and vertical stability caused by direct channel disturbance and changes in flow and sediment regimes of the contributing watershed.

E6 Stream Type

The E6 stream types are channel systems with low to moderate sinuosity, gentle to moderately steep channel gradients, and very low channel width/depth ratios. The E6 stream type is typically seen as a riffle/pool system with the dominant channel materials composed of silt-clay, interspersed with organic materials. Channel slopes are less than 2% with a high number having slopes of less than 0.01%. Due to the inherently stable nature of the bed and banks, this stream type can exist on a wide range of slopes. Sinuosities and meander width ratios decrease, however, with an increase in slope. Streambanks are composed of materials similar to those of the dominant bed materials and are typically stabilized with riparian or wetland vegetation that forms densely rooted sod mats from grasses and grass like plants as well as woody species. Typically the E6 stream channel has high meander width ratios. The E6 stream types are hydraulically efficient forms as they require the least cross sectional area per unit of discharge. The narrow and relatively deep channels maintain a high resistance to plan form adjustment which results in channel stability without significant downcutting. The E6 stream channels are very stable unless the stream banks are disturbed and significant changes in sediment supply and/or streamflow occur.

F5 Stream Type

The F5 stream type is a sand dominated, entrenched, meandering channel, deeply incised in gentle terrain. The "top of bank" elevation for this stream type is much greater than the bankfull stage which is indicative of the deep entrenchment. The F5 stream type can be deeply incised in alluvial valleys or in lacustrine deposits, resulting in the abandonment of former floodplains. The F5 channels have slopes that are generally less than 2%, exhibit riffle/pool bed features, and have width/depth ratios that are high to very high. The dominant channel materials are sand with lesser accumulations of gravel and some silt-clay. Sediment supply in the F5 stream types is moderate to high, depending on stream bank erodibility conditions. Depositional features are common in this stream type, and over time, tend to promote development of a flood plain inside of the bankfull channel. Central and transverse bars are common, and related to the high sediment supply from stream banks and the high width/depth ratio. Stream bank erosion rates are very high due to side slope rejuvenation and mass-wasting process which enhance the fluvial entrainment of eroded bank materials. Riparian vegetation plays a marginal role in streambank stability due to the typically very high bank heights which extend beyond the rooting depth of riparian plants. Exceptions to this are the F5 stream types in the Northeast, Northwest, and Southeast United states where the relatively longer growing seasons and

ample precipitation results in the establishment of riparian vegetation that tends to cover the entire slope face of channel banks.

G5 Stream Type

The G5 stream type is an entrenched, moderately steep, step/pool channel deeply incised in sand materials. Channel sinuosities are relatively low, as are the width/depth ratios. These "sandy gully" stream types transport great amounts of sediment due to the ease of particle detachment and fluvial entrainment. The G5 stream channels are generally in a degradation mode derived from near continuous channel adjustments, due to excessive bank erosion. Bedload transport rates can easily exceed 50% of total load; with active, extensive, consistent channel erosion more typical than not. Exceptions may occur where very dense woody vegetation helps stabilize the toe of the stream bank slopes. The G5 stream type is similar in character to A5 channels, except G5 channel gradients are less than 4% and, tend to be more sinuous with somewhat higher width/depth ratios, due to the gentle channel slopes. The "slope continuum" concept is applied for the "gully" stream types if the observed reach exhibits slopes less than 2%. Such a reach is given the designation of G5c. The lower gradient gully reaches are generally observed developing within a previously meandering, low gradient system with floodplains such as C5 situated in wide alluvial valleys. These stream types are very sensitive to disturbance and tend to make significant channel adjustments to changes in flow regime and sediment supply from the watershed.

7.4 Future Conditions

Regime geometry for future scenarios was predicted using SAM for each of the precision cross sections. These regime cross sections were also classified using the Rosgen system. Each of the five parameters required for the Rosgen classification was examined:

(1) Entrenchment ratio. In the previous existing conditions categorization, most entrenchments ratios were clearly in a particular category. Only two of the 21 precision cross sections impacted by the future pumping (A2-f and D3-a) had entrenchment ratios near categorization boundaries. It was assumed that the other 19 sections, whose categorizations were not borderline, would need to undergo significant morphological changes to shift to another category. Because of this, and because regime methods cannot predict entrenchment ratios, all future condition entrenchment ratios were assumed to be the same as the existing condition entrenchment ratios.

(2) Width/depth ratio. This ratio is directly predicted by the SAM regime/stable channel routines.

(3) Sinuosity. As discussed in Chapter 6, sinuosity is not expected to change significantly.

(4) Slope. For all precision cross sections, slope was predicted by the SAM regime method to be less than the 0.001 threshold used in the Rosgen classification system.

(5) Channel material. There is no basis for expecting the channel material to change at any section.

Of the five parameters, only the width/depth ratio could change enough to cause a reclassification from the existing conditions. Table 7-2 provides the width/depth ratios for 1998 cross sections (existing conditions) as well as the SAM regime geometries. Section L1-a is excluded from this table since it is upstream of the proposed flow increases due to pumping.

Note that in Table 7-2, the SAM regime width/depth ratios for the historical and future traces are nearly identical at most cross sections. Therefore, it was only necessary to classify the SAM regime geometry based on the historical bankfull flows. The Rosgen classifications for all the SAM regime geometries, both historical and future, are identical at each cross section.

Table 7-3 summarizes the differences between the width/depth categories for the 1998 surveyed cross sections and the SAM regime geometries. The table also provides the Rosgen classification for the SAM regime geometry, for those cases where they differ from the Rosgen classification for the existing conditions (1998) geometry.

Three of the 21 precision cross sections were classified differently based on the SAM regime geometry when compared to the Rosgen classifications based on the 1998 surveyed cross sections (existing conditions). However, these classification changes are **not** the result of pumping since they apply equally to the SAM predicted historical geometry as well as all the SAM predicted future geometries for the various future flow scenarios.

The width/depth ratios from the 1998 cross sections are in many cases significantly different from those of the 1940 cross sections. Visual inspection of the 1940 and 1998 cross sections (Appendix G) also confirms that many sections have changed substantially. Most of the sections have moved toward the SAM regime dimensions, as discussed in Chapter 5.

By comparing the 1940 and the 1998 width/depth ratios, we can check to see how quickly the ratios moved toward the SAM predicted regime width/depth ratio. For example, the A2-f section had a width depth ratio of 9.8 in 1940, and 12.3 in 1998. The SAM predicted regime width/depth ratio is 23.3. The actual width/depth ratio has moved closer to the SAM regime value, but by very little. This agrees with the Rosgen prediction that the B5c stream type is not very sensitive to disturbances. Table 7-4 provides a summary of the actual and predicted sensitivities of the precision cross sections to morphological changes. Although Section L1-a is not affected by future pumping, it is included in Table 7-4 as check of the Rosgen predicted sensitivities of channel morphology.

Table 7-2. Width/Depth Ratios by Cross Section using SAM Regime Geometry

Reach	1998 cross section	SAM predicted stable (regime) geometry based on historical and future trace bankfull flows						
		HISTOR	Mdnp	Md300	Md480	Wtnp	Wt300	Wt480
A2-f	12.3	23.3	23.2	23.1	23.2	23.0	23.1	23.1
B3-a	11.2	25.7	25.7	25.7	25.9	25.7	25.6	25.5
B3-e	10.5	16.2	16.2	16.1	16.2	16.0	16.0	16.1
C2-d	29.0	28.7	28.9	28.9	28.7	28.9	28.7	28.7
C2-j	11.4	31.1	31.4	31.4	31.4	30.8	31.0	31.0
D3-a	12.1	8.9	8.9	8.9	8.9	8.9	8.9	8.9
D3-d	13.4	9.5	9.5	9.5	9.4	9.5	9.5	9.5
D3-f	8.3	24.4	24.3	24.3	24.3	24.3	24.3	24.4
D3-h	13.2	12.5	12.5	12.5	12.6	12.5	12.5	12.5
D3-k	13.3	10.3	10.2	10.2	10.3	10.3	10.3	10.2
D3-l	14.5	10.2	10.2	10.2	10.2	10.1	10.1	10.0
E2-a	13.2	13.1	13.0	13.0	13.0	13.0	13.0	13.0
E2-f	9.8	15.2	15.2	15.2	15.3	15.1	15.2	15.2
E2-j	18.9	12.3	12.4	12.4	12.3	12.3	12.3	12.3
F2-a	12.2	19.5	19.6	19.3	19.3	19.3	19.3	19.3
H2-i	19.1	13.9	13.6	13.6	13.6	14.8	14.8	14.8
H3-f	17.5	43.2	43.2	42.9	43.2	44.4	44.4	43.9
I4-a	17.8	19.1	19.3	18.9	19.2	18.7	18.7	18.8
J1-a	74.7	55.3	55.3	54.6	55.6	57.3	57.3	57.7
J1-e	50.0	48.8	48.1	48.1	49.1	50.7	50.7	51.1
K3-j	17.3	16.7	16.7	16.7	16.7	17.5	17.5	17.3

The Rosgen classification system does a reasonably good job of predicting the rate of change of the channels. Eleven sections changed at approximately the rate the Rosgen classification suggested, while two did not. Results at three sections were not conclusive, while 4 other cross sections could not be analyzed as the predicted SAM width/depth ratio was opposite the direction of the historical trend. No determination could be made for two additional cross sections because of the negligible change in the width/depth ratio between 1940 and 1998.

The qualitative rate of change predictions given in Table 7-4 can be considered in conjunction with the width change predictions in Chapter 6. Those reaches with a low or intermediate predicted rate of width/depth change may be expected to take longer to change than the conservatively low values presented in Table 6-8.

Table 7-3. Rosgen Classification of Existing Condition (1998) Cross Sections and SAM Regime Geometry

Reach and section	Rosgen class based on 1998 cross section	Sensitivity of the class to disturbances in flow or sediment transport, per Rosgen	Width/depth category for 1998 cross section	SAM predicted width/depth ratio for historical conditions and all future scenarios	Rosgen class for SAM predicted regime geometry, if different*
A2-f	B5c	Low	Moderate to High / Low	Moderate To High	-
B3-a	B5c	Low	Low / Moderate to High	Moderate To High	-
B3-e	B5c	Low	Low / Moderate to High	Moderate To High	-
C2-d	G5c	Very High	Moderate to High	Moderate To High	-
C2-j	B5c	Low	Low / Moderate to High	Moderate To High	-
D3-a	B6c	Low	Moderate to High / Low	Low*	
D3-d	C6c	High	Moderate to High / Low	Low	E6
D3-f	E6	Low	Low	Moderate To High	C6c
D3-h	C6c	High	Moderate to High / Low	Moderate To High / Low	-
D3-k	B6c	Low	Moderate to High / Low	Low / Moderate To High	-
D3-l	B6c	Low	Moderate to High	Low / Moderate To High	-
E2-a	C6c	High	Moderate to High / Low	Moderate To High / Low	-
E2-f	E6	Low	Low	Moderate To High	C6c
E2-j	C6c	High	Moderate to High	Moderate To High / Low	-
F2-a	C5c	High	Moderate to High / Low	Moderate To High	-
H2-i	C4c	High	Moderate to High	Moderate To High / Low	-
H3-f	C5c	High	Moderate to High	Moderate To High	-
I4-a	B5c	Low	Moderate to High	Moderate To High	-
J1-a	C6c	High	Moderate to High	Moderate To High	-
J1-e	C6c	High	Moderate to High	Moderate To High	-
K3-j	C5c	High	Moderate to High	Moderate To High	-

* Per the Rosgen system, all B streams with moderate entrenchment ratios should have width/depth ratios that are classified as "moderate to high." In the existing conditions (1998) cross sections, all B classified sections had entrenchment ratios greater than 10. This makes all of them moderate to high, (ratio > 12) or potentially moderate to high within the error limits given by Rosgen (ratio > 10). The D3-a section has a SAM regime predicted width/depth ratio of 9.5 which is clearly in the low category. Rosgen mentions, however, that the B6 stream type has the lowest width/depth ratios of the all B stream types, due to cohesive banks. Because of this, and because the primary categorization is by entrenchment ratio, the SAM regime geometry for the D3-a section was classified as B6c, unchanged from the 1998 classification.

Table 7-4. Analysis of Rosgen Stream Type Sensitivity Based on 1940, 1998, and SAM Predicted Width/Depth Ratios

Reach and section	Rosgen class based on 1998 cross section	Sensitivity of class to flow or sediment transport disturbance per Rosgen	1940 width/ depth ratio	1998 width/ depth ratio	SAM predicted width/ depth ratio (historical bankfull flow)	1940 to 1998 qualitative change in width/ depth ratio*	Rate of change agrees with Rosgen sensitivity?
A2-f	B5c	Low	9.8	12.3	23.3	Low	Yes
B3-a	B5c	Low	9.3	11.2	25.7	Low	Yes
B3-e	B5c	Low	7.7	10.5	16.2	Low	Yes
C2-d	G5c	Very High	14.7	29.0	28.7	High	Yes
C2-j	B5c	Low	10.2	11.4	31.1	Low	Yes
D3-a	B6c	Low	15.4	12.1	8.9	Intermediate	Perhaps
D3-d	C6c	High	27.9	13.4	9.5	High	Yes
D3-f	E6	Low	11.1	8.3	24.4	**	**
D3-h	C6c	High	17.1	13.2	12.5	High	Yes
D3-k	B6c	Low	16.2	13.3	10.3	Intermediate	Perhaps
D3-l	B6c	Low	16.1	14.5	10.2	Low	Yes
E2-a	C6c	High	36.0	13.2	13.1	High	Yes
E2-f	E6	Low	13.2	9.8	15.2	**	**
E2-j	C6c	High	31.7	18.9	12.3	High	Yes
F2-a	C5c	High	12.2	12.2	19.5	Low	No
H2-i	C4c	High	27.2	19.1	13.9	Intermediate	Perhaps
H3-f	C5c	High	20.0	17.5	43.2	**	**
I4-a	B5c	Low	13.8	17.8	19.1	High	No
J1-a	C6c	High	60.5	74.7	55.3	**	**
J1-e	C6c	High	51.5	50.0	48.8	***	***
K3-j	C5c	High	17.5	17.3	16.7	***	***
L1-a	F5	High	15.6	20.2	23.27	High	Yes

* Those sections that moved 35% of the way or less toward the SAM predicted width/depth ratio were deemed to have low change, those sections that moved 65% of the way or more toward the SAM predicted width/depth ratio were deemed to have high change, and those sections whose width/depth ratio moved between 35% and 65% of the way toward the SAM predicted with/depth ratio were deemed to have an intermediate rate of change.

** No determination can be made because the SAM predicted width/depth ratio is not in the same direction as the historical trend.

*** No determination can be made because of the small difference in the SAM predicted width/depth ratio versus the 1940 and 1998 values.

8 Vegetation

8.1 General

This section presents an overview of the possible effects of increased flows and long-term changes in the channel morphology of the Sheyenne River Channel on the riparian vegetation due to pumped releases from Devil's Lake. Conversely, a qualitative examination of the possible effects of long-term changes in riparian vegetation on the Sheyenne River channel morphology is also presented.

8.2 Methodology

Because a field vegetation survey was not conducted for this study, a representative list of riparian vegetation species was determined from a review of the Baldhill Dam and Lake Ashtabula Operational Management Plan (USACE, 1993c), which references the study titled, "Soil Survey, Vegetation Analysis, and Interpretation of the Baldhill Dam/Lake Ashtabula Project Lands, North Dakota", North Dakota State University, 1982, by W.T. Barker and H. Omodt. It was assumed for the purpose of this study that the riparian species found near Lake Ashtabula and listed in the above report, are similar to the vegetation along the Sheyenne River study reach.

Several studies related to the flood tolerance of vegetation were obtained and reviewed. The primary reference used to determine the flooding tolerance for the list of selected species was the publication, "Flood tolerance in plants: a state-of-the-art review", (Whitlow and Harris, 1979). The baseline information obtained was used to compare the flooding effects for the "no-pumping" (future without project) and "pumping" alternatives.

The long-term channel change effects on vegetation and the effects of long-term vegetation changes on channel morphology were assessed qualitatively using the results of the geomorphic analysis.

8.3 Riparian Vegetation Communities

The riparian vegetation species along the Sheyenne River were assumed to be similar to those found near Lake Ashtabula and are taken from the Baldhill Dam and Lake Ashtabula Operational Management Plan (USACE, 1993c). The vegetation communities in the Sheyenne River Basin can be divided into four broad physiognomic groups: grassland, wetland, shrubland, and woodland. The vegetation communities include the high prairie, mid prairie, disturbed mid prairie low prairie, disturbed low prairie, meadow, marsh, prairie thicket, river bottom forest, prairie forest, and shelterbelts (USACE, 1993c).

The high prairie communities are located on steep slopes and knolls, which lose most of their moisture through runoff. The mid prairie includes level areas and mid-slopes where the amount of moisture available approximates that received from precipitation. The low prairie generally includes lower slopes that receive moisture from runoff but have well-drained soils. The meadow community is found where the gravitational water remains in

the upper soil horizon for at least several weeks during the spring of each year. The marsh community occurs where there is water in the plant-rooting zone for several months each year and is marked by shallow and deep marsh. The prairie thicket community develops on north facing slopes and in drainage ravines, which receive extra moisture from runoff. There are numerous shelterbelts, which were planted mainly for recreation and wildlife habitat purposes. Introduced species such as smooth bromegrass and Kentucky bluegrass dominate much of the grassland. The river bottom forest community occurs along the river and is the most diverse of all the vegetation communities.

This study concentrates on the river bottom forest community because it includes riparian species that would be most directly impacted by the proposed project. The dominant tree species in the river bottom forest are green ash, box elder, and American elm. Secondary tree species include basswood, cottonwood, and bur oak. The herbaceous lay is composed of prairie grasses and forbs (broadleaf flowering plants distinct from grasses, sedges, and bushes). Prairie grasses may include Kentucky bluegrass, smooth brome, blue grama, western wheatgrass, big bluestem, little bluestem, switchgrass, and porcupine needlegrass. Common forbs found in meadow areas may include Canada thistle, sow thistle, narrowleaf sunflower. Forbs in shallow marsh areas near the river may include waterparsnip, rough bugleweed, wild mint, swamp betony, European water plantain, arrowhead, common reed, alkali bulrush, giant burreed. Forbs in the deep marsh may include tule bulrush, softstem bulrush, common cattail, and narrowleaf cattail. Shrubs found in this community include common chokecherry, juneberry, Virginia creeper, Missouri gooseberry, western snowberry, riverbank grape, common pricklyash, poison ivy, and sandbar willow. Table 8-1 lists these species and their relative tolerance to flooding.

The flooding tolerance is described in a relative sense using the terms very tolerant, tolerant, somewhat tolerant, and intolerant (Whitlow and Harris, 1979). The flooding tolerance of species that could not be found in the literature is listed as unknown. Very tolerant species are able to survive deep, prolonged flooding for more than one year. Tolerant species are able to survive deep flooding for one growing season, with significant mortality occurring if flooding is repeated the following year. Somewhat tolerant species are able to survive flooding or saturated soils for 30 consecutive days during the growing season. Intolerant species are unable to survive more than a few days of flooding during the growing season without significant mortality.

Table 8-1. List of Riparian Species and Their Relative Tolerance to Flooding

Common Name	Scientific Name	Relative Flood Tolerance
Trees		
Green ash	*Fraxinus pennsylvanica*	Very tolerant to tolerant
Box elder	*Acer negundo*	Tolerant
American elm	*Ulmus Americana*	Tolerant
Basswood	*Tilia Americana*	Somewhat tolerant
Cottonwood	*Populus deltoids*	Tolerant
Bur oak	*Quercus macrocarpa*	Tolerant
Shrubs		
Common chokecherry	*Prunus virginiana*	Unknown
Juneberry	*Amelanchier alnifolia*	Unknown
Virginia creeper	*Parthenocissus inserta*	Tolerant
Missouri gooseberry	*Ribes missouriense*	Somewhat tolerant
Western snowberry	*Symphoricarpos occidentalis*	Unknown
Riverbank grape	*Vitis reparia*	Tolerant
Common pricklyash	*Zaqnthoxylum americanum*	Unknown
Poison ivy	*Toxicodendron rydbergii*	Tolerant
Sandbar willow	*Salix exigua*	Somewhat tolerant
Forbs		
Canada thistle	*Cirsium arvense*	Unknown
Sow thistle	*Sonchus uliginosus*	Somewhat tolerant
Narrowleaf sunflower	*Helianthus maximilianii*	Unknown
Waterparsnip	*Sium suave*	Unknown
Rough bugleweed	*Lycopus aspera*	Unknown
Swamp betony	*Stachys palustris*	Unknown
European water plaintain	*Alisma plantago-aquatica*	Unknown
Arrowhead	*Sagittaria cuneata*	Somewhat tolerant
Alkali bulrush	*Scirpus maritimus*	Unknown
Giant burreed	*Sparganium coccinea*	Unknown
Tule bulrush	*Scirpus acutus*	Unknown
Softstem bulrush	*Scirpus validus*	Somewhat tolerant
Common cattail	*Typha latifolia*	Somewhat tolerant
Narrowleaf cattail	*Typha augustifolia*	Unknown
Grasses		
Kentucky bluegrass	*Poa pratensis*	Somewhat tolerant
Smooth brome	*Bromus inermis*	Unknown
Blue grama	*Bouteloua gracilis*	Unknown
Western wheatgrass	*Agropyron smithii*	Unknown
Big bluestem	*Andropogon gerardi*	Intolerant
Little bluestem	*Andropogon scoparius*	Intolerant
Switchgrass	*Panicum virgatum*	Somewhat tolerant
Porcupine needlegrass	*Stipa spartea*	Unknown

8.4 Flooding Effects on Vegetation

Several studies conducted independently have established that flooding can adversely impact vegetation. Flooded conditions cause the depletion of free oxygen in the soil. The absence of oxygen creates a reducing environment in the soil that favors the growth of anaerobic bacteria. These organisms produce a variety of byproducts that are toxic to plants. Therefore, under flooded conditions, a plant has to contend with a lack of oxygen as well as toxic soil conditions (Whitlow and Harris, 1979).

Riparian vegetation is especially sensitive to changes in minimum and maximum flows. It is possible to cause substantial changes in riparian vegetation without changing mean annual flow (Auble et al., 1994).

In general, the duration of inundation rather than the depth of inundation appears to be the determining factor for the survival of vegetation under flooding conditions. The duration of flooding that vegetation can endure depends upon various factors including temperature, soil type, water depth, and the age of the stand.

The seasonal timing of flooding is very important to the survival of woody plants. Dormant season (winter) flooding usually has little effect on woody plants. Plants tend to withstand longer periods of flooding at lower temperatures because the oxygen requirements are lesser in cooler weather. In contrast, flooding during the growing season (spring and summer) can severely damage developing vegetation. Inundation during high midsummer temperatures can easily kill many species.

The depth of flooding during the growing season can influence the degree of injury to, or the survival of, woody plants.

The age of a tree is also an important factor in determining the tolerance to flooding. In general, older, taller, and more mature trees that have their leaves above water may be subjected to less severe conditions than seedlings.

Woody species and trees are one of the hardest hit vegetation classes because they cannot survive lengthy inundation. Green ash appears to be the most tolerant tree species followed by cottonwood, American elm, box elder, and basswood.

Some grasses are more tolerant than trees to longer periods of seasonal inundation. Field studies conducted by McKenzie in Western Canada on reed canary grass (*Phalaris arundanacea*) and western wheat grass (*Agropyron smithii*) showed that these species exhibited strong tolerance to long periods of flooding (Rhoades, 1967).

In this study, flooding was considered to have occurred whenever the future simulated flows over the next 50 years equaled or exceeded the adopted historical bankfull flows at each cross-section. For example, the historical adopted bankfull flow for section A2-f (see Section 4.5) is 1,400 cubic feet per second (cfs). Therefore, future flooding was considered to occur when the flow exceeded 1,400 cfs. The future conditions pumped flow alternatives (300 cfs and 480 cfs) for the moderate and wet climate scenarios were

compared with the corresponding "no-pump" alternatives to determine the additional time in which overbank flooding greater than or equal to a specified duration would occur. Because the duration of flooding is critical to determining the effect on vegetation, the comparison was based on the number of days of continuous flooding. The comparison was made for flood flows that exceeded bankfull for at least 1, 5, 10, 15, 20, 30, 40, 50, 75, and 150 continuous days.

The results indicate that under the moderate climate scenario over the next 50 years, compared to the "no-pump" alternative, the 300 cfs constrained pumping alternative may cause the flow to exceed bankfull and result in up to 50 continuous days of additional flooding during at least 1 or 2 of those years. For the 480 cfs unconstrained pumping alternative under the moderate climate scenario, the flow may exceed bankfull and cause up to 150 continuous days of additional flooding during at least 4 years out of the 50.

Compared to the "no-pump" alternative under the wet climate scenario, the 300 cfs constrained pumping alternative may cause the flow to exceed bankfull and result in 30 to 50 days of continuous flooding during at least 3 to 7 years out of the 50 analyzed. Similarly, the 480 cfs unconstrained pumping alternative under the wet climate scenario may cause the flow to exceed bankfull and result in up to 150 days of continuous flooding during at least 29 years out of the 50. This additional flooding is expected to occur mainly in the upper reaches of the Sheyenne (approximately section H3-f to section K3-j).

A comparison of the flood tolerance of various species to the projected flooding duration of the pumping alternatives shows that all species listed as "intolerant" and "somewhat tolerant" cannot be expected to survive the additional flooding due to the 480 cfs unconstrained pumping for either the moderate or wet scenarios. The 300 cfs constrained pumping alternative can be expected to cause some flooding damage from which the vegetation could be expected to recover, provided flooding is not repeated in consecutive years.

It was concluded from the above comparison that although both pumping alternatives have the potential to damage the floodplain vegetation to varying extents, the 300 cfs constrained pumping alternative would cause much less damage than the 480 cfs unconstrained pumping alternative for both the moderate and the wet climate scenarios.

The increased flows in the river due to pumping may have other indirect adverse effects apart from flooding. Flow alteration downstream of dams and channel straightening activities can cause stream channel degradation, a fact well documented in the literature. The effect of altered flow regimes downstream of dams on riparian trees such as willows, cottonwoods, and poplars has also been widely studied. Riparian vegetation establishment is dependent upon the dominant fluvial geomorphic processes that form surfaces suitable for establishment. Successful establishment from seed occurs only in channel positions that are moist, bare, and protected from removal by subsequent disturbance. Point bars form ideal surfaces for the growth of trees (Scott et al., 1996). If

depositional surfaces such as point bars are lost as a result of processes such as degradation, the successful establishment from seed is prevented.

Similarly, if depositional surfaces such as point bars remain continuously inundated during the active growing season due to pumped flows, the successful establishment from seed on these surfaces will be prevented. The active growing season usually lasts from May through October and most of the pumped releases into the Sheyenne River would occur during this season. To evaluate the effect of the maximum increases in stage on in-channel depositional surfaces, a range in maximum depth increase of 4 to 8 feet was assumed. This value is based on field observations and the assumption that a 4 to 8 feet increase in stage would inundate most depositional surfaces. It was further assumed that this increase in stage would have to be continuously sustained for 150 days or more to prevent the successful establishment of vegetation.

A comparison of the "no-pump" flow depths to the flow depths for the two pumping alternatives under the moderate and wet climate scenarios during the active growing season was made for 50 years into the future. For the moderate climate scenario, the 300 cfs constrained pumping alternative does not cause any significant increase in flow depth. The 480 cfs unconstrained pumping alternative could cause 4 to 7 feet of increase in stage above what it would be without pumping during an additional 1 to 5 years out of the 50 under the moderate climate scenario.

For the wet climate scenario, the 300 cfs constrained pumping alternative could cause 4 to 6 feet of increase in stage above what it would be without pumping during 2 to 8 years out of the 50, mostly in the upper reaches. The 480 cfs unconstrained pumping alternative for the wet climate scenario could cause up to 7 feet of increase in stage during as many as 22 of the 50 years.

The above results indicate that though both the pumping alternatives have the potential to prevent the establishment of seed on riverine depositional surfaces, the 300 cfs constrained pumping alternative would cause much less damage than the 480 cfs unconstrained pumping alternative for both the moderate and wet climate scenarios.

Dr. Bonnie Alexander, Assistant Professor of Biology at Valley City State University in Valley City, North Dakota is familiar with the Sheyenne River Valley vegetation and actively conducts research on vegetation in that area. Dr. Alexander was contacted by telephone and reported the presence of an exotic, invader species called the Eurasian water milfoil (*Myriophyllum spicatum*) in a backwater area of the Sheyenne River near Valley City, North Dakota. According to Dr. Alexander, this species could propagate downstream more easily as a direct consequence of increasing flows in the Sheyenne. Eurasian milfoil spreads by fragmenting and transporting itself downstream through flowing water. Each plant fragment can then take root and grow into a new plant. Further investigation is recommended to verify the presence and effect of this species.

8.5 Vegetation and Bank Stability

Riparian vegetation has an important effect in stabilizing streambanks. In general, all root systems reinforce the soil and increase stability. Fine roots are more useful than thick roots. Most banks devoid of vegetation will collapse when they are saturated with water. Riparian vegetation improves the drainage of bank soils by using the water present in the banks and increases stability. Riparian vegetation such as grasses can decrease the velocity and the erosive action of water. The surcharge or the weight of the vegetation usually does not have an affect on bank stability unless it is located on steep banks that are not capable of supporting themselves. In some cases, the weight of the vegetation can decrease the stability of the bank depending on the slope of the bank, and type of soil. For example, the weight of large trees on the top of a steep cutbank slope can actually trigger bank failure, as was observed during the field visit.

Bank erosion and failure are natural stream channel processes. Bank erosion is the particle-by-particle loss of the bank material due to the shear stresses exerted by the water on the banks. The particle-by-particle loss can be observed along exposed banks that are devoid of vegetation. Bank failure is the sudden collapse of a portion of the bank material into the river. Bank failures are most easily observed along cutbanks in meander bends and occur due to the removal of the bank material along the toe. Although bank erosion and failure are natural processes, the rates of bank erosion or failure can be accelerated by changes in the hydraulic and geomorphic variables.

8.6 Long-Term Channel Change Effects on Vegetation

The Sheyenne River is a typical low-gradient meandering stream with low width-depth ratios. The banks are generally well vegetated with grasses and trees.

The geomorphic analysis examined the trends in the historic, current, and future channel dimensions of the Sheyenne River Channel. The trends in channel width are mixed and the river has been narrowing in some reaches and widening in others since 1940. However, it is believed that the Sheyenne River channel has been generally adjusting its dimensions towards regime conditions for the last 60 years and is currently relatively stable (see Chapter 5).

The geomorphic analysis also examined the predicted long-term channel changes using the regime theory. The results indicate that compared to the “no-pump” condition, the future change in regime channel dimensions due to pumping are minor to insignificant. The channel width is predicted to increase by a maximum of 3 feet for the moderate trace with a pumping rate of 300 cfs, and a maximum of 4 feet for the moderate trace with a pumping rate of 480 cfs. Similarly, the channel width will increase by a maximum of 2.5 feet for the wet trace with a pumping rate of 300 cfs, and a maximum of 5 feet for the wet trace with a pumping rate of 480 cfs. The predicted channel depth change is insignificant (less than 0.25 feet) for both pumping alternatives. This indicates that some bank erosion and minor bank failures might be expected, however, the future channel stability should not be significantly altered as a result of the proposed pumping.

It should be noted that the geomorphic analysis does not account for the stabilizing influence of riparian vegetation because most geomorphic techniques neglect the presence of vegetation. This means that the predicted channel width increases are conservative estimates and the actual width increases should be less than predicted.

Field evidence indicates eroding cutbanks around meander bends and failed banks with fallen trees at some locations. There is an abundance of riparian grasses and trees that help stabilize the banks. The current channel instability observed at cutbanks around meander bends is normal. In general, the channel appeared to be relatively stable. The bank erosion observed at some locations may be attributed to greater flows in the river due to the higher than normal precipitation in recent years.

Localized channel instability may occur if the flows are increased due to pumping over a long period, and as the channel tries to adjust to the new flow regime. The increased flows will cause increased stages and durations of inundation. The banks will be more saturated than in the past. Banks without vegetation may not be able to drain the excess moisture and localized slumping may occur. Shear stresses and velocities along the bed and banks will also be increased which in turn will increase the rate of bank erosion. It may be expected that the banks will fail at some locations and the river will widen at these locations until a regime condition or dynamic equilibrium is reached.

Although the existing riparian vegetation increases the resistance of the bank to erosion and failure, it is expected that some vegetation along the edges of the banks will be lost as the banks widen. This is because the current vegetation is not thick enough and bank failure is evident in locations of increased hydraulic stresses. The loss of vegetation along the banks will make the banks more susceptible to erosion. The failed bank material will be deposited along the toe of the banks and will be gradually entrained.

Based on the above discussion it was concluded that the effect of long-term channel change will be limited to near-bank riparian vegetation loss in some reaches due to localized bank failures and may be considered minor in nature.

8.7 Long-Term Vegetation Changes Effects on Channel Morphology

Based on the preceding discussions of long-term flooding effects and channel change, the long-term vegetation change for the 300 cfs constrained pumping alternative for the moderate and wet climate scenarios is expected to be minor. Therefore, the influence of long-term vegetation changes for this alternative on the channel morphology is also expected to be of a minor nature.

The previous analyses predicted that the long-term flooding effects due to the 480 cfs unconstrained pumping alternative for both the moderate and wet climate scenarios can have a significant adverse impact on vegetation. The loss of near-bank riparian vegetation as well as the loss of vegetation in the floodplain will have negative effects on the bank stability. The lack of vegetation will decrease the drainage through the banks and the floodplain soils resulting in over-saturation and increased water tables. A direct result could be widespread bank failures and increased overland erosion that could clog

the channel with large amounts of eroded sediment until quasi-equilibrium conditions are reached. However, the loss of vegetation is thought to have more of an effect on the rate of erosion to reach the predicted ultimate values (discussed in preceding chapters) rather than the values themselves.

8.8 Conclusions

Both pumping alternatives have the potential to damage the floodplain vegetation to some extent. However, the 300 cfs constrained pumping alternative would cause much less damage than the 480 cfs unconstrained pumping alternative under either the moderate or the wet climate scenario.

The species listed as "intolerant" and "somewhat tolerant" in Table 8-1 cannot be expected to survive the increased inundation due to the 480 cfs unconstrained pumping alternative for both the moderate and wet scenarios. The 300 cfs constrained pumping alternative can be expected to cause some flooding damage from which the vegetation could be expected to recover, provided flooding is not repeated in consecutive years.

It should be noted that a detailed field vegetation survey was not conducted as a part of this study. The species listed in Table 8-1 are based on the assumption that the vegetation near Lake Ashtabula is similar to that along the Sheyenne River corridor. We recommend that the presence of these species and their corresponding flooding tolerance be verified by a plant biologist.

Both pumping alternatives have the potential to prevent the establishment of seed on riverine depositional surfaces. However, the 300 cfs constrained pumping alternative would cause much less damage than the 480 cfs unconstrained pumping alternative for both the moderate and wet climate scenarios.

The effect of long-term channel change on the vegetation will be limited to near-bank riparian vegetation loss in some reaches due to localized bank failures and may be considered minor in nature.

The influence of long-term vegetation changes for the 300 cfs constrained pumping alternative on the channel morphology is expected to be of a minor nature for both the moderate and wet climate scenarios. However, long-term vegetation changes due to the 480 cfs unconstrained pumping alternative could have significant adverse impacts on channel stability for both climate scenarios. The loss of vegetation is thought to have more of an effect on the rate of erosion to reach the predicted ultimate values (discussed in preceding chapters) rather than the values themselves.

9 Predicted Project Effects

9.1 General

Specific analyses to estimate changes in the geomorphology of the Sheyenne River for both future without project (no pumping) and with project (pumping) conditions were described in previous chapters of the report. This chapter summarizes the overall impact of the proposed project on the River.

9.2 Changes in Channel Dimensions

Changes in channel dimensions were predicted by selecting the dominant (or channel forming) discharge at each precision cross section (Chapter 4) and applying these to regime equations (Chapter 5). The SAM stable channel methodology, using the Brownlie D_{50} equation for sediment concentration, was found to predict channel parameters for existing conditions closest to those observed. Therefore, this relationship was also used to predict future channel dimensions. In addition, it was noted that from 1940 to 1998, for most of the precision cross sections, hydraulic parameters were changing in a direction consistent with regime equation predictions.

For future conditions, top width, average depth, and slope were examined for six different scenarios which were classified by future climatic conditions (moderate or wet) and the amount of pumping considered (no pump, 300 cubic feet per second (cfs) constrained, and 480 cfs unconstrained). Each scenario is labeled first by the future climate and then by the pumping amount to yield the following abbreviations for the 6 scenarios: Mdnp, Md300, Md480, Wtnp, Wt300, and Wt480.

Under moderate climate pumping scenarios, top widths are expected to change only slightly from no pumping futures: up to 3 feet for the 300 cfs scenario and 4 feet for the 480 cfs scenario. For wet future pumping scenarios, top widths also will increase only 3-5 feet over the no pumping scenario results. Changes in depth are predicted to be negligible for all of the pumping versus no pumping futures. Adjustments in channel slope are also expected to be very minor.

9.3 Changes in Planform

Comparison between the river planform in 1998 and as early as 1951 shows that the river appears to be in a quasi-stable state. The proposed change in flow in the river will affect this stable state and the river will attempt to establish a new stable state. According to theoretical calculations the river will change its meander length, meander amplitude, and channel shape to accomplish this.

Theoretical equations that predict meander length and amplitude as a function of channel width were applied using 1998 channel widths and the results then compared with measured values from the 1998 orthophotographs. The comparison showed mixed agreement between the computed and measured values. However, as the focus of the study is on the *change* in these parameters between no pump and pumping conditions, and because other methods are not currently available, the equations were applied to

future pump and no pump alternatives under both climatic scenarios. In general, changes due to project conditions were small, with higher (480 cfs) pumping scenario causing greater change than the lower (300 cfs) one.

Changes in the predicted meander length between the with and without pumping futures are relatively small for the moderate climate scenarios. Maximum changes of 33 feet and 44 feet were predicted for the Md300 and Md480 scenarios, respectively. These changes would be applied to the entire meander length, between 500 and 1,500 feet for existing conditions. The results for the wet climate scenarios follow a similar pattern, with a predicted maximum increase in meander length of 28 feet and 57 feet for the Wt300 and Wt480 scenarios, respectively.

The predicted change in meander amplitude between with and without project conditions is also small, with maximum values of 14 feet and 19 feet for the Md300 and Md480 scenarios, respectively. Maximum predicted changes between with and without project conditions are 12 feet and 24 feet for the Wt300 and Wt480 scenarios, respectively. These predicted changes would be applied to existing meander amplitudes, measuring 60 to 650 feet under current conditions.

9.4 Changes in Erosion Rates

The current erosion rate was calculated to be 27 acres per year for the length of the Sheyenne River studied. This rate takes into account only erosion occurring while the river is in its current quasi-stable state. After the river is removed from this steady state it is difficult to determine what time period is necessary to establish a new steady state. It can however be assumed that erosion rates will increase during that time, particularly in the wet scenarios where the difference between predicted and current theoretical calculations is the largest. Computed rates presented in Chapter 6 predict that width adjustments should occur within the life of the project (50-100 years or less) while overall system adjustment will take much longer, perhaps 300 to 1,000 years.

9.5 Stream Classification

Precision cross sections were classified using the Rosgen system (as described in Chapter 7) for two purposes: 1) to aid in communication when discussing the channel reaches and, 2) to predict approximate rates at which the morphology of the sections might change in response to the future pumping scenarios. In spite of possible limitations in the predictive capability of the Rosgen system, the results are still useful when viewed in conjunction with the regime channel and planform analysis results described in Chapters 5 and 6. Predicted channel adjustment rates could be slower than those estimated from the regime channel and planform analyses for certain cross sections where the Rosgen system predicts slow rates of adjustment.

9.6 Vegetation

The increased flows from the pumping scenarios will cause increased stages and durations of inundation. The amount of inundation experienced by various plant species will have a direct effect on plant survivability. In addition to potential weakening of the bank due to vegetative loss, shear stresses and velocities along the bed and banks will

also be increased which in turn will increase the rate of bank erosion. It may be expected that the river will widen until a regime condition or dynamic equilibrium is reached. It should be noted that none of the regime methods employed consider the added resistance of banks to erosion due to vegetation. Thus, predicted widening may be less than computed herein if vegetative effects are considered.

Both pumping alternatives have the potential to damage the floodplain vegetation to some extent. However, the 300 cfs constrained pumping alternative would cause much less damage than the 480 cfs unconstrained pumping alternative under either the moderate or the wet climate scenario.

The species listed as "intolerant" and "somewhat tolerant" in Table 8-1 cannot be expected to survive the increased inundation due to the 480 cfs unconstrained pumping alternative for both the moderate and wet scenarios. The 300 cfs constrained pumping alternative can be expected to cause some flooding damage from which the vegetation could be expected to recover, provided flooding is not repeated in consecutive years.

Both pumping alternatives have the potential to prevent the establishment of seed on riverine depositional surfaces. However, the 300 cfs constrained pumping alternative would cause much less damage than the 480 cfs unconstrained pumping alternative for both the moderate and wet climate scenarios.

The effect of long-term channel change on the vegetation will be limited to near-bank riparian vegetation loss in some reaches due to localized bank failures and may be considered minor in nature.

The influence of long-term vegetation changes for the 300 cfs constrained pumping alternative on the channel morphology is expected to be of a minor nature for both the moderate and wet climate scenarios. However, long-term vegetation changes due to the 480 cfs unconstrained pumping alternative could have significant adverse impacts on channel stability for both climate scenarios. The loss of vegetation is thought to have more of an effect on the rate of erosion to reach the predicted ultimate values rather than the values themselves.

9.7 Adjustment of River after Periods of Prolonged Pumping

As described in the preceding sections, pumping of water from Devils Lake to the Sheyenne River is expected to have an effect on the morphology of the latter. New quasi-equilibrium conditions have been predicted for the project scenarios. The time necessary for the transition from one morphologic state to another can only be roughly estimated and will depend on many factors including bank resistance and vegetation. Initial width adjustment is expected to occur relatively quickly, perhaps measured in decades. However, overall adjustment of the Sheyenne River system to new hydrologic conditions (due to pumping and/or climatic shifts) is expected to take hundreds of years.

From the preceding analyses, it appears that the assumption of moderate or wet climatic conditions will have more of an effect on changes in channel behavior than whether or

not pumping is occurring. However, between pumping scenarios for a given climate condition, the larger pumping scenario (480 cfs) is predicted to have a much greater effect on channel morphology than the smaller (300 cfs) scenario, especially in regards to impact on vegetation.

10 References

Auble, G. T., Friedman, J. M., and Scott, M. L., 1994. "Relating Riparian Vegetation to Present and Future Streamflows," *Ecological Applications*, 4(3).

Biedenharn, D.S. Copeland, R.R., Thorne, C.R., Soar, P.J., Hey, R.D., and Watson, C.C., 2000 (August). "Effective Discharge Calculation," U.S. Army Corps of Engineers, Engineering Research and Development Center, *ERDE/CHL TR-00-15,* Washington, DC.

Brownlie, W.R. 1981. "Prediction of flow depth and sediment discharge in open channels." *Report No. KH-R-43A*, California Institute of Technology, W.M. Keck Laboratory of Hydraulics and Water Resources, Pasadena, CA.

Chow, V.T., 1959. *Open Channel Hydraulics*. McGraw-Hill, Inc., New York, NY.

Copeland, R.R., 1994. "Application of channel stability methods – case studies." *Technical Report HL-94-11*, U.S. Army Corps of Engineers, Waterways Experiment Station, Vicksburg, MS.

Dunne, T., and Leopold, L. B., 1978, *Water in Environmental Planning.* W. H. Freeman and Company, San Francisco, CA.

Julien, P.Y., and Wargadalam, J., 1995. "Alluvial channel geometry: theory and applications." *J. Hydr. Engrg.*, ASCE, 121(4), 312-325.

Leopold, L. B., Wolman, M.G., and Miller, J.P., 1964. *Fluvial Processes in Geomorphology,* W. H. Freeman and Company, San Francisco, CA.

Leopold, L. B., and Wolman, M.G., 1960. "River Meanders," *Geol. Soc. Am Bull.* v. 71, pp. 769-794.

Rhoades, E.D., 1967. "Grass Survival in Flood Pool Areas," *Journal of Soil and Water Conservation*, Volume 22, No. 1, January-February.

Rosgen, D.L., 1996. *Applied River Morphology*, Wildland Hydrology, Pagosa Springs, CO.

Scott, M.L., Freidman, J.M., and Auble, G.T., 1996. "Fluvial Process and the Establishment of Bottomland Trees," *Geomorphology* No. 14.

Simons, D.B., and Albertson, M.L., 1963. "Uniform water conveyance channels in alluvial material." *Trans., ASCE*, 128(1), 65-167.

USGS (U.S. Department of the Interior, Geological Survey), Office of Water Data Coordination, 1982 (March). "Guidelines for Determining Flood Flow Frequency*," Bulletin #17B*, Reston, VA.

USACE, 2000 (July). "HEC-GeoHMS, Geospatial Hydrologic Modeling Extension, User's Manual," *CPD-77*, Hydrologic Engineering Center, Davis, CA.

USACE, 1999 (June). "Design Memorandum, Pool Raise for Flood Control, Baldhill Dam and Reservoir, Sheyenne River, Valley City, North Dakota," Saint Paul District, St. Paul, MN.

USACE, 1998a (August). HEC-RAS Version 2.2, "User's Manual", *CPD-68*, Hydrologic Engineering Center Davis, CA.

USACE, 1998b (March). Draft "User's Manual for the SAM Hydraulic Design package for Channels," Vicksburg, MS.

USACE, 1994 (October). "Channel Stability Assessment for Flood Control Projects," *Engineer Manual 1110-2-1418*, Washington, DC.

USACE, 1993a (March). "Hydrologic Frequency Analysis," *Engineer Manual 1110-2-1415*, Washington, DC.

USACE, 1993b (August). "HEC-6, Scour and Deposition in Rivers and Reservoirs, User's Manual," *CPD-6*, Hydrologic Engineering Center, Davis, CA.

USACE, 1993c, (Jan). "Baldhill Dam and Lake Ashtabula Operational Management Plan, Final Approval, Saint Paul District, St. Paul, MN.

USACE, 1992 (May). "HEC-FFA Flood Frequency Analysis, User's Manual," *CPD-13*, Hydrologic Engineering Center, Davis, CA.

Vanoni, V. A., 1977, "Sedimentation Engineering," *ASCE Manuals and Reports on Engineering Practice- No. 54*, American Society of Civil Engineers, New York, NY.

Whitlow, T. H., and Harris, R.W. 1979, "Flood Tolerance in Plants: A State-of-the-art Review," *Waterways Experiment Station Technical Report E-79-2,* Vicksburg, MS.

Wiche, G. J. and S. W. Pusc (1994), *Hydrology of Devils Lake Area, North Dakota,* North Dakota State Water Commission Water Resources Investigation 22, prepared by the U.S. Geological Survey in cooperation with the North Dakota State Water Commission, Bismarck, ND.

Yang, C.T. 1984. "Unit Stream Power Equation for Gravel," *Journal of Hydraulic Engineering*, ASCE, Vol. 110, No. HY12, pp. 1783-1797.

Yang, C.T. 1973. "Incipient Motion and Sediment Transport," *Journal of Hydraulic Engineering*, ASCE, Vol. 99, No. HY10, pp. 1679-1704.